

ISSN 0385-2520

ROCK MAGNETISM
and
PALEOGEOPHYSICS

volume 5

1978



Published by the

ROCK MAGNETISM AND PALEOGEOPHYSICS RESEARCH GROUP IN JAPAN

P R E F A C E

This volume is the annual progress report of the Rock Magnetism and Paleogeophysics Research Group in Japan for the year 1978. As the previous volumes were so, this volume is a collection of summaries or extended abstracts of various research works carried out in our group. Many of the reports contain substances which may be changed or revised as the research work continues. In this respect, this volume contains many tentative results.

Except for the ones written as pure progress reports, the papers in this volume will be published in academic journals in full detail and length. This volume may be referenced, but if a paper is published in such an academic journal, readers are requested to quote the paper from that journal. We hope that this volume is a useful source of advance information of recent works on rock magnetism and paleogeophysics in Japan.

This volume also constitutes a scientific report of the Rock Magnetism and Paleogeophysics Research Group in the Japanese Geodynamics Project. We would like to acknowledge the partial financial support from the Ministry of Education for this publication and for the investigations included in this volume as a part of the Geodynamics Project.

November 1978

Masaru KONO
Editor

ま え が き

本書は、Geodynamics Project (GDP) II-1-(2)「古地磁気学的方法」の研究グループの報告書として刊行されるものである。岩石磁気学・古地球物理学研究グループでは、以前から Annual Report の形で英文の報文集を刊行してきた。(Annual Progress Report of the Rock Magnetism (Paleogeophysics) Research Group in Japan, 1963, 1964, 1965, 1967, 1968.) これらの報文集は、諸外国の研究者の間でもかなり広く活用されている。こういった実績を継続するためにも、GDPの研究報告書ではあるが英文に依っている。日本国内の研究者の方々に、いく分御面倒をおかけすることになるが、このような事情なので御了承いただきたい。

報文の配列の仕方は、便宜的なものであるが、一応大まかに(1)残留磁化の性質・実験方法 8編, (2)古地磁気層序・年代決定 8編, (3)古地球磁場強度・テクトニックな問題 6編という分類かしてある。

"Rock Magnetism and Paleogeophysics" は extended abstract 集であるのでここにおさめられた報文は progress report 的なものを除いて、いずれは完全な形の論文としてさまざまな学術誌に投稿・発表される予定である。発表予定が特にはっきりしているものについては、各論文末尾にそのことが付記してある。従ってこの報文集から引用されることは自由であるが、本論文が発表されたものについてはそちらを引用されるよう御配慮をお願いしたい。

1978年11月

古地磁気学・古地球物理学研究グループ

ROCK MAGNETISM AND PALEOGEOPHYSICS SYMPOSIUM

The Tenth Rock Magnetism and Paleogeophysics Symposium was held on 16th and 17th August, 1977 at the Joint Universities' Seminar House, Kawabata, Miyagi Prefecture.

PALEOINTENSITIES, TECTONIC PROBLEMS

H. Tanaka	Paleointensities of the Geomagnetic Field Determined from Recent Four Lava Flows of Sakurajima Volcano	87
H. Tanaka	Geomagnetic Paleointensities During the Past 30,000 Years in Japan	95
M. Kono	Paleomagnetism and Paleointensity Studies of Scottish Devonian Volcanic Rocks	98
S. Sasajima, Y. Otofuji, K. Hirooka, and F. Hehuwat	Suparka, Suwijanto Paleomagnetic Studies on Sumatra Island: On the Possibility of Sumatra Being Part of Gondwanaland	104
H. Kinoshita	Paleomagnetism of the Ocean Sediments of Shikoku Basin and Daito Area Obtained by the Deep Sea Drilling Project, Cruise Leg 58, by Glomar Challenger II	111
H. Miki, N. Isezaki, K. Yaskawa and H. Inokuchi	Magnetic Anomaly Lineations in the Philippine Sea	118
Author Index		125

INTENSITY VARIATION OF ONE-AXIS ARM WITH ANGLE

Tsutomu SUEISHI*

Department of Physics, Faculty of Engineering Science,
Osaka University, Toyonaka, Japan

Introduction

Recently anhysteretic remanent magnetization (ARM), which is acquired by a rock subjecting it to a decreasing alternating field superimposed on a small direct field, has been used for many paleomagnetic investigations (for example, Opdyke et al, 1973), because it has characteristics similar to those of thermo-remnant magnetization (TRM). But it is possible to classify ARM to three types as follows ; (1) bias direct field is rotated with specimen in the alternating field using a three-axis tumbler (Stephenson and Collinson, 1974). (2) bias direct field and alternating field are parallel. (3) they are perpendicular (Denham, 1976).

In every cases, the direction of remanent magnetization is coincident with that of direct magnetic field (Rimbert, 1958), but the difference of them could not yet be understandable. In this study, I investigate the variation of one-axis ARM with the angle between direct and alternating field.

Sample

For this investigation, 20 samples has been used. They are granites, basalts, deep-sea or lake sediments and the samples used for archaeomagnetism like baked earths. Most of them were collected in Japan (table).

ARM / IRM Ratio of the Samples

Sueishi et al (1977) estimated the magnetic stability of several sediments by measuring the ratio of intensity of ARM to that of saturation isothermal remanent magnetization (SIRM). This ratio has similar meaning to Königsberger's ratio (Q_t) when it is taken into account that ARM and IRM has characteristics similar to those of TRM and induced magnetization respectively. The ratio ARM (alternating field peak intensity is 1 kOe with 1 Oe direct field parallel to the alternating field) to IRM (1 kOe) of present samples are shown in the table with the data of median deduced field (MDF, indicator of coercive force) of ARM formed on the samples.

In general, granite and basalt specimens which presumably contain magnetic minerals dominated by multi-domain show the tendency that both the ratio ARM to IRM and MDF are small. On the other hand, sediments where ferromagnetic minerals are perhaps composed of single domain have the characteristic to the contrary. Especially, deep-sea ones have very large value of the ratio ARM to IRM. The archaeological specimens take small value of the ratio ARM to IRM and large MDF. They possibly contain the ferromagnetic minerals which are dominated by, what is called, pseudo-single domain.

Result

The data of intensity change of one-axis ARM with angle are shown in the figure. The transverse ARM (t ARM) intensity of sediments and archaeo-

* Present address : Kobe Municipal Office, Ikuta-ku, Kobe 650, Japan

Sample	ARM / IRM	M.D.Field (ARM)
Iwadate (granite)	1.96 %	49 Oe
Tsuruga (granite)	1.22 %	90 Oe
Kitagami (granite)	1.27 %	85 Oe
Asahi (granite)	0.59 %	103 Oe
Oshima (basalt)	1.59 %	292 Oe
Miyake-shima (basalt)	2.24 %	240 Oe
Pagan island (basalt)	1.13 %	122 Oe
Fuji (basalt)	2.19 %	86 Oe
KH73-4-7 (deep-sea sedi.)	12.9 %	220 Oe
KH70-2-5 (deep-sea sedi.)	20.7 %	208 Oe
KH68-4-20 (deep-sea sedi.)	21.8 %	238 Oe
Biwa (73 m, lake sedi.)	5.90 %	382 Oe
Biwa (171 m, lake sedi.)	9.30 %	413 Oe
Takakura-dera (pottery)	2.66 %	365 Oe
Sakai (baked earths)	1.01 %	300 Oe
Sakai (hearth)	1.96 %	375 Oe
Ceylon (baked earths)	1.61 %	137 Oe
GDP15-12 (deep-sea sedi.)	4.07 %	260 Oe
Guam island (sedimentary rock)	1.92 %	173 Oe
synthesized magnetite (1 %)	3.37 %	207 Oe

table. Sampling place or core name of the samples used for this study with the data of the ratio ARM (1 kOe alternating field coaxial with a constant field of 1 Oe) to IRM (1 kOe) and the median deduced field of ARM.

logical samples decrease to about half value of longitudinal ARM (1 ARM) intensity. On the other hand, granite and basalt specimens show no definite intensity variation with angle, and yet some specimens have rather more intensive t ARM than 1 ARM intensity. The synthesized magnetite's 1 ARM is about 1.5 times as intense as its t ARM. This result is in good agreement with the data by Rimbart (1958). She showed that 1 ARM is about 1.4 times as intense as t ARM using pure magnetite specimen. The above-mentioned result seems not to depend upon the magnetized direction of samples.

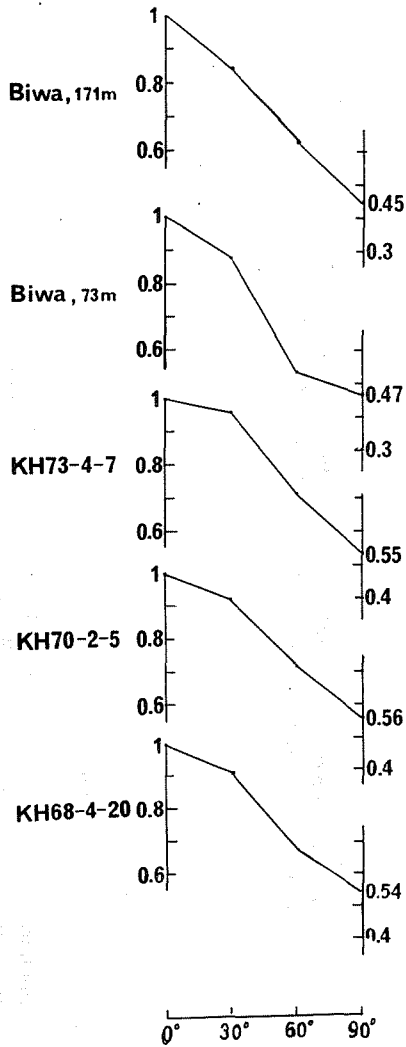
The ratio t ARM to 1 ARM can be regarded as an indicator of magnetic stability against the " secondary component " like the ratio ARM to IRM.

Consideration

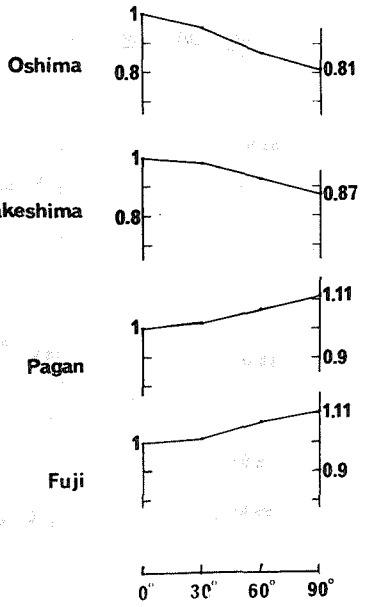
It is essentially troublesome matter to theoretically explain such result because one-axis ARM is formed on the sample under the such condition as " anisotropy of agitation ". But there could be some possible explanations ; (1) the peak of blocking coercive force spectra of t ARM shifts to the higher compared with that of 1 ARM. (2) the interacting field in each ferromagnetic grain might be different according to the angle between direct and alternating field.

It is necessary that when one-axis ARM is produced in the laboratory, the angle between them should be noted, especially when ARM is formed under present earth's magnetic field (for example, Niitsuma, 1977).

sediment



basalt



granite

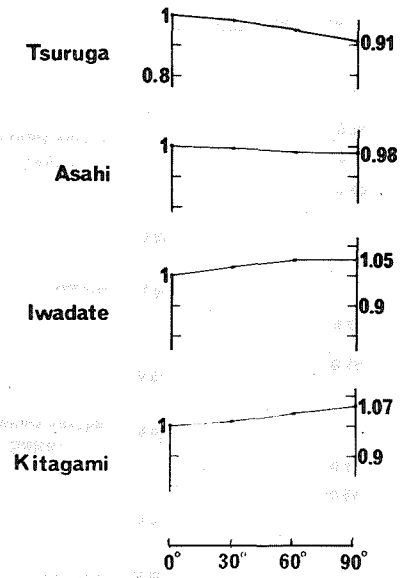
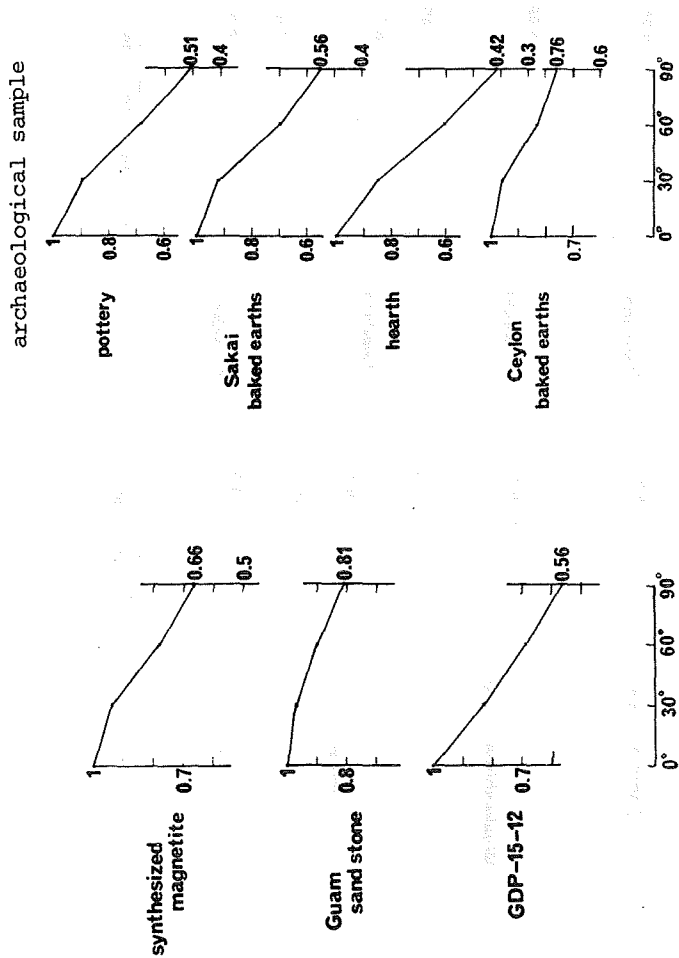


Figure. Intensity variation of one-axis ARM with angle between direct field and decreasing alternating field.



another samples ; synthesized magnetite has a density of 1 % with a particle size of less than one micron.

References

- Denham, C.R. (1976) *Earth Planet. Sci. Lett.*, 29, 422.
 Niitsuma, N. (1977) *Rock Magnetism and Paleogeophysics*, 4, 65.
 Opdyke, N.D., Kent, D.V. and Lowrie, W. (1973) *Earth Planet. Sci. Lett.*, 20, 315.
 Rimbert, F. (1958) Ph.D. Thesis, Paris Univ.
 Stephenson, A. and Collinson, D.W. (1974) *Earth Planet. Sci. Lett.*, 23, 220.
 Sueishi, T., Kawai, N. and Kobayashi, K. (1977) *Rock Magnetism and Paleogeophysics*, 4, 29.

COMPARISON OF THE DIRECTIONS OF CRM AND TRM IN SOME ANDESITIC ROCKS

Yositugu INOUE

Department of Geology, Faculty of Science,
Shinshu University
Asahi 3-1-1, Matsumoto 390, Japan

1. Introduction

It is well known that titanomaghemite phase (γ -phase) is unstable with respect to heating. Therefore, this phase found along rims and cracks of titanomagnetite (β -phase) grains is often called "low temperature oxidized titanomaghemite".

Though it is difficult to manage the unstable phase, mineralogical and magnetic properties of γ -phase is well established (Ozima and Larson, 1967, 1970; Ozima and Sakamoto, 1971; Readman and O'Reilly, 1972). On the other hand, what sort of remanence is acquired by natural γ -phase is not accurately known. Recently works on this problem are summarized by Johnson and Hall (1978).

Although Momose and Inagaki (1973) tried to discriminate chemical remanent magnetization (CRM) of γ -phase from thermo-remnant magnetization (TRM) of β -phase in one rock sample, it is reported that no stable CRM was detected. They suggest that the result may be due to the large grain size of the ferromagnetic minerals contained therein, and that further experiments are required. In this paper successful results of experiment to discriminate and compare the directions of remanences of the two phases in a rock sample are described.

2. Samples, Experiment and Results

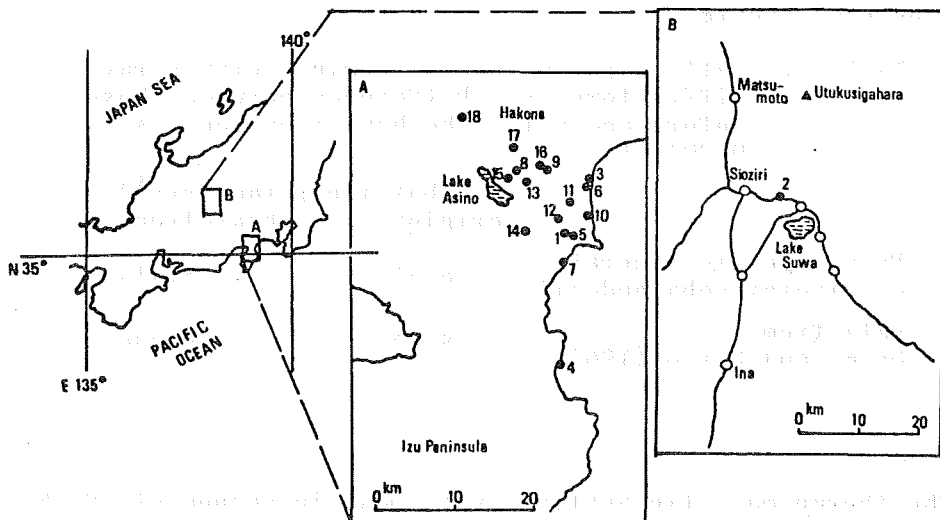


Fig.1 Sampling sites; 1 Siroisityoba, 2 Sioziri-Toge, 3 Komekami, 4 Usami, 5 Kaziya, 6 Nebukawa, 7 Inamura, 8 Hutagoyama, 9 Sarusawa, 10 Nagasakayama, 11 Siraitogawa

12 Makuyama, 13 Bunkoyama, 14 Yugawara Parkway, 15 Hakone-En, 16 Sukumo-Gawa, 17 Sōunzan, 18 Otome-Toge.

Orientated samples of lava flows whose initial remanence may be due to TRM were collected at thirty-three sites scattered in and around Hakone Volcano and Sioziri-Toge near Matsumoto City. To discriminate and compare the remanences of β -phase and γ -phase in a rock sample by the method demonstrated by Momose and Inagaki (ibid.), it is necessary to select samples containing stable ferromagnetic minerals. Such samples should be excluded as those including minerals oxidized or changed by heating of thermal demagnetization at each Curie temperature of β -phase. Among them those from eighteen sites (Fig.1) were selected that contain both β -phase and γ -phase, of which the latter was observed along rims and cracks of the β -phase crystals. The selection was performed under the reflection microscope and by thermo-magnetic analysis. The successful result of experiments mainly on the Siroisityoba andesite are described below.

After the initial thermo-magnetic analyses* Curie point (T_{c2}) of ferromagnetic minerals heat-treated at 680-950°C in 10^{-3} - 10^{-4} Torr for several hours was estimated respectively. In ten cases were observed large descents of Curie points from initial values (Fig.2). Differences in relative value of saturation magnetizations and lattice parameters between those before and after the heat treatment were so small, say a few percents and less than 0.01 Å respectively, that the descent of Curie point is considered as an effect of the breakdown of γ -phase (Ozima and Larson, 1967). Consequently it is judged safely that the new Curie points (T_{c2}) correspond with those of β -phase. In other samples Curie points ascended, i.e., the initial Curie point (T_{c1}) was lower than T_{c2} . It was caused probably by "unmixing" of γ -phase (Ozima and Larson, 1970) or by high temperature oxidation. Table 1 shows the lattice parameter change of ferromagnetic minerals in Siroisityoba andesite by heat treatment.

Table 1. Lattice parameters determined with x-ray diffractometer. Difference between those before and after the heat treatment is 0.001 Å.

	Lattice parameter (Å)	
	original	heat-treated
Ferromagnetic minerals of Siroisityoba andesite	8.415	8.414
Data from Ozima and Larson (1967)	8.430	8.430

* The thermo-magnetic analyses were made in vacuum of 10^{-3} Torr unless otherwise stated.

Table 2. Properties of selected samples

Samples	ferromagnetic minerals		Tc ₁ (°C)	Tc ₂ (°C)	NRM		susceptibility (emu/gr.)	Qn
	average grain size	composition			intensity (emu/gr.)	MDF* (Oe)		
1. Siroisityoba andesite	60 μm	β ≫ γ	500	360	6-10x10 ⁻⁴	70	9.84x10 ⁻⁴	2.1
2. Sioziri-Toge andesite	15 μm	β ≫ γ	500	320	7-12x10 ⁻⁴	75	-	-
3. Komekami andesite	50 μm	β ≫ γ	500	380	4-5x10 ⁻⁴	78	9.48x10 ⁻⁴	1.9

MDF*, peak field

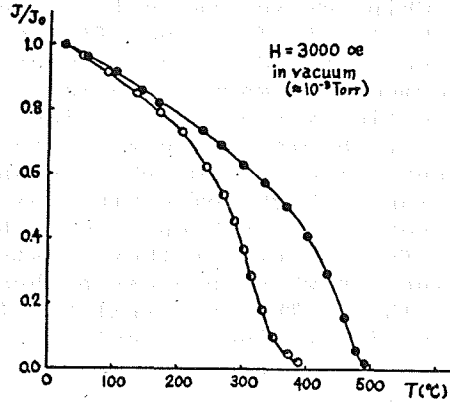


Fig. 2 Heating processes of Js-T curves for Siroisityoba andesite

solid circles, original specimen
open circles, specimen heat treated at 680°C in 10⁻³ Torr for 3 hrs.

The Curie point descended from 500°C to 300°C.

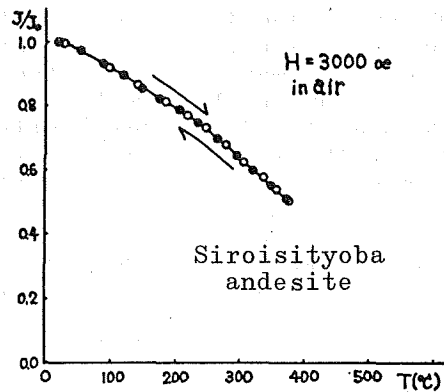


Fig. 3 Test of ferromagnetic minerals with respect to heating at Tc₂ in air for 1 hr.

solid circles, heating process
open circles, cooling process

Both of the curves coincide each other.

Chips or separated ferromagnetic minerals of ten samples were heated to T_c , and after a certain time of preservation they were cooled to room temperature. All this procedure was performed in a magnetic balance, and "in air". The preservation time was one hour. These conditions are similar to those of thermal demagnetization. If the ferromagnetic minerals are subjected to some phase change (for instance, breakdown, unmixing or high temperature oxidation), the process of cooling represented by J_s - T curve must be different from that of heating. As a result of these tests samples from three sites were obtained in which process of heating and cooling coincide with each other. They are suitable for thermal demagnetization without destroying the natural remanence of γ -phase (Fig.3).

Various properties obtained from them are summarized in Table 2.

Thermal demagnetization on core specimen of Siroisityoba andesite was successfully carried out. After thermal demagnetization at T_c (380°C) a remanence was found to be maintained still in each specimen. The intensity of the remanence was 35 to 40 percents of that of the initial natural remanent magnetization (NRM). The remanence is neither the TRM component of β -phase resulting from incomplete demagnetization nor the CRM component newly induced in the electric furnace, but it is the CRM component of NRM preserved in γ -phase. This is understood from the following.

1) Blocking temperature (T_B) of β -phase determined from gradual thermal demagnetization is ca. 350°C (Fig.4).

2) Samples are set one after another in random directions in the furnace, and the result is that the remanences in them resemble to each other in intensity and direction.

3) Similar remanences are also observed after the thermal demagnetization in the μ -metal shielded furnace (inner field = 50-200 γ) of the Tokyo University.

4) Under the reflection microscope no phase change of the ferromagnetic minerals is detected after thermal demagnetization.

5) J_s - T curve of a specimen after thermal demagnetization is similar to the initial one.

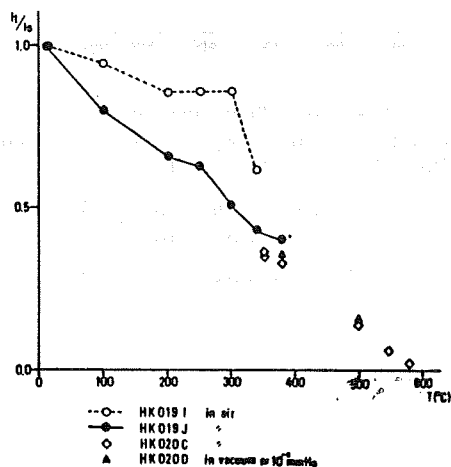


Fig.4 Gradual thermal demagnetization for Siroisityoba andesite

Open circles, Thermal demagnetization was made after demagnetization.

The other signs, Thermal demagnetization was made on original specimen.

Newly induced CRMs are found after the thermal demagnetization higher than 380°C .

The average direction of these remanences of γ -phase is compared with that of af(25-50 Oe) demagnetized core specimens which may represent a superimposed direction of TRM of β -phase and CRM of γ -phase(Fig.5), using Fisherian statistics(Table 3). Little difference is found between the two directions of TRM and CRM.

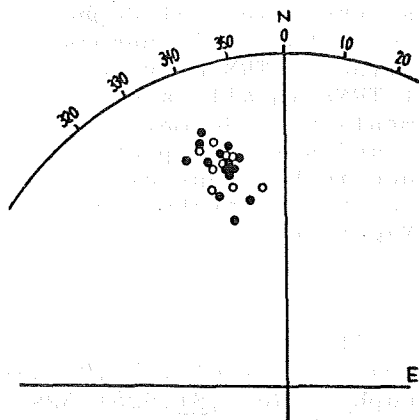


Fig.5 Stereographic projection of remanences of Siroisityoba andesite on Schmidt's net.

Inclinations are all positive.

Solid circles, after thermal demag. (CRM).

Open circles, after af demag. (TRM+CRM).

Original NRM's are more scattered probably because of unstable VRM.

Table 3. Fisherian statistical comparison of (CRM) and (TRM+CRM).

	*1	*2
mean direction declination	N 14°3 W	N 14°2 W
inclination	+35°2	+33°6
precision parameter	63	124
radius of 95% confi. circle	5°1	4°8
number of points	14	9
angle between two directions	1°7	

*1 After thermal demagnetization at T_{c2} (CRM).

*2 After af(25-50 Oe) demagnetization(TRM+CRM).

3. Discussions

The ferromagnetic minerals contained in Siroisityoba andesite are coarse in grain size, and might have originally been a β -phase mineral with $x=0.3$ (calculated from T_c ; Akimoto, 1955). So it may be assumed that the remanence of γ -phase is CRM which was subjected to the external field of that time when the low temperature oxidation proceeded(Johnson and Merrill, 1973; Johnson and Hall, 1978). If such is true, the above-mentioned results are explained as follows. The low temperature oxidation proceeded and ended just after the cooling of the lava, and CRM was acquired in the same direction of TRM of β -phase.

Recently the writer carried out low temperature cleaning (Ozima et al., 1964), instead of af demagnetization, of NRM's of Siroisityoba andesite. By this experiment the above-

mentioned result that CRM of γ -phase is similar to TRM of β -phase in direction is again demonstrated with more sound reliability. Further experiments are now being executed by the writer, which will probably yield the same results. The same result is obtained also by Momose (unpublished) on samples of Utukusigahara andesite.

The properties of CRM described above seems to be general in γ -phase minerals of other andesites, whose initial β -phase mineral is titanomagnetite with $x=0.3-0.4$. But it is unknown whether these CRMs succeeded the direction of TRM or were acquired just after the acquisition of TRMs in all cases.

However, these results of experiments provide more reliable paleomagnetic data of Siroisityoba andesite and probably of others. It may be due to the difference in horizons of sampling that the paleomagnetic data of Siroisityoba andesite described above differ from those of Nagata et al. (1975).

4. References

- Akimoto, S. (1955) Jap. J. Geophys., 1, 1-31.
Akimoto, S. and I. Kushiro (1960) J. Geomag. Geoelectr., 11, 94-110.
Johnson, H.P. and J.M. Hall (1976) J. Geophys. Res., 81, 5281-5293.
Johnson, H.P. and J.M. Hall (1978) Geophys. J. R. astr. Soc., 52, 45-64.
Johnson, H.P. and R.T. Merrill (1972) J. Geophys. Res., 77, 334-341.
Johnson, H.P. and R.T. Merrill (1973) J. Geophys. Res., 78, 4938-4949.
Johnson, H.P. and R.T. Merrill (1974) J. Geophys. Res., 79, 5533-5534.
Kobayashi, K. (1959) J. Geomag. Geoelectr., 10, 99-117.
Kuno, H. (1950) J. Fac. Sci. Univ. Tokyo, II, 7, 257-279.
Marshall, M. and A. Cox (1971) Nature, 230, 28-31.
Marshall, M. and A. Cox (1972) J. Geophys. Res., 77, 6459-6469.
Momose, K. and S. Inagaki (1973) Rockmagnetism and Paleogeophysics, 1, 7-8.
Nagata, T., S. Akimoto, S. Uyeda, Y. Simizu, K. Kobayashi and H. Kuno (1957) J. Geomag. Geoelectr., 9, 23-41.
Ozima, M. and E.E. Larson (1967) J. Geomag. Geoelectr., 19, 117-127.
Ozima, M. and E.E. Larson (1970) J. Geophys. Res., 75, 1003-1018.
Ozima, M. and N. Sakamoto (1971) J. Geophys. Res., 76, 7035-7046.
Ozima, M., M. Ozima and T. Nagata (1964) J. Geomag. Geoelectr., 16, 37-40.
Readman, P.W. and W.O'Reilly (1972) J. Geomag. Geoelectr., 24, 69-90.
Sasajima, S. (1961) J. Geomag. Geoelectr., 12, 190-251.

SECONDARY COMPONENT OF REMANENT MAGNETISM IN MORIYAMA DEEP DRILLING CORE

Masayuki TORII

Department of Geology and Mineralogy, Faculty of Science, Kyoto University, Kitashirakawa, Sakyo-ku, Kyoto 606, Japan

Introduction

Paleomagnetic investigation often encounters an obstruction of stable secondary component which can not be easily removed by any demagnetization techniques. This difficulty is frequently observed in sediments or sedimentary rocks.

Such an obstruction was discussed in a paper of Kawai et al. (1978). They studied paleomagnetism of a long core from the underground strata of the Kobiwako Group at the eastern coast of Lake Biwa (Moriyama City). The core samples were composed of lacustrine sediments and expected to include the Brunhes/Matuyama geomagnetic polarity epoch boundary. Natural remanent magnetization was measured of all specimens and they appeared to be disturbed by the secondary components in most cases (Fig. 1). No significant removals of the secondary components were observed by both alternating field and thermal method for demagnetization.

Property of remanent magnetization of this core is reexamined in this short report.

Results and Discussion

Specimens were selected from very fine sand and silt of the core for this experiments. They were gradually dried in a laboratory. The measurement of remanence was carried out by the Schonstedt spinner magnetometer (SSM-1A). Intensity of the remanence is mostly an order of 10^{-6} cgsemu/gr.

1) Storage test

Specimens were subjected to alternating field demagnetization of 150 Oe (peak field) prior to the storage. They were stored in the geomagnetic field of 0.46 G. Remanences were repeatedly measured after 24 hours, 8 days and 119 days storage. Most of the remanent vectors after 119 days storage were apparently turned toward the direction of an applied field as shown in Fig. 2. Then they were treated again by alternating field of 200 Oe. The original direction is recovered by this demagnetization. The remanence acquired during the storage may be viscous remanent magnetization. In this case, the viscous component is properly removed by alternating field demagnetization of several hundreds oersted and is not a major factor suppressing the primary component of the remanence.

2) Alternating field demagnetization

The results of progressive alternating field demagnetization up to 400 Oe are typically shown in Fig. 3. Specimens were sampled from the site closely near the volcanic ash layer (553 m) whose polarity was reversed. Remanences of these specimens are therefore expected to be reversed.

Specimen of volcanic ash (a) is exceptionally quite stable against alternating field. Specimen (b) shows considerable decay of the resulting intensity of remanence (J), but retains close direction to the original. Specimens (c) and (d) show large swing of remanent vectors, and irregular change of J. It may be concluded that stable end point of remanence can

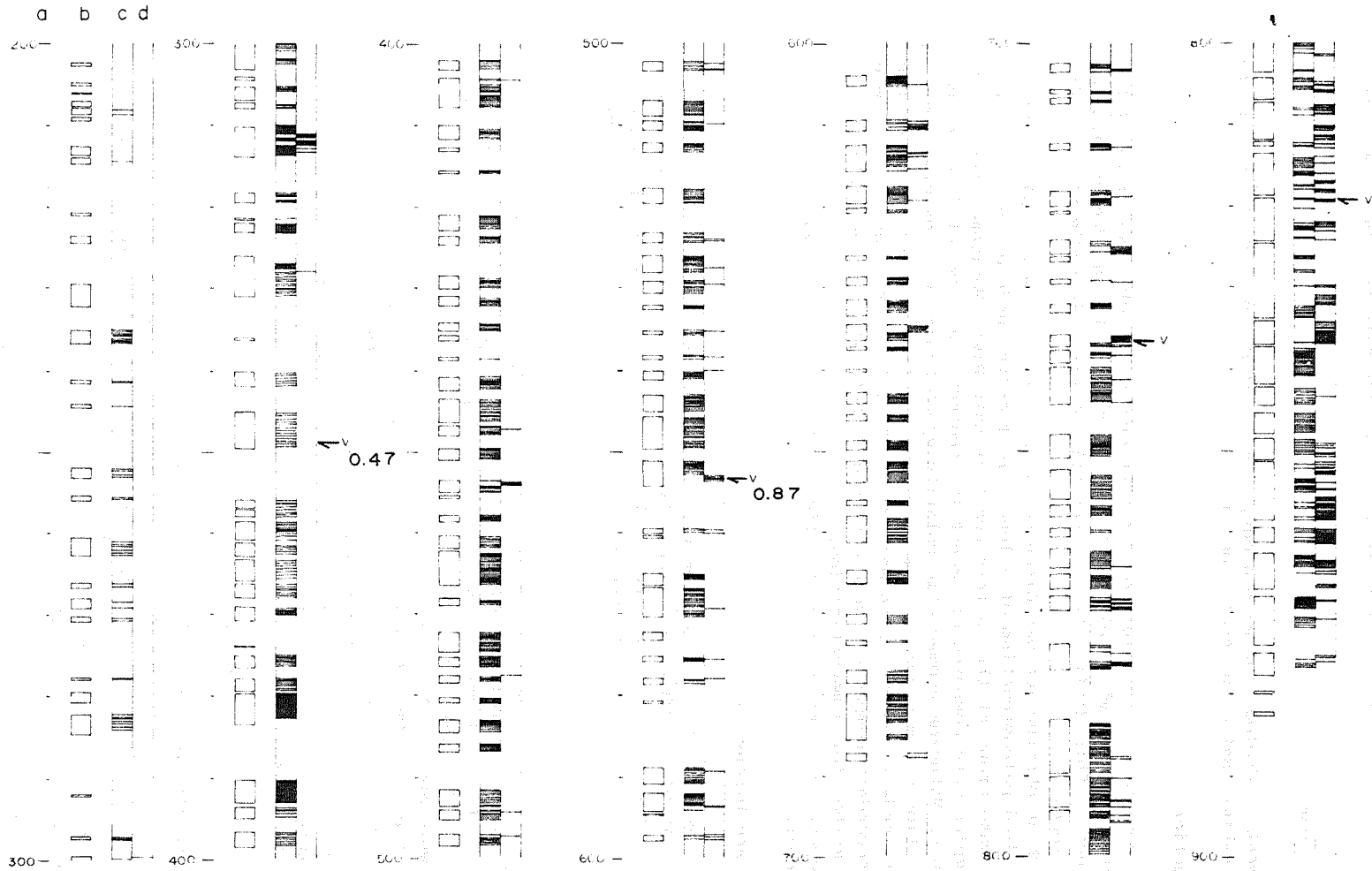


Fig. 1. NRM of Moriyama core samples by Kawai et al. (1978). a: drilled depth b: location of core sample c: down inclination d: up inclination 'v' indicates location of volcanic ash layer and numbers show fission track age of them by Takemura et al. (1977).

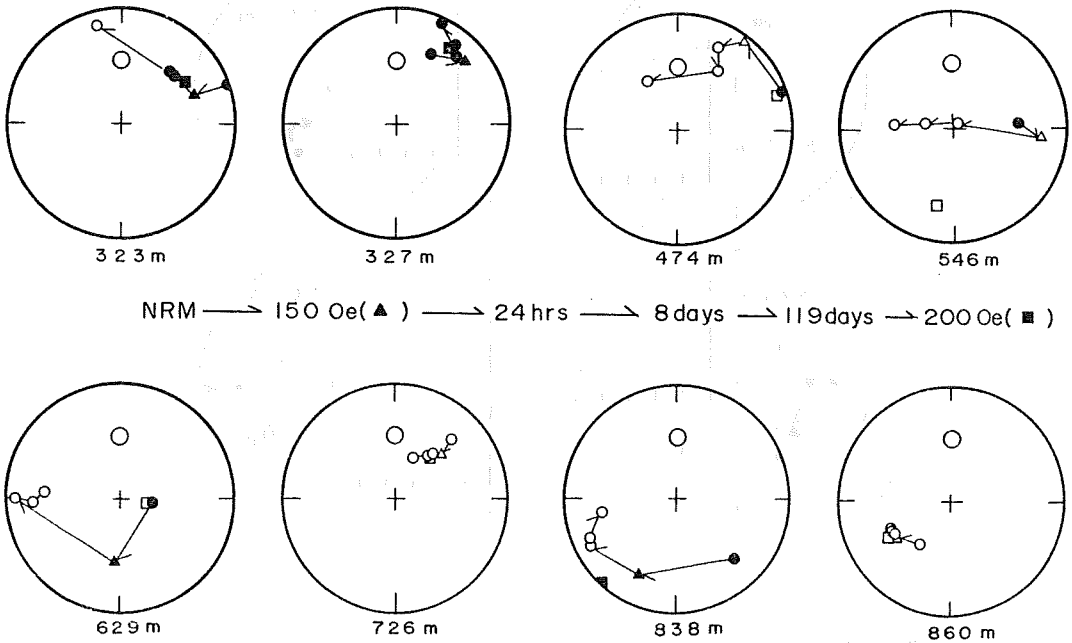


Fig. 2. Results of storage test on Schmidt equal area projection. Open symbol is upper hemisphere. Closed symbol is lower hemisphere. Large open circle is direction of storage field.

not be found out by alternating field demagnetization in this case.

3) Thermal demagnetization

Thermal demagnetization was carried out as follows: Specimens were heated in the non-inductive electric furnace in the open air. Heating in nitrogen atmosphere was also tried. But it resulted an extreme increase of J , which may be due to the reduction of specimens. Magnetic field at a sample holder in the furnace was reduced less than 50 gamma with an orthogonal set of three Helmholtz coils and double-layered μ -metal tube around the furnace.

Fig. 4 shows the typical results of thermal demagnetization. On the case of (a) and (b), J increases abruptly when the demagnetization temperature exceeds 300°C . Directional change of the remanence is rather anomalous. No significant change of the direction is observed in (c). Reversal of the remanent vector is observed in (d).

Meanwhile, the remanences showed rather unstable behavior caused by thermal treatment. Exponential decay of J during measurement with spinner magnetometer was observed in most cases. Remanent vectors also attain parallel direction to the storage field when they are stored only a few days

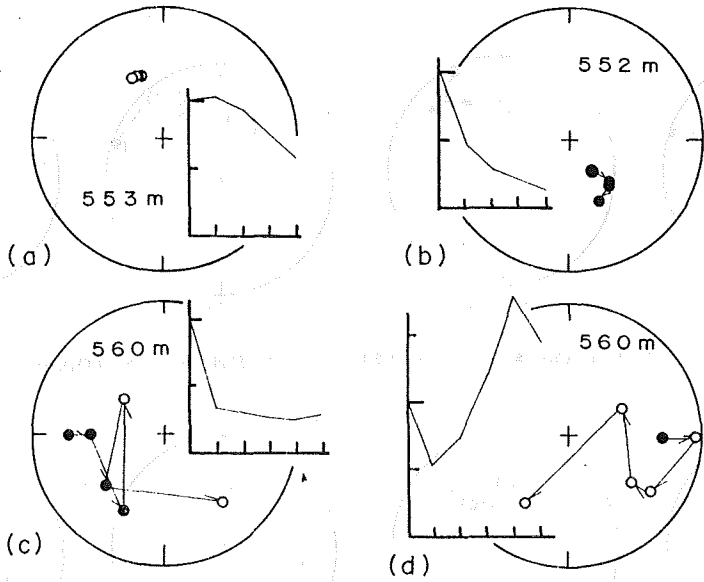


Fig. 3. Results of alternating field demagnetization. Each unit on abscissa is 100 Oe (peak field).

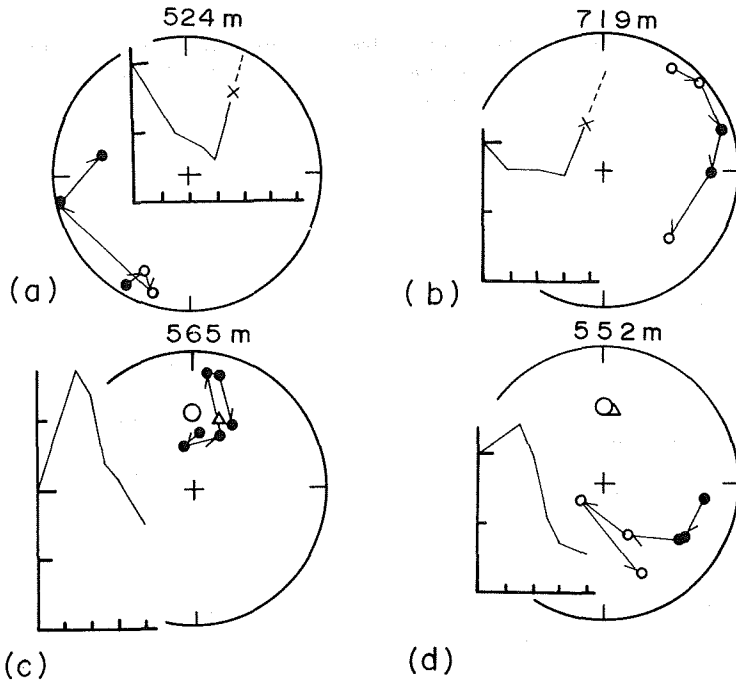


Fig. 4. Results of thermal demagnetization. Each unit on abscissa is 100°C . Large open circle in (c) and (d) is direction of storage field after heating. Triangle is direction of remanence after storage.

after thermal demagnetization.

Thermal demagnetization supposedly yields stable end point of the remanence. However, these results indicate that a fairly soft magnetic component is produced by heating. They may lead results of thermal demagnetization confusion.

4) Thermo-remanent magnetization experiment

To study the change of magnetic property caused by thermal treatment, following experiment on several specimens was carried out about thermo-remanent magnetization (TRM). Specimens were arranged into two groups. Group A has a little component of secondary magnetization*. On the other hand, primary component is assumed to be covered with secondary component in the case of group B**. They are treated in the furnace at the temperatures of 100°, 150°, 200°, 300° and 410°C in the direct field of 0.3 Oe. At each step of the TRM they were subjected to progressive alternating field demagnetization up to 400 Oe. Change of J against demagnetization field is shown on a log scale (Fig. 5). Distribution pattern of remanent coercivity is available for each step of TRM from the diagram of normalized intensity in the Fig. 6. Specimens were demagnetized at the temperature of 430°C after the last step of TRM(410°C). Value of J after this demagnetization is indicated by asterisks in Fig. 5.

Differences in the magnetic property observed between group A and group B are summarized as follows: i) Sudden increase of J is observed at the temperature above 200°C for the group A. Such a behavior is not clearly recognized for the group B. ii) Coercivity of resulting remanence is relatively soft comparing with the original. Especially, the portion of low coercivity is increased by heating process in the case of of group A. iii) J do not decrease to the original level after thermal demagnetization. Fairly large amount of J is remained undemagnetized for the group A.

These result may lead us to a following speculation. If there are "magnetic embryos" in all horizon of the core which grows to be secondary components, the difference between the two group will be ascribed to the degree of growth of the "embryo". In the case of the group A with a little secondary component, the growth of the "embryo" starts rapidly by heating the specimen above room temperature. In the case of the group B, however, considerable amount of the "embryo" has already grown to the stable secondary component during the geologic time. It may be one of the plausible idea to interpret the result of present experiment.

Quite similar phenomenon has been discussed by Watkins et al. (1974). They found unstable behavior of the remanence in their specimens of Italian marine sediments after heating. Hayashida (1978) also discussed on the property of secondary component which could not be properly removed by the method of demagnetization. His specimens were obtained from the correlative land section to this core.

TRM experiment suggests the production of new magnetic carrier caused by heating. On the other hand, it may be evident that the subsequent oxidation is occurred during heating. Effects on the magnetic property of both production and oxidation are probably inseparable. Specimens after heating

* Specimens of 327 m and 411 m (in the Brunhes normal epoch) have normal polarity of remanence. Specimen of 864 m (in the Matuyama reversed epoch) has reversed polarity.

** Specimens of 547 m, 682 m and 797 m (in the Matuyama reversed epoch) have normal polarity which is regarded as a spurious magnetization.

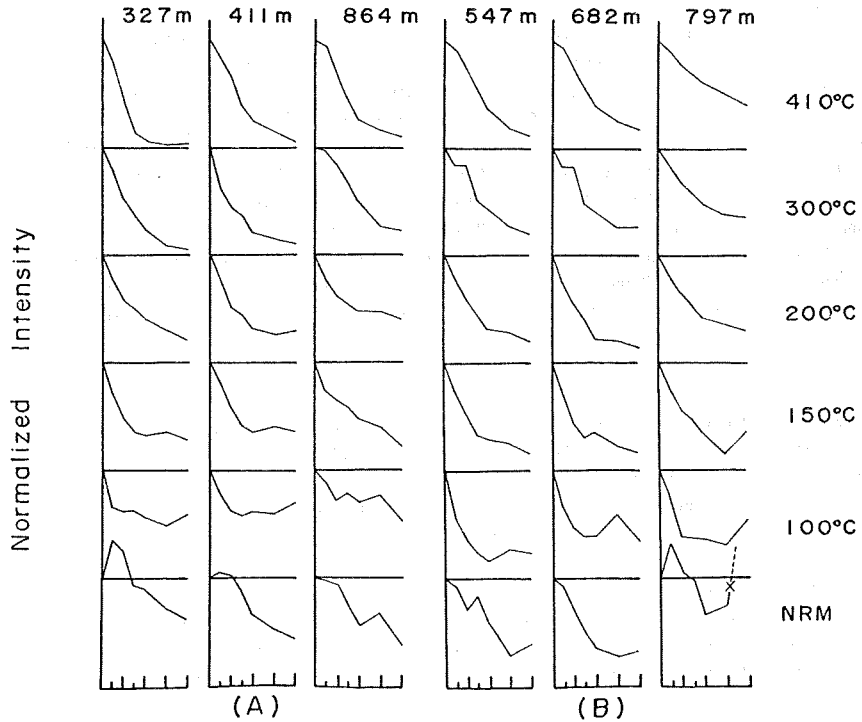
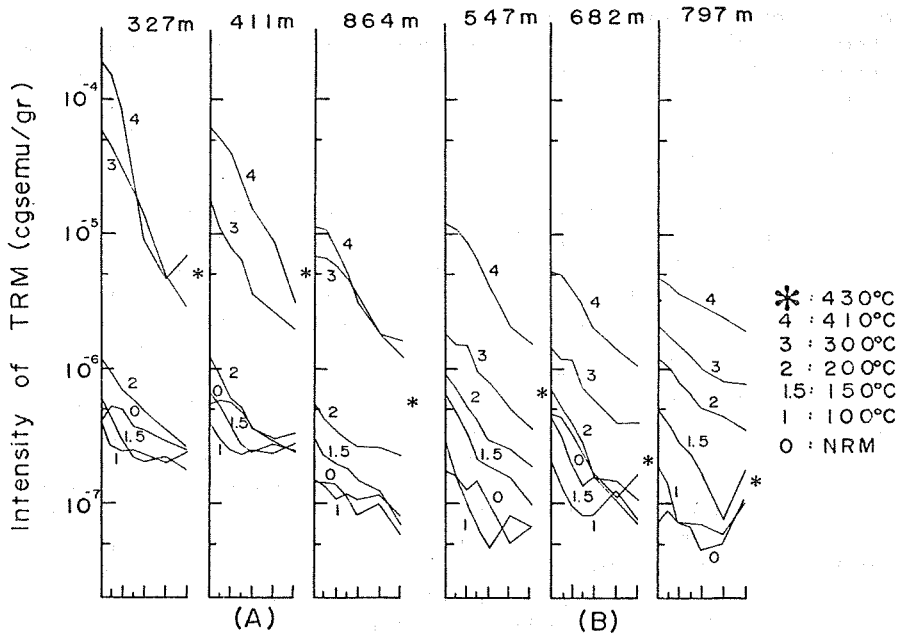


Fig. 5 (upper). Progressive alternating field demagnetization of TRM at various temperatures. Each unit on abscissa is 100 Oe
Fig. 6 (lower). Variation of normalized intensity at each step of TRM in upper figure.

turn their colour from dark bluish gray to light brown. But identification of minerals is not made in the present study. It seems to be difficult to identify magnetic minerals because of thermal instability of them.

Further experiments, such as critical identification of the magnetic minerals before and after thermal treatment, are required.

References

Hayashida, A. (1978) Master Thesis of Kyoto University
Kawai, N., T. Nakajima, N. Natsuhara, S. Sasajima, M. Torii, Y. Otofujii,
A. Hayashida, J. Nishida and S. Horie (1978) *Paleolim. Lake Biwa Japanese Pleist.*, 5, 95.
Takemura, K., S. Nishimura, T. Danhara and T. Yokoyama (1977) *ibid.*, 4, 79.
Watkins, N.D., D.R. Kester and J.P. Kennett (1974) *Earth Planet. Sci. Lett.*, 24, 113.

FIELD DEPENDENCE OF PALEOINTENSITY DETERMINED BY THE THELLIER METHOD

Hidefumi TANAKA

Department of Applied Physics, Tokyo Institute of Technology,
Meguro-ku, Tokyo 152

Introduction

Paleointensity determination is very important field in paleomagnetism and the Thellier method (Thellier and Thellier, 1959) is most reliable because it can check the presence of non-ideal behavior such as changes in TRM characteristics during the heat treatment by the linearity of the NRM-TRM relation. Although many basic studies about the Thellier method (Coe, 1967; Coe and Grommé, 1973; Kono, 1974; Khodair and Coe, 1975; Kono and Tanaka, 1977), they were mainly concerning with the mechanisms of the non-ideal behaviors of the remanent magnetization in the course of heat treatments and how to succeed in the paleointensity experiment. There were no study concerning to the dependence of the determined intensity by the Thellier method on the paleointensity value. When we obtain an extraordinary large or small paleointensity values by the Thellier method, there remain still some suspicions about the obtained intensity values. It is worthwhile to ascertain the success of the Thellier method by making the following experiments. First, TRM's are produced to natural rock samples in various magnitude of the laboratory magnetic field, and paleointensities are determined using those samples by the Thellier method. It is aimed to check whether the intensity values the same as the actual laboratory field intensities are obtained.

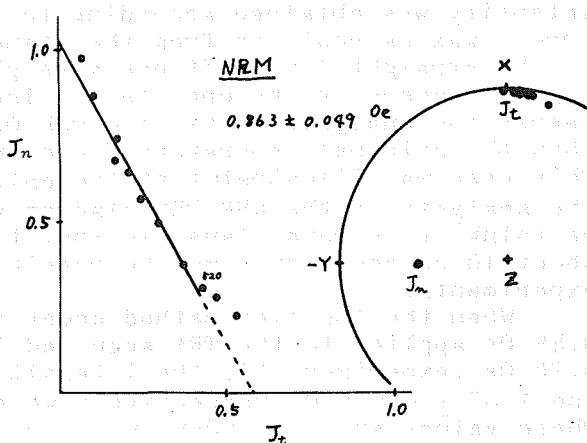
Samples

Samples used in this study are sampled from the Kotaki pyroclastic flow, Asama volcano, central Japan. These samples are suitable for this study, because the Thellier method is always successfully applied in any atmosphere in the furnace (Kono, 1969). This Kotaki pyroclastic flow is dated as about 2,000 years B.P. by radio-carbon dating, and yields a large paleointensity value of 0.84 Oe (Kono, 1969) that is concordant with the world-wide secular change of the geomagnetic paleointensity. The paleointensity value obtained from this flow by the Thellier method making use of our instrument agrees well with the result by Kono (1969) as shown in Fig. 1. This indicates that our instrument works well.

Experimental Procedures

Two different types of experiment were performed. First is that TRM's made under the laboratory field of various intensities are all attributed to the paleointensity experiment by the ordinary Thellier method under the laboratory field of 0.49 Oe (experiment 1). Second is that those TRM's made under various magnitude of the field are attributed to the Thellier

Fig. 1. NRM-TRM diagram for a sample from Kotaki pyroclastic flow (NRM). The intensity value of 0.86 ± 0.05 Oe was obtained where the error was calculated from the standard error of the slope of the straight line.

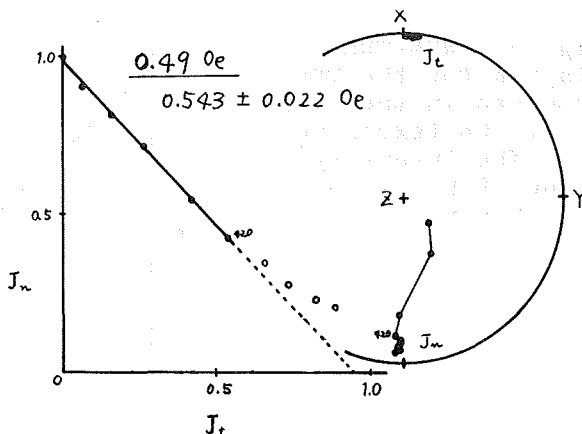


method under the magnetic field the same magnitude as the original laboratory one (experiment 2). Nine values of intensities ranging from about 0.02 to 10 Oe were used in experiment 1 to produce TRM's that are treated as the original NRM's in the Thellier method, and four values of 0.02, 0.2, 2 and 10 Oe were used in the experiment 2. All the experiment was performed in air.

Results from TRM's produced in the medium magnetic field

Three specimens which acquired TRM's in the field intensity of 0.196, 0.49 and 0.98 Oe were attributed to the Thellier method under the laboratory field of 0.49 Oe (experiment 1). Fig. 2 illustrates the NRM-TRM diagram (Arai diagram; Nagata et al., 1963) for the TRM produced in the field of 0.49 Oe. Plots in NRM-TRM diagram deflect a little from a straight line at higher temperatures as shown in Fig. 2. When NRM's deflect from the original NRM directions more than 10 degrees at some temperatures, plots on a NRM-TRM diagram corresponding to these temperatures were rejected from the linear regression analysis of the straight line. 0.543 ± 0.022 Oe about 10 percent larger than the original laboratory field

Fig. 2. NRM-TRM diagram for the TRM produced in the field of 0.49 Oe (experiment 1). The intensity value of 0.543 ± 0.022 Oe was obtained.



intensity was obtained according to this criteria, and the error was calculated from the standard error of the slope of the straight line. If one more plot corresponding to a higher temperature by one step is included to the linear regression analysis, 0.511 ± 0.024 Oe only 4 percent larger than the original laboratory field intensity is obtained. This case may illustrate that the criteria above mentioned for the analysis of the NRM-TRM diagram works not very well. But we think it is more plausible that this result indicate that about 10 percent error may be possible in paleointensity experiments.

When the Thellier method under the laboratory field of 0.49 Oe applied to the TRM acquired in the field of 0.196 and 0.98 Oe (experiment 1), the intensity values of 0.21 ± 0.01 and 1.02 ± 0.025 Oe respectively were successfully obtained. These values are concordant with the original laboratory field intensities.

Results from TRM's produced in the large magnetic field

Three specimens which acquired TRM's in the field intensity of 1.96, 4.9 and 9.8 Oe were attributed to the Thellier method under the laboratory field of 0.49 Oe (experiment 1), and another two specimens having TRM's produced in 1.96 and 9.8 Oe were also attributed to the Thellier method under the respective original laboratory field of 1.96 and 9.8 Oe (experiment 2). Fig. 3 illustrates the NRM-TRM curve for the TRM produced in the field of 4.9 Oe obtained by the experiment 1. Scatter of plots in NRM-TRM diagram seems to be very large, but the abscissa is enlarged by ten times, so the result is successful as indicated by the correlation coefficient of 0.976. The obtained intensity value of 4.59 ± 0.32 Oe is about 6 percent smaller than the original intensity, but considering the error amounted to ± 0.32 Oe the obtained value agrees with the original intensity value.

For TRM's produced in the field of 1.96 and 9.8 Oe, the Thellier method was successfully applied (experiment 1) and the obtained intensity values are 2.01 ± 0.06 Oe and 7.57 ± 0.87 Oe respectively. The former value agrees very well with the original intensity, but the latter is 23 percent smaller

Fig. 3. NRM-TRM diagram for the TRM produced in the field of 4.9 Oe (experiment 1). The intensity value of 4.59 ± 0.32 Oe was obtained.

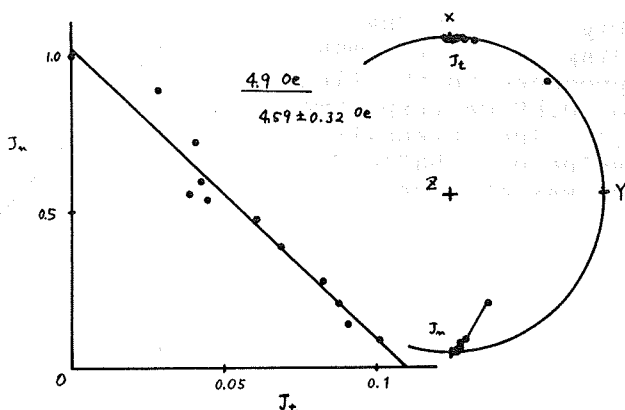
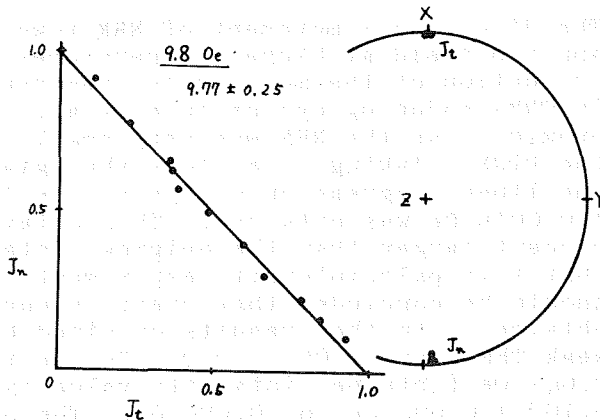


Fig. 4. NRM-TRM diagram for the TRM produced in the field of 9.8 Oe obtained by the Thellier method under the laboratory field of 9.8 Oe (experiment 2). The intensity value of 9.77 ± 0.25 Oe is obtained.



than the original one. This discrepancy between the obtained intensity value and the original intensity value may be due to the non-linearity of field dependence of TRM acquisition in a strong field range.

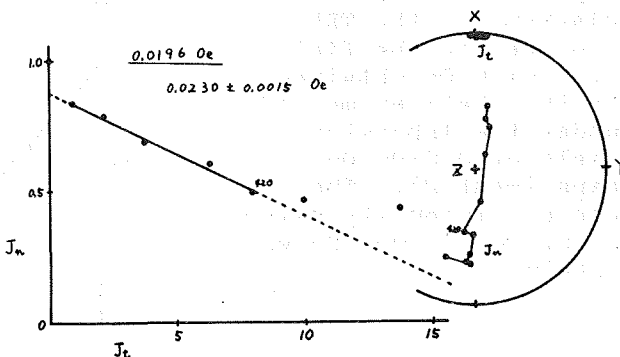
Fig. 4 illustrates the NRM-TRM diagram for the TRM produced in the field of 9.8 Oe obtained by the Thellier method under the same laboratory field as the original field of 9.8 Oe (experiment 2). The successful Thellier method yielded the intensity value of 9.77 ± 0.25 Oe which agrees well with the original field of 9.8 Oe, and this indicates that the addition law of partial TRM holds good in such strong field ranges. The experiment 2 for the TRM produced in 1.96 Oe was also very successful, and the intensity value of 2.08 ± 0.02 Oe agreeing well with the original laboratory field was obtained.

Results from TRM's produced in the weak magnetic field

Three specimens which acquired TRM's in the field intensity of 0.0196, 0.049 and 0.098 Oe were attributed to the experiment 1, and another one specimen having a TRM produced in 0.0196 Oe was attributed to the experiment 2.

Fig. 5 illustrates the NRM-TRM diagram for the TRM produced in the field of 0.0196 Oe obtained by the experiment 1.

Fig. 5. NRM-TRM diagram for the TRM produced in the weak field of 0.0196 Oe obtained by the ordinary Thellier method (experiment 1). The intensity value of 0.0230 ± 0.0015 Oe was obtained.



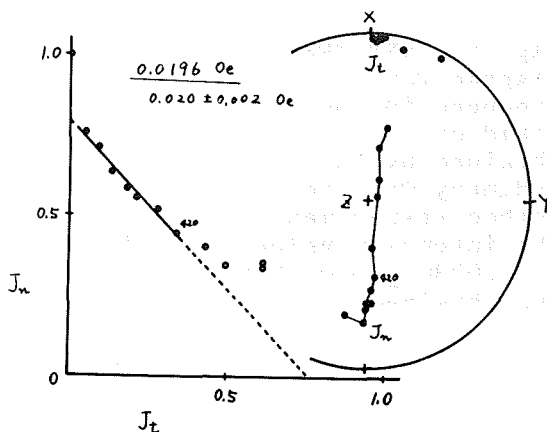
The directional movement of NRM toward the direction of the applied field at higher temperatures is perhaps caused by the production of thermo-chemical remanent magnetization (TCRM) in TRM-producing cycles (Coe et al., 1978), and it was prominent as the NRM was very small in intensity compared to the PTRM. Taking five plots that give a straight line into the linear regression analysis, the intensity value of 0.0230 ± 0.0015 Oe was obtained. This obtained intensity value is 18 percent larger than the original intensity, but considering that this paleointensity experiment is so special case, it should be concluded that pretty accurate intensity value is obtained. Another results obtained by the experiment 1 for weak TRM's are 0.067 ± 0.002 Oe for the original intensity of 0.049 Oe (obtained intensity value is 32 percent larger) and 0.102 ± 0.002 Oe for 0.098 Oe. The paleointensity value of 0.1 Oe seems to be the lower limit that can be correctly obtained by the ordinary Thellier method under the laboratory magnetic field of about 0.5 Oe.

Fig. 6 shows the NRM-TRM diagram obtained by the experiment 2 for the weak TRM produced in the field of 0.0196 Oe. The obtained intensity value of 0.020 ± 0.002 Oe is correctly concordant with the original laboratory intensity of 0.0196 Oe. This successful results of extremely weak paleointensity experiment is perhaps due to that the Thellier method was performed under the special laboratory field of 0.0196 Oe as weak as the original field intensity.

Discussion

The proportionality of TRM to an external field in weak field ranges and the additivity law of PTRM are the main two principles of the Thellier method. It is concluded that the additivity law of PTRM hold good when plots lay on a straight line in the NRM-TRM diagram. Good straight lines were obtained from all the specimen used in this study independent on the kind of the experiment, though in some cases some of the plots deviate from the straight line in low and high temperature steps, but they are probably caused by the secondary component of magnetization and the high temperature oxidation during heat treatment respectively. So, it can be concluded that the

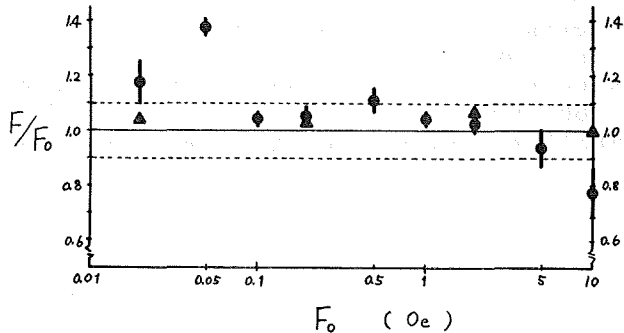
Fig. 6. NRM-TRM diagram for the TRM produced in the field of 0.0196 Oe obtained by the Thellier method under the laboratory field of 0.0196 Oe (experiment 2). The correct intensity value of 0.020 ± 0.002 Oe was obtained.



additivity law of the TRM hold good in very wide range of the intensity of TRM inducing magnetic field. It can also be concluded that the additivity law is valid independently on the existence of a strong NRM component.

The proportionality of TRM to an external field can be checked by examining the ratio of the obtained intensity value to the original laboratory field intensity. The ratios are illustrated in Fig. 7 where the abscissa is the logarithms of the original laboratory field intensity. Squares indicate results by experiment 1 and triangles those by experiment 2. If the possible maximum error in the paleointensity experiment is about 10 percent, it can be said that the Thellier method was successful in very wide range of the intensity, from 0.1 Oe to 5 Oe. The small value of the ratio of the obtained intensity value to the original intensity value in the large field of 9.8 Oe is probably caused by the difference of field dependence of TRM between in 0.5 Oe and in 9.8 Oe, because TRM intensity increases approximately as $\tanh(aH_{ex})$ where H_{ex} is the external field and a is a constant (Nagata, 1961). The cause is unknown for large values of the ratio in the weak magnetic field of 0.02 and 0.05 Oe, but perhaps it is due to both the difference of field dependence of TRM and some experimental errors.

Fig. 7. The ratios of the intensity value obtained by the Thellier method to the original laboratory field intensity. Squares and triangles indicate results by experiment 1 and experiment 2 respectively.



Conclusion

The ordinary Thellier method was applied under the laboratory field of 0.5 Oe to nine specimens of natural andesite which acquired TRM's in known laboratory fields of various intensities ranging from 0.02 to 10 Oe, and another four specimens that have also TRM's produced in various magnetic field were examined by the special Thellier method under the same laboratory field as the known original laboratory field.

All experiments were successful because plots in NRM-TRM diagram gave a straight line. This indicates that the law of additivity was always valid in all the case in this study.

All four specimens used in experiment 2 gave correct intensity values as the known original intensity values, but in the experiment 1 three of nine specimens which acquired TRM's in the fields of extremely small and large intensities

(0.02, 0.05 and 10 Oe) gave uncorrect intensity values whereas other six specimens gave correct values within the error of 10 percent. This indicates that the field dependence of TRM in the extremely weak or large field differs that in the medium field around 0.5 Oe, but it is concluded that the linearity of TRM to the external field hold good for pretty wide range of field intensity.

It is concluded that the Thellier method is reliable for wide range of paleointensity, but if extremely small or large intensity value is obtained, it is desirable to experiment again under the laboratory field of small or large intensities respectively.

References

- Coe, R.S. (1967) J. Geomag. Geoelectr., 19, 157.
Coe, R.S. and C.S. Grommé (1973) J. Geomag. Geoelectr., 25, 415.
Coe, R.S., S. Grommé and E.A. Mankinen (1978) J. Geophys. Res., 83, 1740.
Khodair, A.A. and R.S. Coe (1975) Geophys. J. Roy. Astron. Soc., 42, 107.
Kono, M. (1969) D. Sc. thesis (Univ. of Tokyo, Tokyo) p.58.
Kono, M. (1974) J. Geophys. Res., 79, 1135.
Kono, M. and H. Tanaka (1977) Phys. Earth Planet. Inter., 13, 276.
Nagata, T. (1961) Rock Magnetism, 2nd ed. (Maruzen, Tokyo) p. 195.
Nagata, T., Y. Arai and K. Momose (1963) J. Geophys. Res., 68, 5277.
Thellier, E. and O. Thellier (1959) Ann. Geophys., 15, 285.

STABILITY OF REMANENT MAGNETISM OF SCOTTISH
DEVONIAN LAVA FLOWS

Kan-ichi MOMOSE

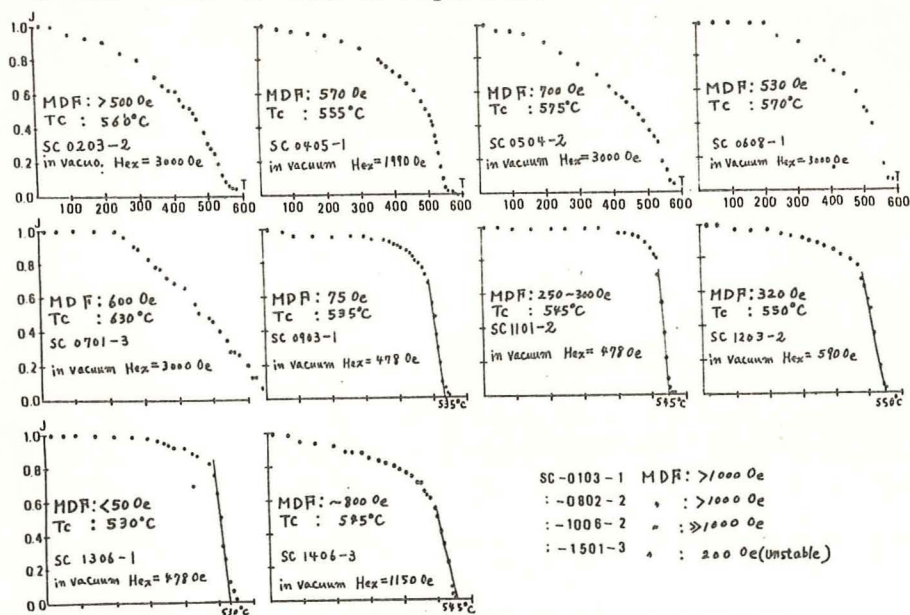
Department of Geology, Shinshu University
Asahi 3-1-1, Matsumoto 390, Japan

M. Kono (University of Tokyo) studied paleomagnetism and paleointensity of some samples from basaltic and andesitic lava flows of the Arbuthnott Group of the Devonian Lower Old Red Sandstone in Scotland.

According to his personal communication their remanent magnetisms characteristically show a high stability against the progressive Af-Demagnetization (Median Demagnetization Field : MDF value applied to some samples was above 1000 Oe) and also a much higher Blocking temperature.

For the purpose of finding the cause of this high stability, the present author made microscopic observation on polished sections and thermomagnetic analysis of respective samples from fourteen lava flows in the field occurrence and compared the results with MDF value of each sample.

(1) Magnetic moments of the samples are classified into three groups, according to the magnitude of the external field (Hex) required for this thermomagnetic analysis (See Figure 1). A-group : Hex 600 Oe : magnetic moment of this group of samples is sufficiently strong enough to be measured, B-group : Hex \approx 3000 Oe ca. : measurable, C-group : Hex $>$ 3000 Oe : even by this magnitude of the applied field, the samples are barely measured. The Figure indicates that the samples No. SC-0103-1, -0802-2, -1006-2 are classed as belonging to C-group. It also shows that the Curie temperature of every sample has a value close to that of magnetite.



Thermomagnetic curve for the Arbuthnott samples.
(The curve only indicates heating process.)

(2) Results of microscopic observation made on polished sections of those samples tell us that : titanomagnetite of the groups except that of A-group is highly oxidized having altered to very much amount of hematite. Even silicate minerals have altered partly to hematite in highly oxidized. Primary titanomagnetite grain is found to be intersected by growth of lamellar hematite, resulting in the diminution of titanomagnetite down to the fractions $3/4$ across. In C-group consisting of most intensively oxidized minerals, occurrence of (X1000) magnified through the oil immersion method.

(3) The MDF value (by Kono's measurement) is put with respect to the thermomagnetic result of each sample. As seen from the Figure the MDF values of A-group range from 50 to 300 Oe, whereas those of both B- and C-groups range from 600 to 1000 Oe.

Summarizing the results stated from (1) to (3), a good coincidence is recognized between the " Apparent intensity ", grain size of magnetic minerals, and MDF of each sample.

High stability of the NRM may be caused by the diminution of grain size due to alteration of magnetic minerals to hematite.

ON THE MAGNETIC SUSCEPTIBILITY ANISOTROPY
OF THE SAMBAGAWA SCHISTS

Takao HIRAJIMA, Yo-ichiro OTOFUJI.
and Sadao SASAJIMA

Department of Geology and Mineralogy,
University of Kyoto, 606, Kyoto, Japan.

Introduction

Many researchers have shown that for schists the minimum magnetic susceptibility axis is vertical to the schistosity plane (S-plane), and the intermediate and maximum axes lie on the S-plane; for example Graham(1954), Balsly and Buddington(1960); Khan(1962), Stone(1963), Hroud, et.al.(1971) and etc. Therefore, magnetic susceptibility anisotropy of a schist is mainly determined by its rock fabrics.

The magnetic susceptibility anisotropy of the Sambagawa schists were determined for the samples collected from the Asemi River area, Kochi Prefecture, where the thermal structure of metamorphic terrain is studied in detail by Higashino(1975). The samples examined are almost free from magnetite and pyrrhotite, then the anisotropy depends on the morphology of ferromagnesian silicates, mainly amphibole and chlorite. The susceptibility ellipsoid can be used as a measure of the morphological preferred orientation of those minerals in the schists.

Experiment

In order to quantify the magnetic susceptibility anisotropy, the spinner magnetometer (Model SSM-1A Schonstedt Instrument) was used throughout. The susceptibility can be approximated by a second rank symmetric tensor k_{ij} which linearly relates the induced magnetization component M_i to each component H_j of the induced field:

$$M_i = k_{ij} H_j \quad (1)$$

where $K = \begin{pmatrix} k_{11} & k_{12} & k_{13} \\ k_{21} & k_{22} & k_{23} \\ k_{31} & k_{32} & k_{33} \end{pmatrix}$ (2)

In using spinner magnetometer, test materials are spun around the Z axis of the instrument coordinates. The direction of induced field is parallel to the Y axis of the system. A sample is spun at three independent positions being set as shown in Fig.1, then following 6 signals, being proportional to $(k_{ii} - k_{jj})$, and the quadrature component to k_{ij} are obtained:

$$\begin{array}{ll} X_1 = H_2 k_{12} & Y_1 = H_2 (k_{22} - k_{11}) / 2 \\ X_2 = H_2 k_{13} & Y_2 = H_2 (k_{11} - k_{33}) / 2 \\ X_3 = H_2 k_{23} & Y_3 = H_2 (k_{22} - k_{33}) / 2 \end{array} \quad (3)$$

where H_2 indicates the magnitudes of induced field along Y axis, X_i and Y_i correspond to spin number.

Principally the eigenvalue of the characteristic equation can be obtained using 6 signals in equation (3), by means of Granar's method(1957). For better accuracy, measurements at the spinning position 4 and 5 (cf. Fig.1) are added to above three positions, and the characteristic equation are solved by least square method, using a program composed by Otofujii(in preparation).

To describe the shape of the susceptibility ellipsoid, a parameter, quotient(q), is defined as follow;

$$(q)=2(k_b-k_a)/3k_c \quad (4)$$

where $k_a, k_b,$ and k_c are the magnitude of the eigenvalue which correspond to the maximum, intermediate and minimum value, respectively. The value of (q), being less than 0.67, represents an oblate ellipsoid and that larger than 0.67 a prolate one.

Hitherto, to measure the magnetic susceptibility anisotropy, torque meter method is considered to give better values than spinner magnetometer method. However, for economy of time consumption, required to handle a large number of sample, the spinner magnetometer was used in this study.

The accuracy of the spinner magnetometer was checked against the torque meter described by Muroi(1974); by comparing the data obtained from the same sample by use of the two different instruments.

The parameter, M-value, determined by the following equation is used as a criterion of the accuracy of the data by spinner magnetometer;

$$M\text{-value}=(Y_1+Y_2-Y_3)/(Y_1^2+Y_2^2+Y_3^2)^{1/2} \quad (5)$$

where Y_i is described in equation(3). Ideally, M-value should be zero.

All of the test samples were fashioned into cylinder, about 2.4 cm in diameter and 2.2 cm in length, the ratio of length to diameter (L/D) being about 0.9. The cylinder axis of the test sample is vertical to the S-plane.

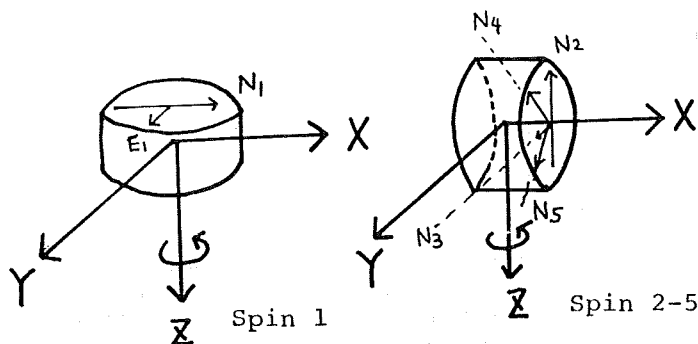


Fig.1. Schematic showing of independent 5 spinning positions. Sample position in each spin is indicated by N_i direction, respectively. N_i lies on the S-plane. X,Y, and Z axes : Instrument coordinates
 N_i, E_i : Sample coordinates

Result and Discussion

First of all, to evaluate the accuracy of the data by the spinner magnetometer, the magnetic susceptibility anisotropy of 10 cylindrical samples were measured by both torque meter and spinner magnetometer. The results are shown in Table 1 and Fig.2. When the directions of the susceptibility axes determined by two different instruments agree within 10° , the M-value ranges from 0.0 to 0.14, as shown in Table 1. Schmidt's equal area projections of the direction of the magnetic susceptibility axes are shown in Fig.2, where the primitive circle represents the S-plane of the schist. In Fig.2, the M-value of sample No.11417 is 0.13. In this sample the directions of the minimum susceptibility axes obtained by two methods are vertical to the S-plane and the intermediate and maximum axes lie on the S-plane. Moreover the direction of the maximum axis is parallel to the apparent lineation of the silicate minerals and the intermediate axis is vertical to it and is on the S-plane.

In another sample, sample No.40-1, M-value is 0.20. In this case, although the directions of the susceptibility axes measured by the torque meter are the same as those of sample No.11417, those determined by the spinner magnetometer have no systematic relation to the S-plane. Judging from this discordance of the direction of the susceptibility axes, the measurement by the spinner magnetometer may be wrong if the M-value exceeds 0.15.

As the result, it follows that the spinner magnetometer can be used to determine the direction of the susceptibility axis, if the M-value is around 0.15 or less. Thus, in the subsequent experiments, the data with the M-value larger than 0.15 were discarded.

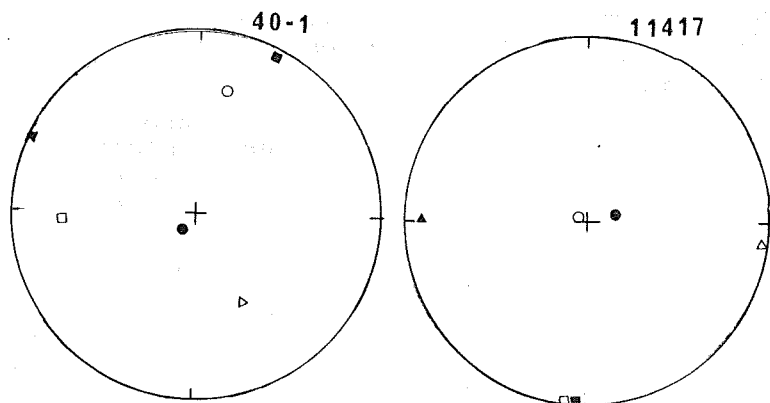


Fig.2. Variation in the direction of the susceptibility axes obtained by two instruments. Circle, triangle and square represents the direction of minimum, intermediate and maximum susceptibility axis, respectively. Open and solid symbols are obtained by the spinner magnetometer and the torque meter, respectively. The primitive represents the S-plane. The M-value of No.40-1 is larger than 0.15, that of No.11417 less than 0.15.

Table 1. Direction of the susceptibility axis, M-value, q parameter and the intensity of NRM, obtained by both the spinner magnetometer and the torque meter. D:declination, I:inclination T:data by the torque meter, S:data by the spinner magnetometer, Ka,Kb and Kc:the maximum,intermediate and minimum susceptibility axis, respectively.

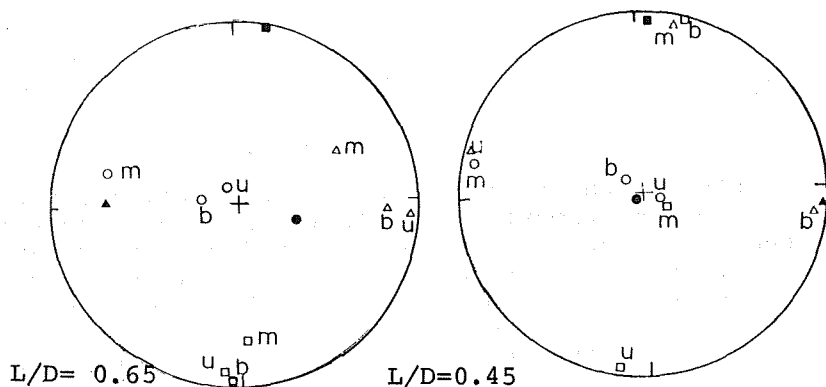
No.		Ka(D)	Ka(I)	Kb(D)	Kb(I)	Kc(D)	Kc(I)	M-value	q	N.R.M.
11420	T	170.3	3.9	80.6	-4.4	39.1	84.2		0.46	
	S	-8.1	-1.2	81.9	-0.9	20.0	88.1	0.05	0.11	4×10^{-7}
256	T	95.3	2.4	5.4	-4.1	-25.3	85.3		0.39	
	S	86.2	-6.8	-2.3	12.5	-31.9	-75.8	0.05	0.18	5×10^{-7}
41	T	185.0	0.2	95.0	-4.0	92.5	86.0		0.44	
	S	5.8	0.5	-84.3	3.7	-77.2	-86.2	0.02	0.32	4×10^{-7}
11422	T	184.2	11.3	95.8	-8.0	40.5	76.1		0.86	
	S	-68.5	63.3	0.2	-10.3	85.5	24.3	0.23	0.56	5×10^{-4}
11416	T	171.1	1.3	-99.2	-14.0	3.6	75.9		0.71	
	S	0.3	1.4	-89.9	9.8	-78.5	-82.6	0.06	0.25	2×10^{-7}
11417	T	180.2	3.2	91.0	-12.7	76.2	76.9		0.44	
	S	8.3	-1.3	-81.8	-2.6	-56.1	87.1	0.13	0.46	2×10^{-7}
40-1	T	25.1	5.4	-64.9	-0.3	208.0	84.6		0.65	
	S	86.7	-21.9	-27.3	-45.2	14.1	36.6	0.20	1.12	2×10^{-4}
11423	T	75.4	43.3	130.5	-31.3	199.4	30.7		0.36	
	S	-31.6	-49.7	20.0	27.8	-85.3	26.7	0.72	0.37	1×10^{-4}
11418	T	142.3	4.0	52.4	-1.2	-20.8	85.8		0.15	
	S	-21.2	2.0	68.7	-1.7	-62.0	-87.4	0.04	0.14	8×10^{-7}
11412	T	-1.1	0.2	88.8	-8.3	90.2	81.7		0.29	
	S	7.5	2.6	-82.5	-0.0	8.5	-87.4	0.00	0.21	1×10^{-7}

Fig.3. Variation on the susceptibility axes and on the q parameter, obtained by both the spinner magnetometer and the torque meter. The same sample was set at different 3 positions in the sample holder of the spinner magnetometer.

SOLID SYMBOL: TORQUE METER
 OPEN " : SPINNER

u : upper position of sample holder
 m : middle
 b : bottom

L/D	quotient		
	upper	middle	bottom
0.65	0.59	0.42	0.29
0.45	0.57	0.42	0.58



Kent(1975) demonstrated by changing the (L/D) ratio of the test samples from 1.25 to 0.50 that the axes of the magnetic susceptibility anisotropy and q'-value ($q'=2(k_a-k_b)/(k_a+k_b-2k_c)$ in his paper) changed for 90° and from 0.0 to 1.5, respectively. Therefore, we must test this problem. The relationship between the q parameter and (L/D) ratio which we have obtained, are shown in Fig.3 and 4. Certainly, the q parameter depends on the (L/D) ratio. Further, as shown in Fig.3, the q parameter and the directions of the magnetic susceptibility axes are also different at the different positions in the sample holder of the spinner magnetometer. However, if we set the test samples at the top or bottom position in the sample holder, the direction of the susceptibility axes obtained by the spinner magnetometer agree well with those obtained by the torque meter. In our experiments, therefore, the samples were set at the bottom position of the sample holder so that the direction of the susceptibility axis obtained by the spinner magnetometer can be used in geological discussion.

Fig.4. Variation on the susceptibility anisotropy with length to diameter ratio of cylindrical specimen obtained by two different instruments.

	L/D	Spinner	Torque
		open symbol quotient	solid symbol quotient
1	0.90	0.5781	1.0029
2	0.65	0.5848	1.2253
3	0.45	0.2871	1.3033

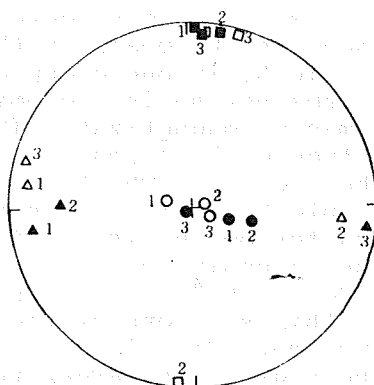
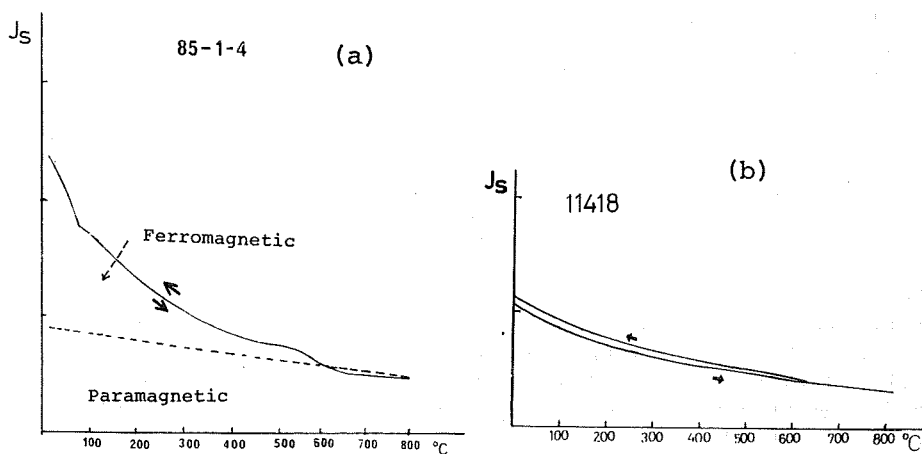


Fig.5. Thermo-magnetic curve. A unit of the longitude is arbitrary. (a) No.85-1-4 belongs to P-F group. (b) No.11418 belongs to P group.



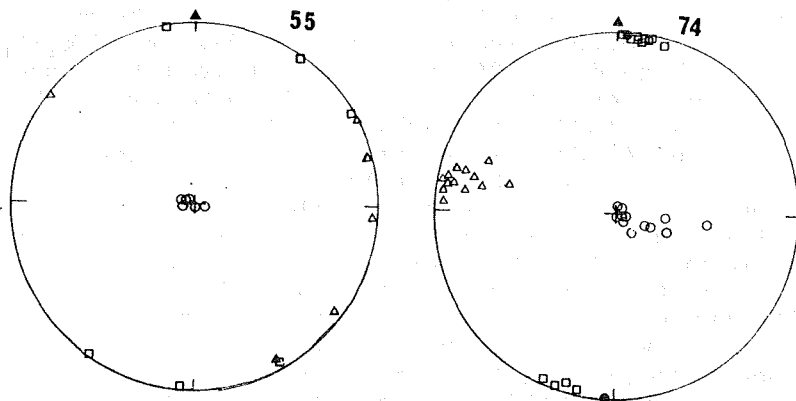


Fig.6. Orientation of the susceptibility axes. The q parameter of No.55 and No.74 is 0.08 and 0.51, respectively.

Next, we must determine the minerals responsible for the magnetism by means of the thermo-magnetic analysis. As shown in Fig.5, in one group of samples, for example sample No.11418, paramagnetism is predominant, and the intensity of the natural remanent magnetization (NRM) is very small, in the order of magnitude of 10^{-7} emu/gr (cf. Table 1). This group will be called the P group. The test materials of another group, for example sample No.85-1-4, possess the properties of both paramagnetism and ferromagnetism. This group will be called the P-F group. The intensity of NRM of the P-F group, in the order of magnitude of 10^{-4} emu/gr, is stronger than the P group. Observation of thin sections of the P-F group of samples indicates that the much more Fe-oxides are included. Moreover, the M-value of the P group is larger than 0.15.

Therefore the magnetic susceptibility anisotropy owes to that of the ferromagnesian silicates such as amphibole and chlorite, and so the susceptibility ellipsoid is related to the morphology of the ferromagnesian silicates.

The test specimens which are cut from 20 blocks of the Sambagawa schists, collected from the different localities, satisfy the aboved conditions, and all of them have a common feature that the minimum susceptibility axis is vertical to and the intermediate and maximum axes lie on the S-plane.

As shown in Fig.6, if the q parameter obtained by the spinner magnetometer is larger than 0.5, the maximum susceptibility axis is parallel to the apparent lineation of silicate minerals, and the intermediate susceptibility axis is vertical to it. If the q parameter is less than 0.30, these two axes scatter on the S-plane, even if the clear lineation exists. Some of the test materials which have small q parameter contain a large amount of chlorite. The amphibole has a needle shape, but chlorite is platy, moreover the basal plane of chlorite tend to be parallel to the S-plane. Therefore one of factors which affects the q parameter is the amount of chlorite, even though the abundance of chlorite alone can not explain all of the samples with scattering axes, and we must await further investigation on this problem.

Reference

Balsley, J.R. and Buddington, A.F., (1960) Amer. J. Sci., Vol. 258-A, p.6,
Fuller, M.D., (1960) Nature, Vol. 186, p.790,
Graham, J.W., (1954) Geol. Soc. Am. Bull., Vol. 165, p.1257,
Granar, L., (1957) Ark. Geof., Band. 3, p.1,
Higashino, T., (1975) J. Geol. Soc. Japan, Vol. 81, p.653,
Ising, G., (1942) Ark. Mat. Astr. Phys., Band. 29-A, p.1,
Kent, D., (1975) Earth Planet. Sci. Lett., Vol. 28, p.1,
Khan, M.A., (1962) J. Geophys. Res., Vol. 67, p.2873,
Muroi, I., (1974) Research note of 'Antei So-ken', No. 1, p.22,
Nagata, T., (1961) Rock Magnetism. 2nd ed. (Maruzen Tokyo) p.75,
Stone, D.B., (1963) Geophy. J. Roy. astr. Soc., Vol. 7, p.375,
Yasukawa, K., (1957) Master thesis of Kyoto University,

ERROR ANGLES WITHIN A SPECIMEN

Isao MUROI

Department of Earth Science, Science Education Institute
of Osaka Prefecture, Osaka 558

1. Introduction

NRM (Natural Remanent Magnetization) of a specimen is generally measured as magnetically uniform (or homogeneous) and its magnetic factors (Declination, Inclination and Intensity) are calculated usually. Nagata (1931) ascertained that the magnetization of igneous rocks from Mt. Amagi and Mt. Usami, Izu Peninsula was uniform.

In fact, it seems that the magnetization of a specimen from some volcanic rocks is not so magnetically uniform as our suppose. Because the magnetic curves from an astatic magnetometer with a recording system (Muroi, 1968) sometimes do not show sinusoidal shape and suggest us that the specimen will be not uniform. The reason why the specimen does not have uniform magnetization, is not so simple and not fully clarified yet. It is shown that the systematic errors due to such inhomogeneity can be averaged out by a suitable procedure of measurement (Creer, 1967).

Roy and Fahrig (1973) used an index meaning a qualitative measure of within-specimen uniformity of magnetic direction.

In this paper, a method that the author tried to calculate an error angle of the within-specimen from the magnetic direction measured by the same astatic magnetometer as above mentioned is described.

2. Measurement of NRM

NRM is measured as follows. A cubic specimen with 2.5 cm in each length is located on a sample stage under the lower magnet and rotated around the vertical axis by a belt driven with a synchronous motor situated at 2 m from the stage. It takes 2 minutes per revolution. Before measuring, six alphabets N, S, E, W, U and D are written on each surface of the cubic specimen.

We assign orthogonal axes x , y and z to the specimen so that z is the vertical axis. x and y are horizontal ones. x is magnetic north and y , magnetic east as shown in Fig. 1.

The specimen takes six positions. On each position of them, the specimen is rotated on

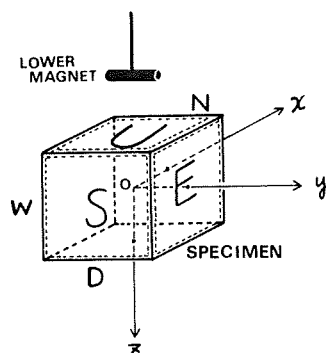


Fig. 1 Specimen in coordinate system under the lower magnet of an astatic magnetometer.

a 0°- 360° circle and is reversely repeated, in upright set. After that, the specimen is inverted and rotated as above. This is similar to the double-spin procedure which is usually carried with a spinner magnetometer (Doell and Cox, 1967).

Output signal in proportion to the deflection is recorded on a chart. Twelve readings are obtained at intervals of 30° in rotation angle from the record, though the record is read from the end of the same curve, when the rotation is reversed. The first order values from these readings are calculated by Fourier analysis. Maximum amplitude showing the magnetic north of the surface of the specimen and phase angle corresponding to the amplitude are obtained. Here is treated the phase angle only. As the two values of the angle are measured by normal and reverse rotation in a surface of the specimen, mean value of the angles is usually used.

Six angles showing each north-seeking direction on each surface of the specimen are obtained from 12 measurements in all. These angles are $\alpha_U, \alpha_D, \beta_S, \beta_N, \gamma_W$ and γ_E . In these symbols, suffix U, D, S, N, W and E mean the nearest surface to the lower magnet of the astatic magnetometer. And from these angles, mean angles α, β and γ between opposite surfaces of the specimen are finally calculated as follows:

$$\alpha = \frac{\alpha_U + \alpha_D}{2}, \quad \beta = \frac{\beta_S + \beta_N}{2}, \quad \gamma = \frac{\gamma_W + \gamma_E}{2} \quad (1)$$

3. NRM direction of a specimen

Magnetic direction (D:Declination and I:Inclination) is calculated from α, β and γ as mentioned above. A graphical technique for obtaining the magnetic direction using stereographic projection is as follows (Graham, 1949; Doell and Cox, 1965; Doell and Cox, 1967). The planes defined by α, β and γ are drawn as great circles on the projection. They usually intersect to form a small error triangle, and the size of this triangle is commonly used as a measure of the precision of the measurement. Its center, defined by the angles D and I, is commonly used as the best estimate of the magnetic direction as shown in Fig. 2.

To find the magnetic direction D and I corresponding to the original orientation of the specimen, the points that three lines drawn from α, β and γ , intersect mutually must be calculated in the projection.

There are four cases that numbers of the intersecting point are 3, 2, 1 and 0. And there are eight quadrants, that is, four quadrants in upper hemisphere and lower one respectively, in this projection net.

Therefore, combinations α, β and γ with these quadrants are 144 in all. 32 cases of them are used here.

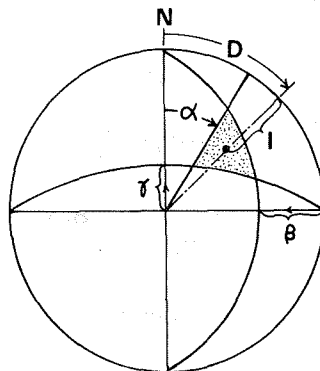


Fig. 2 NRM direction from α, β and γ in a stereographic net.

A definition of the intersecting points ①, ②, and ③ is given: ① intersects with α and β . ②, with β and γ . ③, with γ and α . This definition does not change whichever the quadrant to which the points belong is upper hemisphere or lower one of the projection. These points $D_i, I_i, (i=1,2,3)$ may be written:

$$\textcircled{1} \begin{cases} D_1 = \alpha \\ \tan I_1 = \tan \beta \cdot \sin D_1 \end{cases} \quad (2-1)$$

$$\textcircled{2} \begin{cases} \tan D_2 = \frac{1}{\tan \beta \cdot \tan \gamma} \quad (\beta, \gamma \neq 0^\circ, 180^\circ) \\ \tan I_2 = \tan \beta \cdot \sin D_2 \end{cases} \quad (2-2)$$

$$\textcircled{3} \begin{cases} D_3 = \alpha \\ \tan I_3 = \tan(90^\circ - \gamma) \cdot \cos D_3 \quad (0^\circ < \gamma \leq 180^\circ) \\ \tan I_3 = \tan(270^\circ - \gamma) \cdot \cos D_3 \quad (180^\circ < \gamma \leq 360^\circ) \end{cases} \quad (2-3)$$

where D_2 is corrected to $D_2 + 180^\circ$ when the point belongs to the 2nd and 3rd quadrants, and $D_2 + 360^\circ$ to the 4th quadrant in the projection.

In order to calculate a resultant direction D_0 and I_0 , vector sum of each value of the 3 intersecting points ($D_i, I_i; i=1,2,3$) is given:

$$x = \sum_{i=1}^3 \cos I_i \cdot \cos D_i \quad (3-1)$$

$$y = \sum_{i=1}^3 \cos I_i \cdot \sin D_i \quad (3-2)$$

$$z = \sum_{i=1}^3 \sin I_i \quad (3-3)$$

$$r = \sqrt{x^2 + y^2 + z^2} \quad (4)$$

Hence, the resultant direction, that is, magnetic mean direction of a specimen, D_0 and I_0 is written:

$$\tan D_0 = \frac{y}{x} \quad (5-1)$$

$$\sin I_0 = \frac{z}{r} \quad (5-2)$$

Error angle δ_0 of confidence of 95 % (Fisher, 1953) of a specimen may be also used as $N=3$:

$$\cos \delta_0 = 1 - 3.4721 \left(\frac{3 - r}{r} \right) \quad (6)$$

Precision parameter K_0 of a specimen, if necessary, is given:

$$K_0 = \frac{2}{3 - r} \quad (7)$$

4. Error angles of a specimen

From (1), difference angles between mutual opposit surfaces of a specimen are given:

$$\Delta\alpha_1 = \alpha_U - \alpha_D, \quad \Delta\beta_1 = \beta_S - \beta_N, \quad \Delta\gamma_1 = \gamma_W - \gamma_E \quad (8)$$

Then, error angle δ_1 , which is rather external, is written:

$$\delta_1 = \left\{ \frac{\Delta\alpha_1^2 + \Delta\beta_1^2 + \Delta\gamma_1^2}{3} \right\}^{1/2} \quad (9)$$

On the other hand, 3 angles α_0 , β_0 and γ_0 corresponding to the mean direction (D., I.) are expressed as follows:

$$\alpha_0 = D_0 \quad (10-1)$$

$$\tan\beta_0 = \frac{\tan I_0}{\sin D_0} \quad (10-2)$$

$$\tan\gamma_0 = \frac{\cos D_0}{\tan I_0} \quad (10-3)$$

where α_0 , β_0 and γ_0 must be corrected as the case may be.

Difference angles between observed values α , β , γ and calculated ones α_0 , β_0 , γ_0 are written:

$$\Delta\alpha_2 = |\alpha - \alpha_0|, \quad \Delta\beta_2 = |\beta - \beta_0|, \quad \Delta\gamma_2 = |\gamma - \gamma_0| \quad (11)$$

Then, error angle δ_2 , which is rather internal, is written:

$$\delta_2 = \Delta\alpha_2 + \Delta\beta_2 + \Delta\gamma_2 \quad (12)$$

After all, the total error angle ΔD within a specimen from (9) and (12) may be given by

$$\Delta D = \delta_1 + \delta_2 \quad (13)$$

In (13), error angle δ_2 is used instead of δ_0 as internal error angle, because the error angle δ_0 in (6) is equal to or more than δ_2 and sometimes dispers.

The relation of these angles in the stereographic projection is shown in Fig.3.

Some examples of δ_1 and δ_2 are shown in Fig. 4. In this figure, it is not clear whether these error angles are systematic or not.

This study must be continued by using more specimens in future.

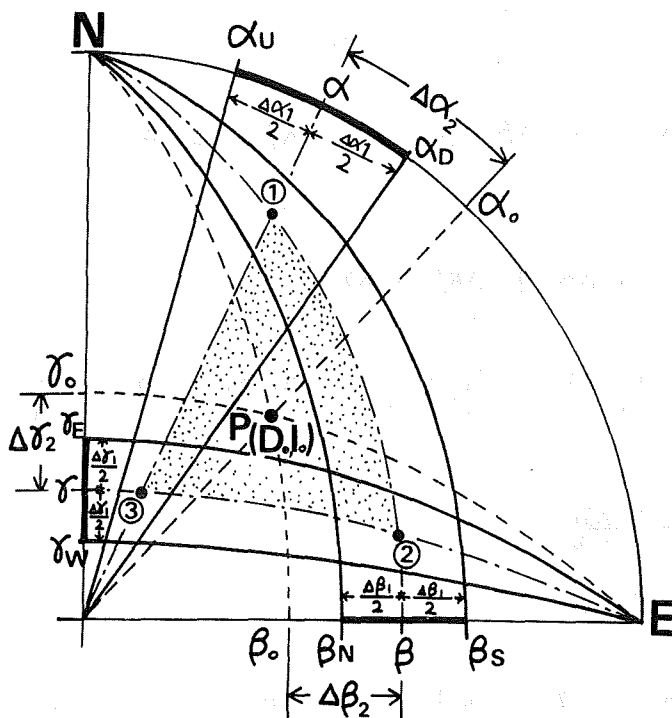


Fig. 3 NRM direction $P(D_o, I_o)$ and error angles from α , β and γ in a stereographic net (downward). Further explanation appears in the text.

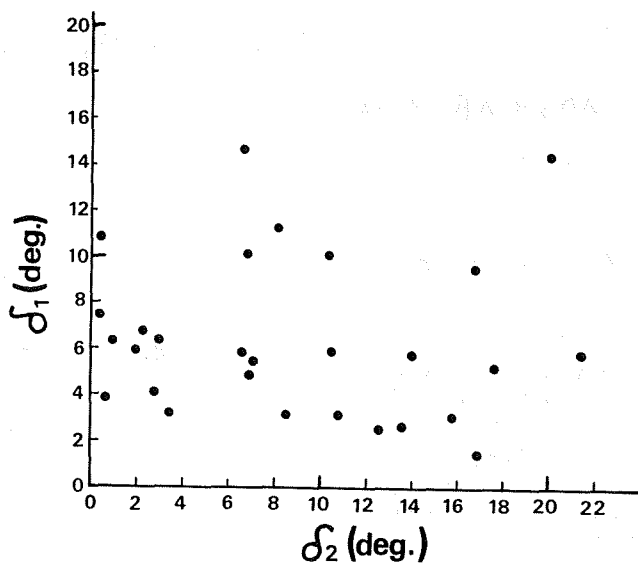


Fig. 4 External error angle δ_1 versus internal error angle δ_2 for specimens of volcanic rocks. The two are independent of each other.

References

- Creer, K. M. (1967) Methods in Palaeomagnetism, (Elsevier, Amsterdam) P.172.
- Doell, R. R. and A. Cox (1965) U.S., Geol. Surv., Bull., 1203-A:1.
- Doell, R. R. and A. Cox (1967) Methods in Palaeomagnetism (Elsevier, Amsterdam) P.196.
- Fisher, R. A. (1953) Roy. Soc. London Proc., ser. A, 217, 295.
- Graham, J. W. (1949) J. Geophys. Res., 54, 131.
- Muroi, I. (1968) 1968 Annual Prog. Rep. Paleogeophysical Res. in Japan, 73.
- Nagata, T. (1931) Zisin, 13, 8.240.
- Roy, J. L. and W. F. Fahrig (1973) Can. J. Earth Sci., 10, 1279.
- Runcorn, S. K. (1967) Methods in Palaeomagnetism (Elsevier, Amsterdam) P.163.

A NOTE ON THE NRM MEASUREMENT BY MEANS OF
A SPINNER MAGNETOMETER.

Haruo DOMEN

Institute of Physical Sciences,
Faculty of Education, Yamaguchi University,
1677-1 Yoshida, Yamaguchi 753, Japan.

As has been well known, the measuring procedure of the remanent magnetization of rocks by means of a spinner magnetometer is such a way that the test specimen feebly magnetized is put inside of the coil and revolved under the constant speed and the e.m.f. produced is picked up and amplified. With the specimen spinning about an axis; say Z-axis of the sample's coordinate system, other two components along with the X- and Y-axes of the sample are simultaneously measured.

In this report, the present author compared the NRM components obtained by means of the spinner magnetometer; Schonstedt's SSM-1A, with the variety of the spinning axes and also with the data obtained by an astatic magnetometer (the present author's hand made, Domen 1965).

Fig. 1 shows the variation of the spin holding of test specimens with several combinations of the different rotation axes of specimen's coordinate system. Figures 2 and 3 show two examples of the data sheets of measuring for the 6- and 24-spin holding respectively.

Rotation axis faced Sensor	Components of sample's NRM	Configurations
1) + X (N)	+Y (E), -Z (V)	
2) + Y (E)	+Z , -X	
3) + Z (V)	+X , -Y	

Fig. 1-1. 3 spin holding.

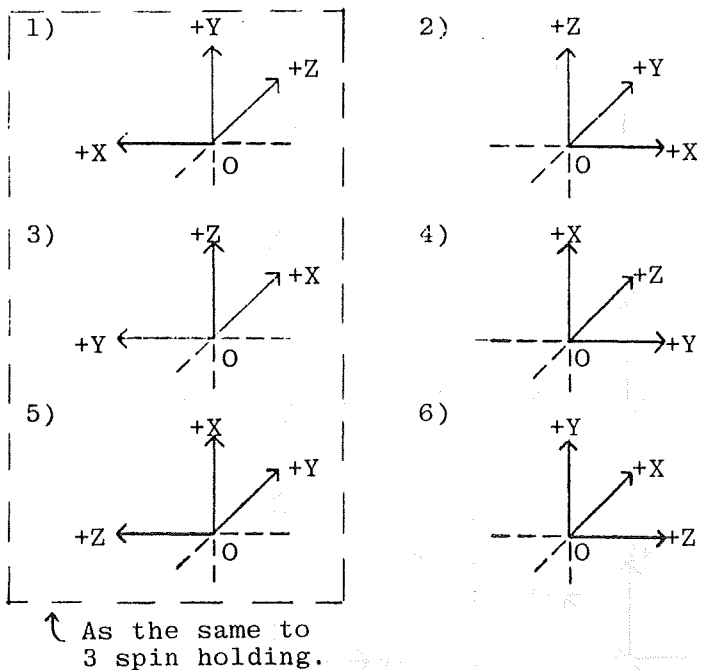


Fig. 1-2. 6 spin holding. Notations for the spin axes and measurable components are the same to those in Fig. 1-1. In following figures (Figs. 1-3, -4) are as well.

Table 1. NRM data obtained by means of spinner magnetometer with the various spin holdings and of astatic magnetometer.

1) Sample; Columbia River Tertiary basalt:
DA-1(Reversed)

"Spinner"

N@	Vector components			I#	NRM Directions	
	+X (N)	+Y (E)	+Z (V)		D(E)	I(D)
3	-0.575	-0.235	-0.615	0.874	-157.8°	-44.7°
6	-0.585	-0.235	-0.613	0.879	-158.1	-44.2
12	-0.584	-0.234	-0.611	0.877	-158.2	-44.4
24	-0.578	-0.233	-0.611	0.872	-158.1	-44.4
"Astatic"				1963*	-162	-35
				1978	-158.8	-43.8

(to be contd.)

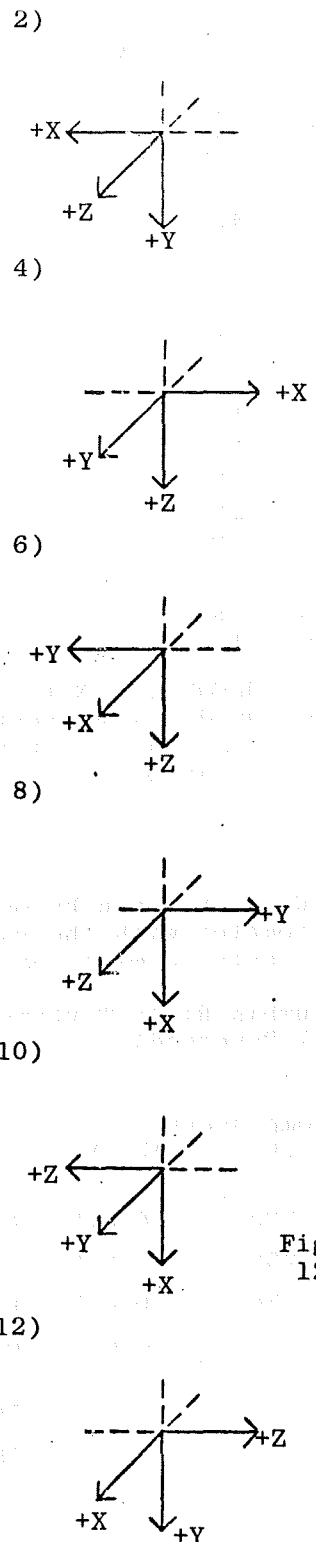
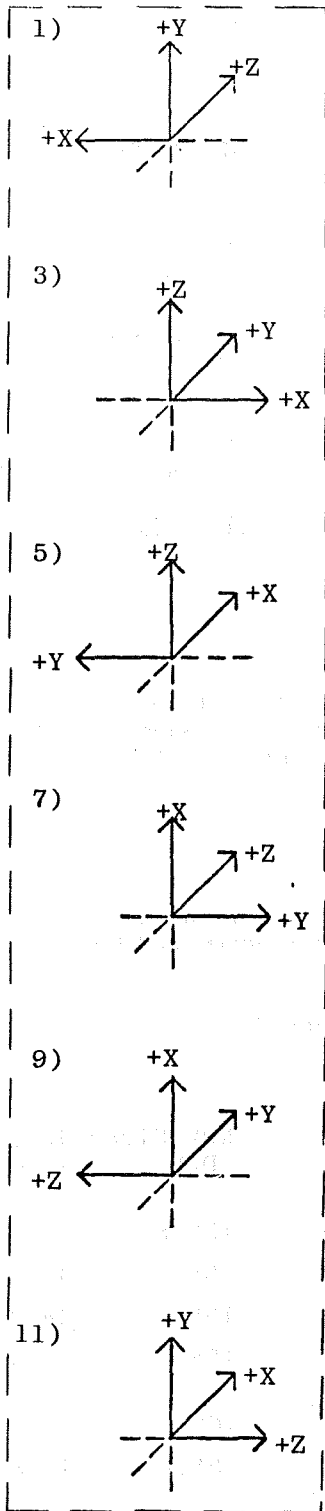


Fig. 1-3.
12 spin holding.

↑ Same to 6 spin

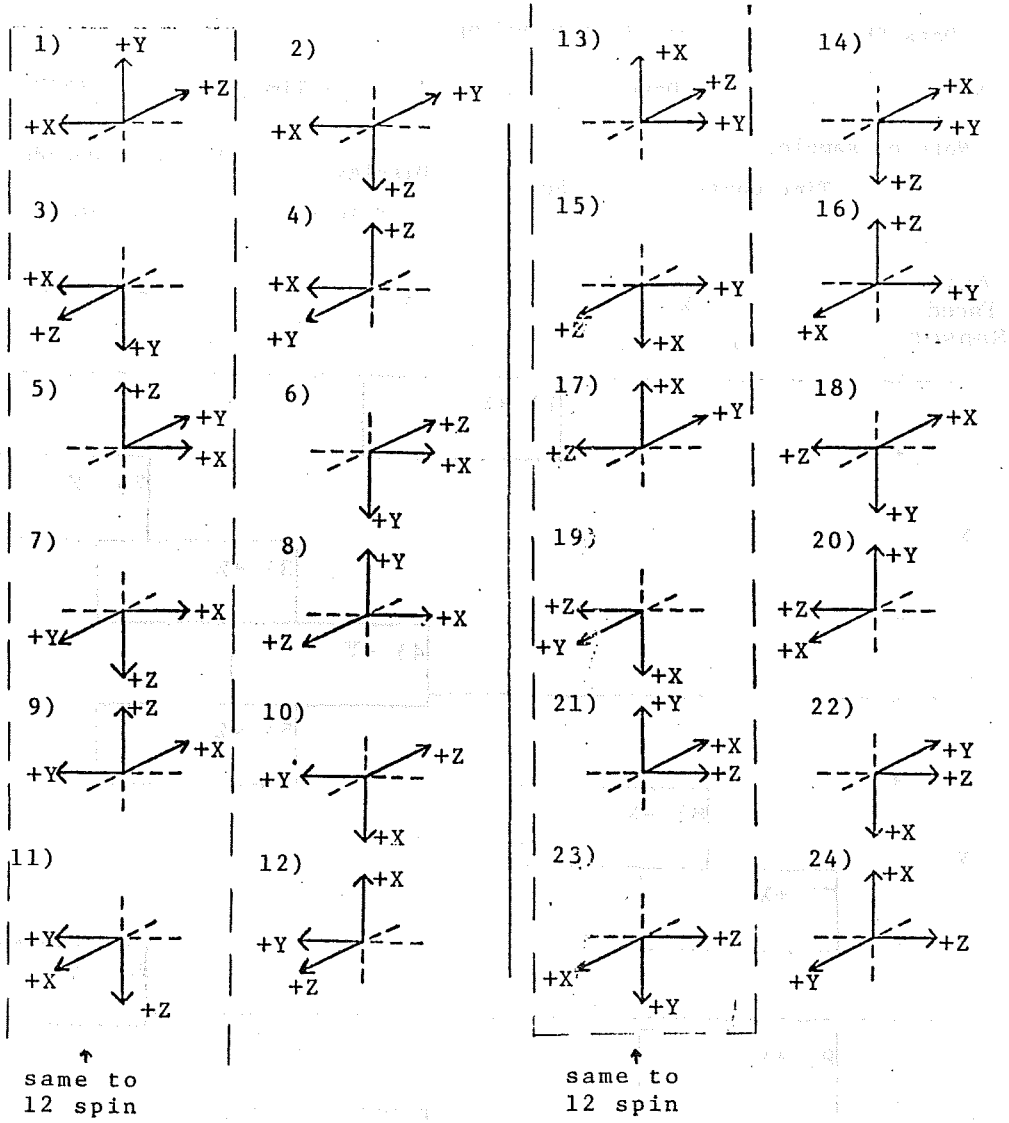


Fig. 1-4. 24 spin holding.

Data Sheet ----- 24 spin holding.

No. _____ Date; _____ / _____ / _____ / Time; _____ AM/PM

Note on sample;

Time Const. _____ Sec. Display _____ Multi. _____ Decade _____
 × 10⁻ _____ × 10⁻ _____

Axis Faced Sensor	X		Y		Z	
	+	-	+	-	+	-
1 +			1			2
2 +				2		1
3 +				1	2	
4 +			2		1	
5 X +				2	1	
6 -				1		2
7 -			2			1
8 -			1		2	
9 +	2				1	
10 +		1				2
1 +	2					1
2 +	1				2	
3 Y -	1					2
4 -		2				1
5 -		1			2	
6 -	2				1	
7 +	1			2		
8 +		2		1		
9 +		1	2			
20 +	2		1			
1 Z -		2	1			
2 -		1		2		
3 -	2			1		
4 -	1		2			
Total						
Mean × 10 ⁻						

Fig. 3. An example of data sheet for the 24 spin holding.

Table 1 (contd.)

2) Sample; same to 1) DA-11(Normal)						
"Spinner"						
@				#		
3	+1.410	+0.680	+0.640	1.691	+25.7	+22.2
6	+1.480	+0.748	+0.670	1.788	+26.8	+22.0
12	+1.486	+0.743	+0.654	1.785	+26.5	+21.5
"Astatic"				1963*	+20	+20
				1978	+25.7	+22.6

@: Mode of "Spin Holding", #: Total vector,
*: Year made measurements. 1963 measurements were done at Geophysics Laboratory, University of Toronto by means of "astatic" made by the present author.

For this examination, the test specimens have been selected from a stock of the Tertiary basalts come from the Columbia River Plateau, Washington, U. S. A., which were mostly submitted to the present author by Professor C. D. Campbell of Washington State University in 1961-63 (Domen 1963, 1965, 1966) and some of those were collected in the summer of 1965 by the present author by himself (Domen & Muneoka 1977).

Two examples of the obtained data are shown in Table 1, from which as has been known, any choice of the varieties of the spin holding gives about the same informations on the NRM of samples as the measurements are performed by means of the spinner magnetometer and also the data obtained by "astatic" are not so much deviated from those from "spinner".

References.

- Domen, H. (1963), A part of "Final Report on NSF Res. Grant G-4643 submitted by C. D. Campbell.
Domen, H. (1965), Bull. Fac. Educ., Yamaguchi Univ., 14, 35.
Domen, H. (1966), *ibid.* 15, 9.
Domen, H. & H. Muneoka (1977), Rock Mag. Paleogeophys., 4, 114.

A PRELIMINARY REPORT ON A PALEO/ROCK MAGNETIC STUDY
OF HOLOCENE BASALT AT KASA-YAMA, YAMAGUCHI PREFECTURE
WEST JAPAN.

Haruo DOMEN

Institute of Physical Sciences,
Faculty of Education, Yamaguchi University,
1677-1 Yoshida, Yamaguchi 753, Japan.

One quarter of a century has gone since the present author made the first sampling and measurements of the NRM and of some other magnetic properties on the Holocene calc-alkali basalts come from Kasa-Yama (Kasa-no-Yama), on the coast of the Sea of Japan, at the east end of Hagi City, Yamaguchi Prefecture, west Japan. The Mt. Kasa-Yama is an Aspite overlain Tholoide with the small crater (an extinct), which is well known as the smallest (?) all over the world. And it has an altitude of only ca.100 m.

In this spring (May 1978), the present author attacked these basalt flows and collected several rock samples at the top part of the Aspite. Five chunks were drilled out from one sample of 10×10×20 cm of the size and each drilled chunks were cut into two or three plugs as the test specimen which has about 25 mm with diameter and the same size in height for the NRM measurements; performed by means of both an astatic and a spinner magnetometers. The former magnetometer is a hand made by the present author himself (Domen 1965) and the latter is a commercial one; Schonstedt's SSM-1A, which has newly been introduced to the Domen's laboratory on this March by the special financial aid from the Ministry of Education, Japan.

Table 1. Mean NRM directions of Kasa-Yama basalt
by means of both astatic and spinner.

1987 (this study)		"Aspite"					
Magnetometer	N	D(E)* ± S.D.	I(D) ± S.D.	K	α _{95%}		
Astatic	14 [†]	-8.7° ± 7.5°	+54.1° ± 4.4°	84	4°		
Spinner	19 [†]	-8.2 13.5	+51.7 8.4	84	8		
1960 (see Ref., Domen 1960, 1965)		"Aspite"					
Astatic	20 [§]	-38.6 18.7	+63.4 8.4	16	8		
Sampling sites of these samples are differ from 1978.							
1960 (")		"Tholoide (Crater)"					
Astatic	9 [§]	-15.8 16.0	+64.5 6.9	45	7		

* Declination from the astronomical north,
† Numbers of test specimens,
§ Numbers of samples.

The obtained data on the NRM of these samples submitted are entered in Table 1 together with the previous data (Domen 1960, 1965). However specimens submitted to the "spinner" are a few more than those to "astatic", the mean direction of NRM obtained by means of "astatic" shows smaller standard deviation and also has one half of $\alpha_{95\%}$ compared with that of "spinner" in spite of the same order of K-values from both measurements.

Other samples now have been submitting to the paleomagnetic measurements. On the other hand, the following items of experiments are undertaken; thermo-magnetic analysis, Af-demagnetization, also thermal and chemical (Domen 1967) demagnetizations. X-ray analysis on those ferromagnetic rock forming minerals extracted from these samples is going to be performed. And those will be submitted to an electron probe micro analyzer in the near future.

References.

- Domen, H. (1960), Bull. Fac. Educ., Yamaguchi Univ., 9, 31.
" (1965), J. G. R., 70(2), 425.
" (1967), Bull. Fac. Educ., Yamaguchi Univ., 16, 25.

PALEOMAGNETISM OF KOMYOIKE VOLCANIC ASH HORIZON SEDIMENTS IN OSAKA GROUP

Kazuaki MAENAKA

Faculty of Literature, Hanazono College, Tsubonouchi, Nakagyo, Kyoto 604

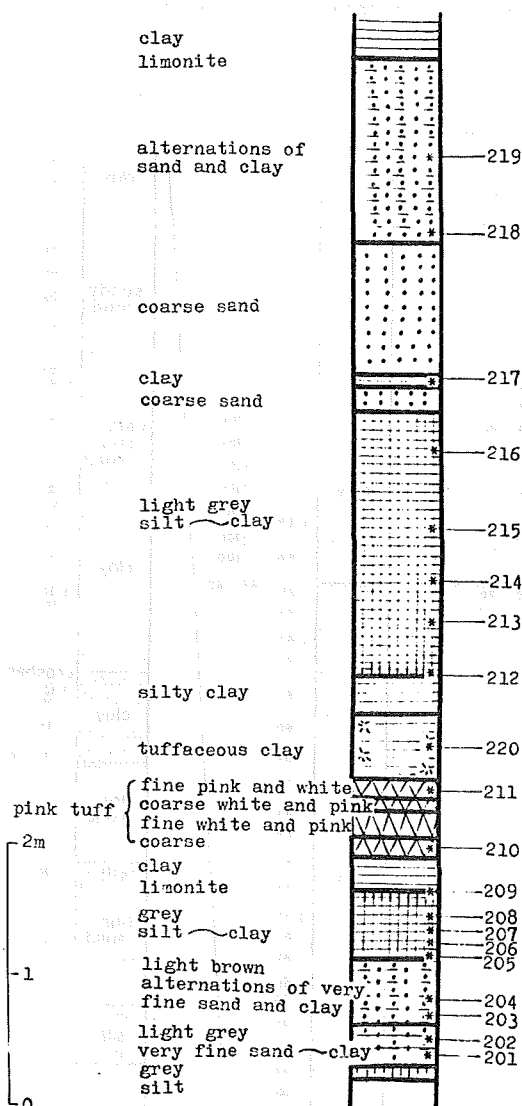


Fig. 1. Stratigraphic column of Pink horizon sediments.

Osaka Group, one of the most typical Plio-Pleistocene Series in Japan, is composed of unconsolidated gravels, sands, silt and clay beds of limnic, fluvial and marine origin with many volcanic ash layers (Ithara et al., 1975). The upper half of the Osaka Group consists of alternations of marine and non-marine sediments. Most of the marine facies are represented by enclosed specified pyroclastic layers: Ma 0 through Ma 13 in ascending order. A magnetostratigraphic approach has contributed substantially to the dating of the numerous fossils described from the Group. The writer with his collaborators presented a paleomagnetic stratigraphy on the water-laid volcanic ash layers intercalated in the sediments (Ishida et al., 1969, Maenaka et al., 1977). It was found that the deposits were formed during the Brunhes Normal, the Matuyama Reversed, and the Gauss Normal Epochs. The continuous record of past changes of the geomagnetic field by measurement of the weak remanent magnetization such as lacustrine and marine sediments became possible by using a spinner magnetometer. In the present paper, the preliminary result of the paleomagnetic study on the sediments around the Komyoike volcanic ash horizon in Osaka Group are reported.

Komyoike volcanic ash layer is imbedded in the interval between Pink volcanic ash bed and Ma 2 bed, and intermittently distributed only in Senpoku area, southern part of Osaka Prefecture. The paleomagnetic polarity of the Komyoike ash is normal, and the fission track age is 1.1 million years old (Nishimura and Sasajima, 1970). This age is considered to be a reasonable age basing on the geological grounds. The writer (1975) suggested the

the possibility of the existence of unknown event in the Matuyama age. With cooperation of Ishida, Yokoyama and others, more than one hundred oriented samples were collected successively from out-crop sediments at east of Mikita, Izumi City. The uppermost horizon of the exposure is Ma 2, and the lowermost horizon of the exposurer is alternations of sand and clay below the Pink ash. The stratigraphic succession of the collected samples are shown in Figures 1 and 2. Several adjacent cubes (one inch cubic) were prepared from each sample with a band saw of non-magnetic material. The remanent magnetizations of the prepared specimens were measured by a spinner

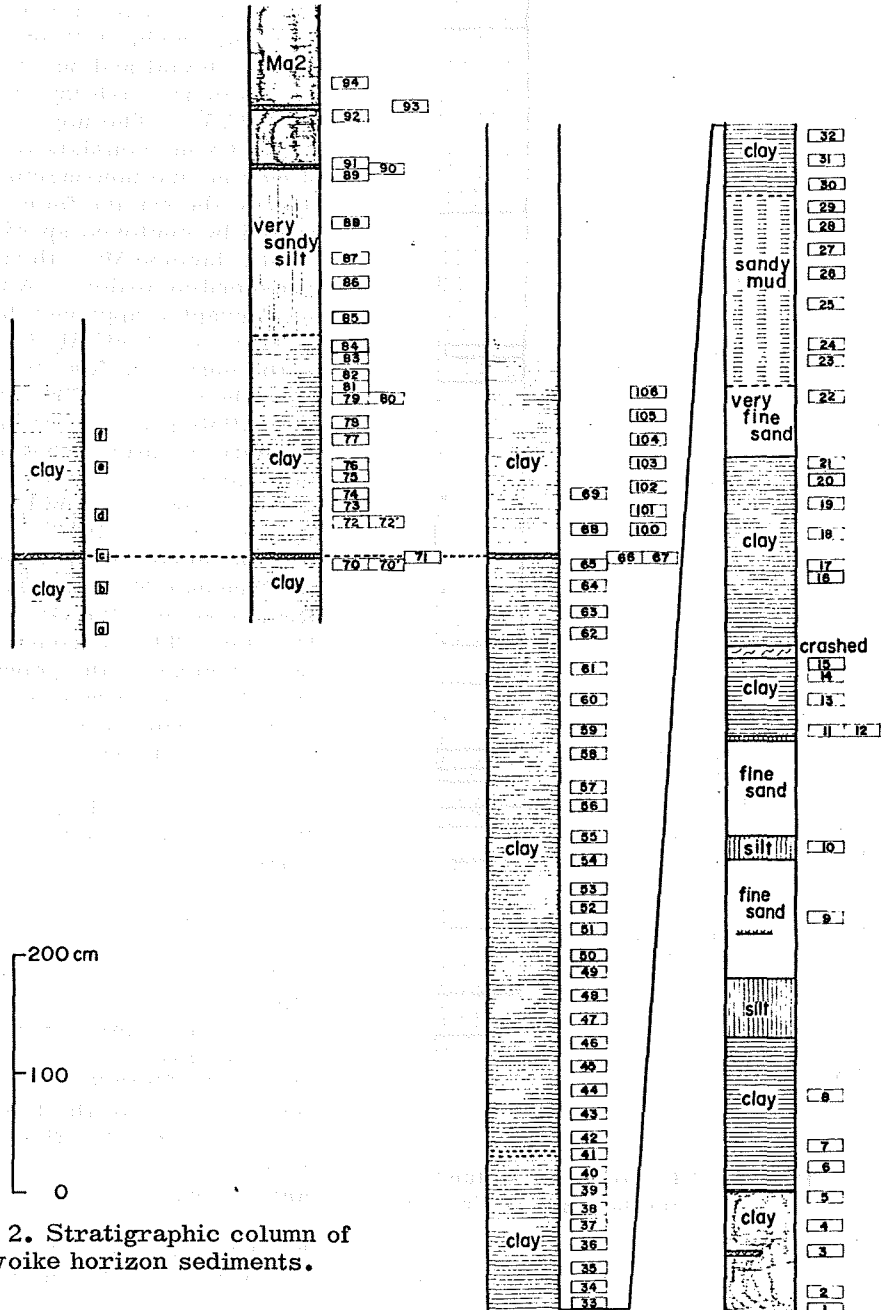


Fig. 2. Stratigraphic column of Komyoike horizon sediments.

magnetometer at Kyoto University. From the result of the preliminary test using a pilot specimen, all specimens were demagnetized in an alternating peak field of 100 oersteds, by means of an instrument equipped with a three axis tumbler. Paleomagnetic results after magnetic cleaning for the relevant sedimentary sequence, which afford a continuous record of the geomagnetic directional change, are summarized in Tables 1 and 2. As given in Table 1, the concentration of the remanent magnetization of the sediments obtained from the Pink horizon is rather good and all samples have normal polarity.

Table 1. Paleomagnetic data after magnetic cleaning for Pink horizon sediments.

Sample Number	Number of Specimens	Mean Direction			Virtual Pole Position		
		Decli.	Incli.	k	Lat.	Long.	
219	10	19.7 E	68.8	19	67.4 N	168.0 E	
218	6	29.7 E	40.2	18	61.6 N	119.3 W	
217	10	21.7 W	78.2	4	54.9 N	121.1 E	
216	7	13.9 E	54.2	25	78.5 N	128.5 W	
215	5	22.9 E	48.4	10	69.9 N	125.9 W	
214	4	0.4 W	63.5	17	79.4 N	134.0 E	
213	4	27.6 E	23.7	93	56.6 N	99.8 W	
212	3	2.5 W	36.9	18	75.9 N	34.8 W	
209	6	13.9 E	45.0	42	75.7 N	104.7 W	
208	5	11.7 E	52.0	36	74.3 N	88.3 W	
207	6	8.8 E	47.3	72	80.4 N	98.3 W	
206	5	14.1 E	45.7	12	75.8 N	101.7 W	
205	6	3.8 W	39.1	10	77.2 N	27.8 W	
204	5	6.3 E	44.6	35	80.1 N	79.4 W	
203	8	29.5 E	25.4	24	56.0 N	103.4 W	
202	8	4.2 W	42.8	8	79.6 N	22.8 W	
201	4	2.5 W	43.3	59	80.4 N	30.7 W	

On the other hand, the concentration of the remanent magnetization of the Komyoike horizon sediments is not so good. The stratigraphical sequence of the Komyoike horizon is divided into three divisions by the polarity change. The normal polarity of the lower stratigraphic position of the Komyoike horizon (Sample Number 2-30) continues to the normal polarity of the Pink volcanic ash. The long sequence of normal polarity from Pink to Komyoike ashes is ascertained to be expected. The writer tentatively names this long term normal polarity as "Komyoike event" after the type locality of the Komyoike volcanic ash layer. The reversed polarity of the higher ones (above the Sample Number 48), though the topmost has anomalous remanence, is thought to continue to the reversed polarity of the Yamada volcanic ash layer (Maenaka et al., 1977). The middle part (Sample Number 31-47) is considered to be transitional zone from normal field to reversed field. As given in Table 2, the intermediate remanent magnetization is characterized by abnormally low magnitudes of the precision parameter k. It may mean that the scatter of the remanent of the remanent magnetization is large during the periods of the polarity transition. This may be explained by the relative variation in the strength of the non-dipole field to the reduction of the dipole field strength during the field reversal.

Table 2. Paleomagnetic data after magnetic cleaning for Komyoike horizon sediments.

Sample Number	Number of Specimens	Mean Direction			Virtual Pole Position		
		Decli.	Incli.	k	Lat.	Long.	
94	5	152.7 E	51.5	5	18.5 S	159.7 E	
93 a	4	178.6 W	-38.4	3	77.0 S	129.7 E	
92 a	4	132.9 E	49.4	3	11.5 S	175.7 E	
92 c	5	144.7 E	18.7	2	34.7 S	179.3 E	
91	2	174.7 W	-49.0	4	83.5 S	90.1 E	
90	6	114.1 W	-65.4	9	40.2 S	9.3 E	
88	5	164.1 W	-64.4	51	73.2 S	3.5 W	
86	10	170.8 E	-24.9	27	67.0 S	159.0 E	
85	4	177.9 W	-36.3	28	75.6 S	127.6 E	
84	5	155.5 E	-25.0	28	59.2 S	172.5 W	
83	7	170.4 W	-24.2	8	66.5 S	111.4 E	
82	10	166.2 W	-5.5	4	55.8 S	110.4 E	
81	7	162.2 E	-7.8	15	55.2 S	167.8 E	
80	9	174.2 E	-60.4	59	81.7 S	76.3 W	
79	8	124.8 E	-44.0	8	42.1 S	129.3 W	
105	10	164.7 W	-9.7	18	57.2 S	106.5 E	
78	7	166.5 W	-41.9	27	74.4 S	83.2 E	
f	5	146.0 E	-20.3	26	50.8 S	164.0 W	
77	8	170.2 E	-24.2	12	63.8 S	157.6 E	
104	9	159.6 E	-46.2	6	71.2 S	150.9 W	
103	10	169.9 W	-14.8	2	61.4 S	114.2 E	
76	9	166.4 W	-46.5	7	76.6 S	71.7 E	
e	5	138.7 E	-25.1	23	47.1 S	153.9 W	
75	10	178.4 W	-36.3	3	75.6 S	129.4 E	
102	7	85.9 W	-54.4	4	16.0 S	13.8 E	
69	5	59.5 W	-60.7	6	3.7 S	4.4 W	
74	9	168.5 E	-20.9	127	64.1 S	162.1 E	
73	8	163.1 E	-36.3	10	69.3 S	173.9 W	
101	10	64.1 E	-14.7	3	16.4 N	112.9 W	
72	7	179.9 E	-28.1	7	70.4 S	135.8 E	
72'	9	146.3 W	-45.3	19	60.2 S	39.8 E	
100	8	141.3 W	-45.6	7	56.1 S	43.3 E	
c	6	162.8 E	-55.7	11	75.9 S	122.5 W	
66	6	39.3 E	-67.0	8	1.1 S	68.7 W	
67	6	163.6 E	-68.9	11	68.7 S	72.9 W	
71	4	168.8 W	-34.9	11	71.8 S	99.6 E	
70	7	65.6 E	-42.8	6	4.1 N	100.5 W	
70'	7	101.5 E	-60.8	22	30.0 S	102.0 W	
64	4	155.1 W	-78.5	35	53.7 S	29.0 W	
63	6	98.4 W	-67.3	40	30.8 S	3.1 E	
a	7	135.5 E	-57.1	3	54.2 S	116.1 W	
62	5	157.5 E	-72.1	46	62.8 S	71.5 W	
61	7	123.4 W	-86.0	39	38.6 S	35.9 W	
60	10	146.2 E	-70.0	27	59.4 S	84.7 W	
59	6	131.0 E	-65.9	13	51.5 S	98.4 W	
58	5	92.9 E	-60.1	43	23.8 S	100.0 W	
57	8	92.5 E	-56.6	25	21.8 S	103.5 W	
56	10	100.2 E	-64.4	43	30.7 S	96.9 W	
55	7	134.8 W	-17.1	10	41.3 S	66.5 E	
54	7	167.7 E	-59.4	30	78.7 S	100.6 W	
53	7	149.0 W	-74.9	23	56.6 S	18.1 W	
52	6	175.7 W	-63.7	19	78.7 S	28.9 W	

Table 2. (continued)

Sample Number	Number of Specimens	Mean Direction			Virtual Pole Position	
		Decli.	Incli.	k	Lat.	Long.
51	8	172.4 W	-27.4	19	68.9 S	114.7 E
50	10	171.8 W	-46.9	11	80.5 S	85.7 E
49	9	128.3 E	-58.6	37	49.0 S	112.1 W
48	6	173.7 W	-63.5	4	78.3 S	22.0 W
47	10	122.8 W	-37.3	43	38.2 S	43.6 E
46	7	101.3 W	-42.0	2	22.3 S	30.7 E
45	10	154.2 W	-30.6	16	60.7 S	77.0 E
44	8	47.2 E	-66.7	4	3.7 S	73.2 W
43	10	5.4 E	-83.8	14	22.3 S	45.7 W
42	6	74.2 E	-12.2	5	9.3 N	148.7 W
41	6	115.7 E	6.7	8	18.9 S	152.6 W
40	8	13.7 W	-37.4	10	33.0 N	29.2 W
39	8	0.8 E	-64.4	13	9.3 N	45.1 W
38	8	74.1 W	-25.1	4	5.2 N	25.6 E
37	9	155.8 W	-40.6	3	66.1 S	67.3 E
36	6	171.4 W	-56.2	68	82.5 S	21.5 E
35	10	157.6 E	-27.9	9	61.8 S	173.2 W
34	6	173.3 W	-69.4	14	70.8 S	32.2 W
33	4	154.7 W	-72.1	26	61.7 S	15.2 W
32	9	144.7 W	-68.2	12	59.6 S	1.1 E
31	5	166.4 W	-61.6	17	76.5 S	3.0 E
30	10	5.7 E	3.0	1	55.4 N	54.6 W
29	9	45.5 E	0.1	1	35.3 N	105.4 W
28	10	53.6 W	45.1	4	43.7 N	50.6 E
27	8	16.2 W	22.2	1	62.7 N	7.9 W
26	10	144.8 W	70.2	2	3.8 N	115.7 E
25	6	4.4 W	57.6	29	85.0 N	91.6 E
24	7	8.9 W	42.3	21	77.3 N	4.7 W
23	5	1.0 E	46.1	6	82.7 N	51.5 W
22	8	1.3 W	42.3	8	79.8 N	37.8 W
21	6	15.7 E	33.8	6	68.8 N	89.6 W
20	8	39.5 E	33.5	5	51.4 N	120.0 W
19	4	7.7 E	41.8	71	77.6 N	79.3 W
18	5	14.6 E	25.0	6	64.8 N	79.8 W
17	4	6.5 W	32.5	7	72.2 N	23.8 W
16	6	8.5 W	-21.7	28	43.5 N	33.0 W
15	5	6.0 E	22.6	5	66.6 N	59.5 W
14	7	24.6 W	-44.2	3	25.3 N	20.0 W
13	9	36.8 W	42.7	7	56.8 N	38.6 E
12	9	7.4 W	43.4	14	78.8 N	7.8 W
11	5	2.9 W	42.9	24	80.1 N	29.1 W
10	4	10.8 W	38.4	9	74.0 N	5.4 W
9	5	15.5 E	53.7	5	77.2 N	137.3 W
8	6	8.7 W	44.3	28	78.7 N	0.8 W
7	10	8.2 W	54.2	18	83.2 N	52.3 E
6	9	6.1 W	49.6	12	83.4 N	8.4 E
5	6	15.4 W	52.4	20	77.1 N	43.2 E
4	7	4.2 W	47.3	46	83.0 N	12.5 W
3	6	31.5 E	42.0	25	60.8 N	122.2 W
2	7	29.0 E	29.9	5	58.1 N	106.4 W

References

- Ishida, S., K. Maenaka, and T. Yokoyama (1969) Jour. Geol. Soc. Japan, 75, 183.
- Itihara, M., S. Yoshikawa, K. Inoue, T. Hayashi, M. Tateishi, and K. Nakajima (1975) Jour. Geosci. Osaka City Univ., 19, 1.
- Maenaka, K. (1975) Rock Magnetism and Paleogeophysics, 3, 41.
- Maenaka, K., T. Yokoyama, and S. Ishida (1977) Quaternary Research, 7, 341.
- Nishimura, S. and S. Sasajima (1970) Chikyu Kagaku, 24, 222.

THE BRUNHES/MATUYAMA POLARITY EPOCH BOUNDARY
IN THE KOBIWAKO GROUP ON THE WEST COAST OF LAKE BIWA,
CENTRAL JAPAN

Akira HAYASHIDA*, Sadao SASAJIMA* and Takuo YOKOYAMA**

*Department of Geology and Mineralogy, Kyoto University, Kyoto 606

**Laboratory of Earth Science, Doshisha University, Kyoto 602

INTRODUCTION

The purpose of this report is to present the results of a paleomagnetic analysis of lacustrine sediments called the Katata Formation of the Kobiwako Group, which is distributed on the west coast of Lake Biwa in Central Japan (Fig. 1). Studied section along the Kisen River has been expected to include the Brunhes/Matuyama boundary. Paleomagnetic dating of the Kobiwako Group is a key character for the natural history of the Pleistocene time in Central Japan. Detailed survey of the section would provide precise informations for the geomagnetic field behavior during the polarity transition.

Paleomagnetism has provided important data for chronology and world-wide correlations of the Cenozoic strata, and its role on historical geology is very promising. But it is imperative that we are confronted with some difficulties in recognizing a true paleomagnetic history recorded in the sediments, as summarized in Kukula and Nakagawa (1977). Among these problems, post-depositional magnetic overprints are the most serious obstruction to the recovery of original signal of detrital remanent magnetization (DRM), especially as to outcropping strata in the land surface. Although the small amount of unstable viscous remanent magnetization (VRM) is believed to be minimized by alternating field (AF) demagnetization, we are unfortunate at present to have no experimental method that can remove the secondary magnetizations completely from sediment samples. Thermal demagnetization is sometimes adopted successfully to erase the secondary overprints of chemical remanent magnetization (CRM), for instance by Ouliac (1976), Niitsuma (1976), and Roggenthen and Napoleone (1977).

On the Kisen River section of the present study, the preliminary result of measurement of natural remanent magnetization (NRM) has been reported (Hayashida et al., 1976). The measurement was resulted with AF demagnetization up to 200 Oe peak fields. In the present report, the section is reexamined using both of AF and thermal demagnetizations.

GEOLOGICAL SETTING AND PREVIOUS DATA

The Katata Formation is thought to be the uppermost part of the Kobiwako Group, the fresh water sediments of the ancient Lake Biwa. It is composed of clays, sands and gravels with some peat and volcanic ash seams. The detailed stratigraphic description of the Katata Formation is seen in Yokoyama (1975). As shown in the columnar section in Fig. 2, paleomagnetic polarity data and fission track ages of some outstanding volcanic ashes are available for the chronology of the Katata Formation (Nishimura and Sasajima, 1970; Nishimura and Yokoyama, 1973, 1975; Maenaka et al., 1977). These data suggest the Brunhes/Matuyama polarity transition occurred during the deposition of the lower part of the Katata Formation, between the Biotite and Ogoto volcanic ashes.

Fig. 2 also shows the preliminary result of a paleomagnetic survey which was made to determine the exact horizon of the Brunhes/Matuyama

boundary (Hayashida et al., 1976). Samples for the survey were collected along the Kisen River where the good exposures of the Kobiwako Group including the Biotite and Ogoto volcanic ashes are observable. As shown in this figure, the Brunhes/Matuyama boundary is appeared to exist in the muddy sediments about 10 meter above the Biotite volcanic ash layer. However, subsequent thermal demagnetizing test revealed the instability of NRM and production of another magnetic phase during heating process on some of these muddy sediments. So, to refine the previous data and to make clear the horizon of the Brunhes/Matuyama boundary, more samples were taken from the Kisen River section between the Biotite and Ogoto volcanic ashes. Stratigraphic horizon of the samples are marked on the columnar section represented in Fig. 3.

ALTERNATING FIELD DEMAGNETIZATION

Progressive AF demagnetization was carried out on one or two specimens from each site, in steps in peak fields up to 400 Oe. NRM of these pilot specimens was all normal in polarity before any demagnetizing treatments. After the AF demagnetization up to 400 Oe peak fields, they did not show any significant changes in direction of their remanent magnetism towards reversed polarity, except a specimen from sample Z-13. The sample Z-13 is thought to have recovered its original DRM by the partial demagnetization of soft component of magnetization. Other specimens from all sites were routinely demagnetized in the peak field of 200 Oe. Remanent magnetizations resulted from such a demagnetizing treatment for all sites are given in Table 1.

THERMAL DEMAGNETIZATION

Thermal demagnetization was performed with a non-inductive electric furnace shielded by a double layered μ -metal tube and an orthogonal set of three Helmholtz coils. The temperature inside the furnace is controlled with the accuracy as much as $\pm 25^\circ\text{C}$ by an electronic controller which has a Pt-PtRh thermocouple attached to the sample holder. Stray field inside the furnace is measured as less than several tens gamma. Pilot specimens from each site were subjected to the progressive thermal demagnetization at the temperature of every 100 degrees from 150°C up to 450°C or 550°C in the open air.

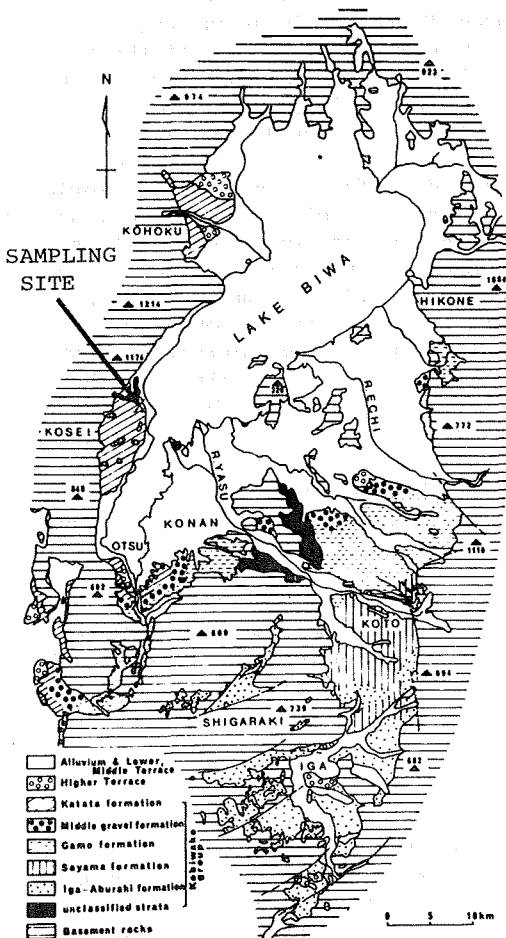


Fig. 1. Map showing the distribution of the Kobiwako Group around Lake Biwa and the sampling site of the present study, the Kisen River section. Base map is from Ikebe and Yokoyama (1976).

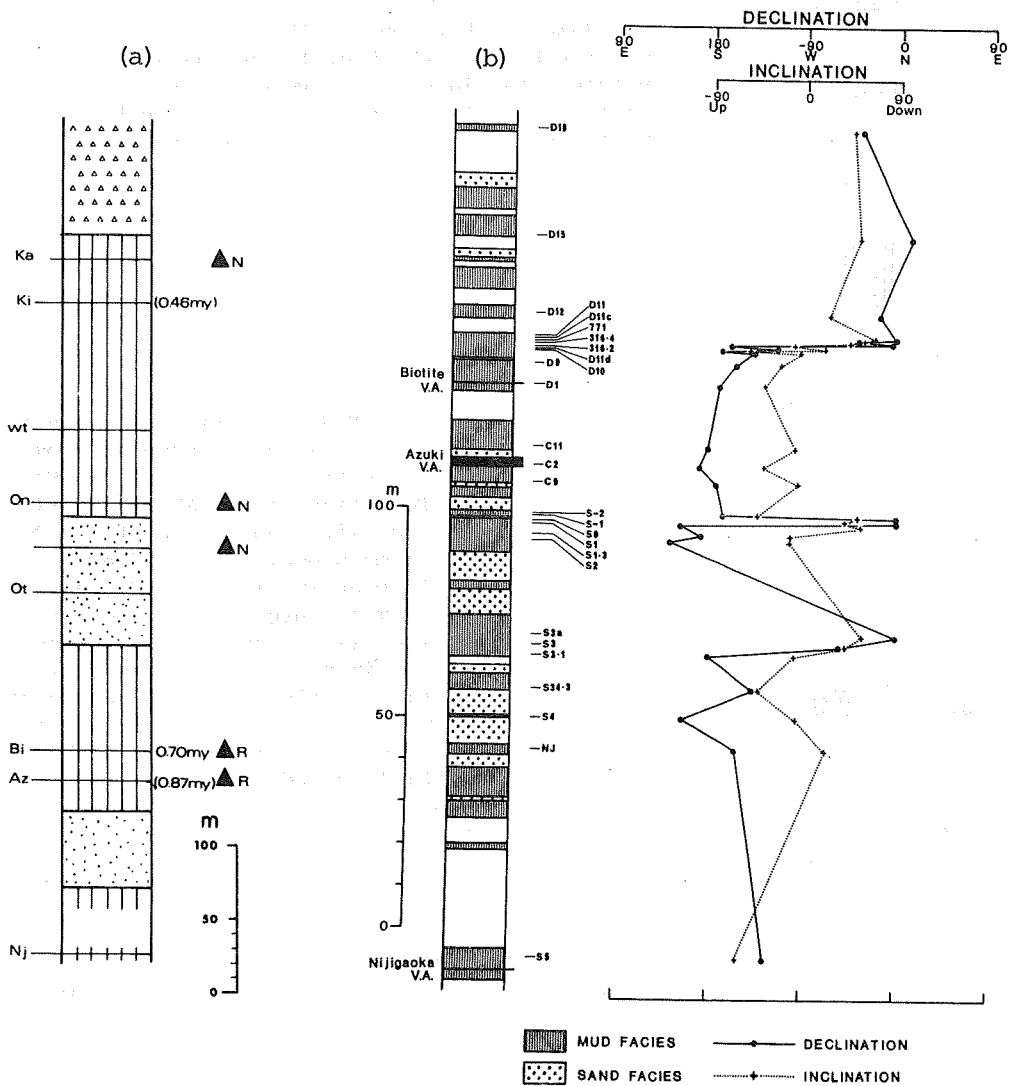


Fig. 2. Stratigraphical data of the Katata Formation of the Kobiwako Group. (a) Typical columnar section of the Katata Formation. Horizontal lines show the volcanic ash layers; Nj: Nijigaoka, Az: Azuki, Bi: Biotite, Ot: Ogoto, On: Ono, Wt: White, Ki: Kinukawa, Ka: Kamiogi volcanic ash layer. Fission track ages and paleomagnetic polarity of some volcanic ashes are also shown. (b) NRM directions of the samples from the Kisen River section of the Katata Formation, after the stability test of AF demagnetization up to 200 Oe peak field. (Hayashida et al., 1976)

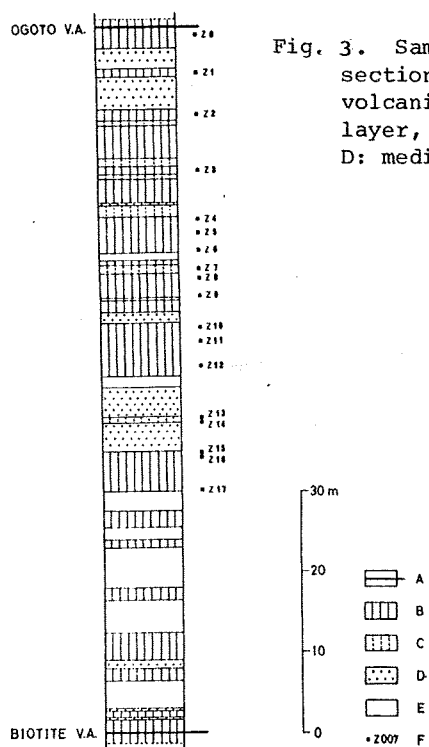


Fig. 3. Sampling horizons on the Kisen River section between the Biotite and Ogoto volcanic ash layers. A: volcanic ash layer, B: silts and clays, C: fine sands, D: medium or coarse sands, E: not observed.

Table 1. Mean direction of remanent magnetization of samples from the Kisen River section of the Katata Formation, after AF demagnetization with peak field of 200 Oe. D: mean declination (degrees) I: mean inclination (degrees) J: mean intensity of magnetization ($\times 10^{-6}$ emu/cc), N: number of specimens, R: resultant vector, k: Fisher's precision parameter, α_{95} : 95% confidence circle radius (degrees), ϕ : latitude of VGP, λ : longitude of VGP.

Identification	D	I	J	N	R	k	α_{95}	ϕ	λ
K-1(Ogoto v.a.)	26.4	47.0	10.8	3	2.999	1613.	3.1	66.5	236.0
Z-0	- 1.8	54.2	0.24	4	3.993	419.4	4.5	88.5	29.6
Z-1	- 4.5	54.5	0.29	4	3.924	39.40	14.8	86.1	45.3
Z-2	- 2.1	48.3	0.72	4	3.933	44.46	13.9	83.8	333.5
Z-3	- 4.7	56.3	0.46	2	1.929	14.06	72.6	85.8	71.1
Z-4	8.4	48.9	3.58	4	3.988	248.2	5.8	81.1	260.8
Z-5	8.9	47.5	15.0	4	3.998	1252.	2.6	80.0	264.8
Z-6	- 0.2	44.5	10.2	4	3.973	112.6	8.7	81.0	316.9
Z-7	- 6.7	49.1	0.70	4	3.967	91.62	9.7	82.3	4.8
Z-8	6.0	40.5	4.27	4	3.996	679.6	3.5	76.8	290.9
Z-9	- 1.7	53.5	3.61	4	3.963	82.05	10.2	88.2	8.3
Z-10	21.6	57.7	3.36	4	3.991	341.6	5.0	72.5	209.4
Z-11	12.6	41.2	5.87	4	3.991	333.9	5.0	74.1	269.0
Z-12	-58.4	36.4	0.11	4	2.375	1.846	-	36.9	45.9
Z-13	122.7	-15.0	0.23	4	3.002	3.007	64.5	-30.9	212.4
Z-14	1.2	57.7	0.60	4	3.792	14.42	25.1	86.8	152.6
Z-15	30.0	88.1	0.21	3	2.843	12.77	36.0	38.4	138.3
Z-16	189.0	46.4	0.30	4	3.633	8.182	34.2	-26.5	127.0
Z-17	26.1	61.2	3.13	4	3.993	441.3	4.4	68.6	198.9

Remanent magnetization of some specimens began to change their polarity towards the reversed direction by the thermal demagnetization at 150°C or 250°C. After heating up to 250°C or 350°C, however, remanent magnetization of most specimens turned into completely unstable one. They showed extraordinary high intensity at the first moment of measurement by the spinner magnetometer (Schonstedt's SSM-1A), the next moment changing on and on through the continuous measurement. This behavior of unstable magnetization is represented in Fig. 4, for example. As shown in the figure, the magnetic intensity changes exponentially with time, and it indicates that an extremely unstable component of magnetization is being demagnetized in the field-free space of the spinner magnetometer. The sensor of the spinner magnetometer and a specimen under the measurement are defended with μ -metal shield from the geomagnetic field in the laboratory, and the ambient field is neutralized under ± 10 gamma in the direction of the sensor. The unstable component has such a short relaxation time as a few seconds or so, that the polarity of these specimens is changed while they are inverted by hand. This unstable magnetization is suggested to be isothermal remanent magnetization (IRM) carried by a new ferrimagnetic minerals produced during the heating process and to have been acquired under the geomagnetic field in the laboratory while the specimen was brought from the furnace to the magnetometer for measurement.

It is also supposed that we might be allowed to know the primary magnetization after the thermal demagnetization if this IRM component were entirely erased. In fact, after sufficiently long-term spinning like several tens of minutes by the spinner magnetometer, the resulting intensity and direction of such specimens is possible to be regarded as those of the primary magnetism. But this method of IRM demagnetization is capable only for the specimens after the thermal treatment of lower temperature than 300°C. The following heating at higher temperature make such soft component of magnetization more stable, and it becomes impossible to demagnetize the IRM component sufficiently in the zero-field space of the spinner magnetometer.

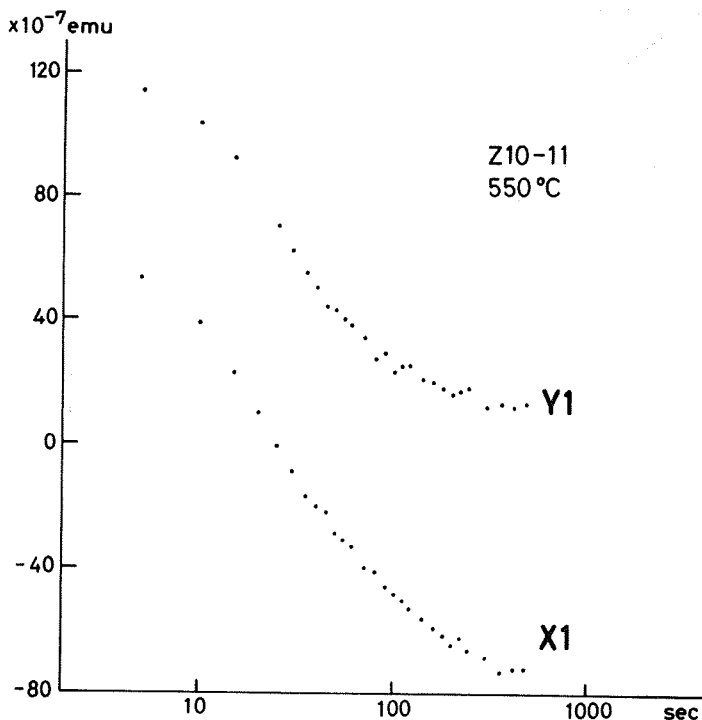


Fig. 4. Changes of the highly unstable magnetization during the measurement by spinner magnetometer, after thermal demagnetization at 550°C. X1 and Y1 indicate two rectangular components of magnetization.

As the consequence, the resulting magnetization after treatment of higher temperature tends to direct to the bottom of the specimen, namely the vertically down direction in the laboratory process, in which direction the resultant IRM is to be acquired. Results of the progressive thermal demagnetization represented in Fig. 5 are obtained by above mentioned method, and such behavior of magnetization after thermal treatment at 450°C or 550°C is also shown in this figure.

DISCUSSION

Although the thermal demagnetization test revealed the existence of the secondary CRM component in sediments of the Kisen River section which could not be cleaned up by AF demagnetization, the alteration of magnetic minerals by heating treatment is an impediment to recovery of the original DRM. Fig. 6. shows the acquisition curves of anhysteretic remanent magnetization (ARM) of four specimens from the same site. Three of them had been thermally demagnetized at temperatures of 250°C, 350°C and 450°C, and another had been left unheated. Coercivity spectra of their saturation ARM are also represented in the figure. Here the secondary ferrimagnetic phase is shown to be increasingly produced by the heating up to 350°C. The decreased ARM by the heating up to 450°C suggests its growth to another phase. A possible interpretation of this phenomenon is that the increasing dehydration and subsequent oxydation of iron hydroxides or iron-bearing

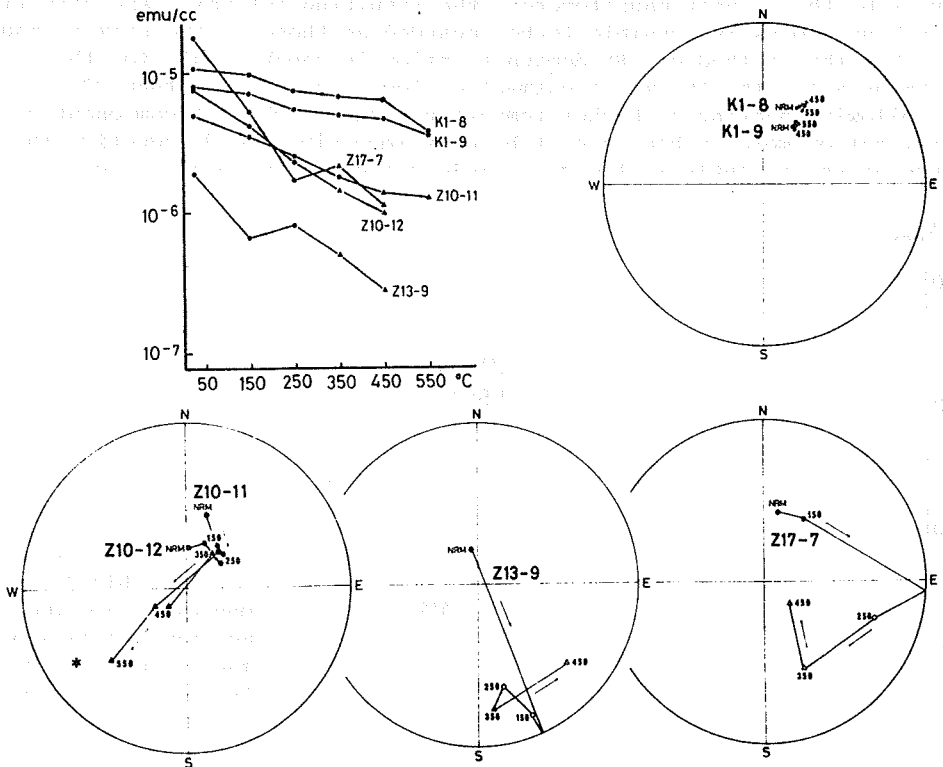


Fig. 5. Changes of intensity and direction of magnetization by progressive thermal demagnetization. Directions and intensities represented by triangles are determined after the IRM demagnetization in the spinner magnetometer. Asterisk show the direction of the bottom of specimens. Sample K1 is from the Ogoto volcanic ash, which shows stable magnetization through thermal demagnetization up to 550°C.

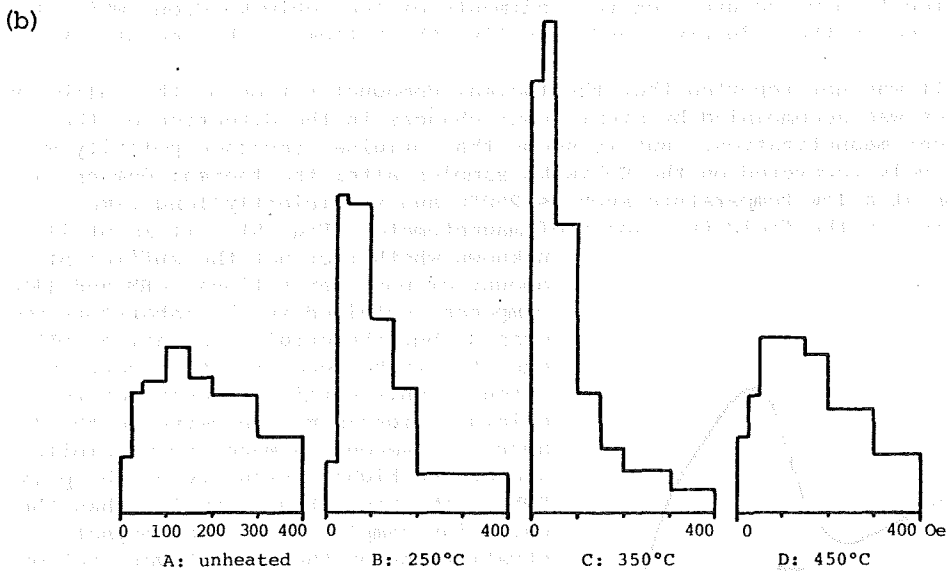
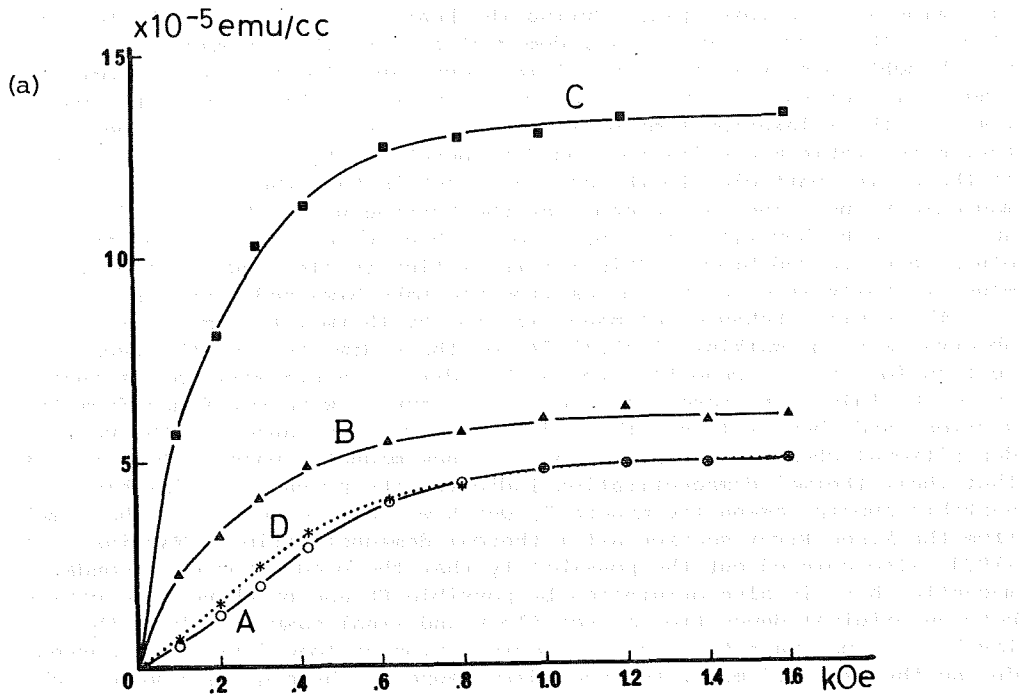


Fig. 6. (a) ARM acquisition curves versus peak AF intensity. Alternating fields are generated parallel to the direct field, the geomagnetic field in the laboratory (0.46 G). Samples were taken from the same site. A: unheated, B: after 250°C, C: after 350°C, D: after 450°C thermal demagnetization. (b) Coercivity spectra of saturation ARM obtained by progressive AF demagnetization up to 400 Oe.

clay minerals are taken place during the heating process. In the beginning stage of the progressive thermal demagnetization, the new magnetic minerals are thought to be very small particles comparable to the critical magnetic domain size of superparamagnetism, representing the highly unstable magnetism with the relaxation time of few seconds or so. It is also suggested that more stable magnetization could be developed by the following growth of these fine particles to the coarser crystals than the critical superparamagnetic value. The last product by the heating up to 450°C or 550°C is appeared to be hematite, for such samples had turned their colour from bluish grey to red-brown. This interpretation is also suggested by thermomagnetic analysis of clay samples from the Lake Biwa sediments (Fig. 7).

The similar behavior of magnetization by thermal treatments was observed also by Watkins et al. (1974) on the sediments from the type section for the Pliocene/Pleistocene boundary at Santa Maria de Catanzaro in south Italy. Any reversely magnetized samples were not found from the section, and they explained their data to have been caused by the post-depositional chemical precipitation of a new magnetic phase. They reported that their thermal demagnetization indicated the presence of "highly unstable superparamagnetic mineral", which was also observed in the samples from the Kisen River section after thermal demagnetization. Watkins et al. (1974) also pointed out the possibility that the production of secondary magnetic phase is also originated by possible Eh and pH changes occurring between original deposition at sea floor and final sampling above the sea level. If such magnetic mineral precipitation of long duration occurred during the last 0.7 m.y., the secondary magnetic phase grows a more stable component showing the normal polarity. Such environmental changes are expected to have occurred on the sediments of the Kobiwako Group which have deposited in the reductive condition like the bottom of the recent Lake Biwa.

It was not reported that the thermal demagnetization of the Calabrian samples was accompanied by significant changes in the direction of their remanent magnetization. But it seems that original reversed polarity was relatively recovered on the Kobiwako samples after the thermal demagnetization at a low temperature such as 250°C and sufficiently long-time spinning in the field-free space of magnetometer (Fig. 5). It is still unknown whether or not the sufficient amount of post-depositional CRM and IRM component obtained in the laboratory was erased, but the original signal of DRM is expected to be recovered to a certain extent. This partial recovery of the original signals may be owing to the less amount of secondary magnetic precipitation and/or the higher intensity of the primary DRM of the Kisen River samples than the Calabrian samples. Thus the magnetostratigraphy of the Kisen River section can be tentatively described. Fig. 7 shows the directions of the remanent magnetization after the thermal demagnetization up to 250°C or 300°C. These directions were determined after the demagnetization of IRM component of the magnetization in the spinner magnetometer as mentioned before. Results of the mean directions after the AF demagnetization with peak field of 200 Oe (Table 1) are also plotted on the figure. As shown here,

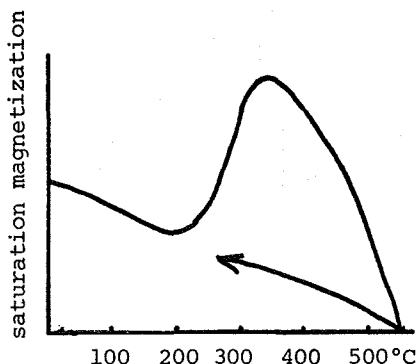


Fig. 7. Generalized result of thermomagnetic analysis of the Lake Biwa sediments.

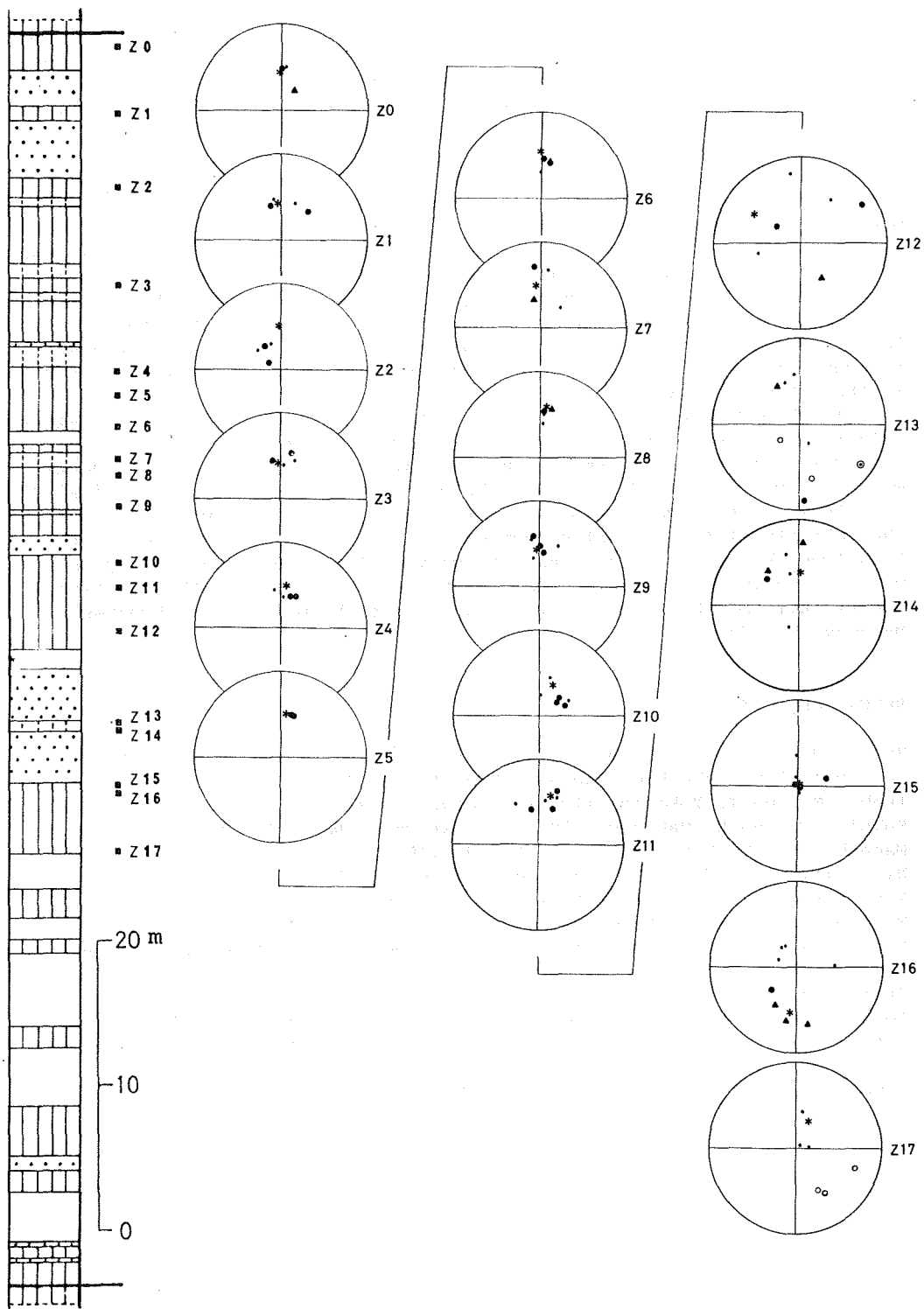


Fig. 8. Stereographic projection of paleomagnetic results. Small points and large circles show the direction of remanent magnetization before and after thermal demagnetization at 250°C or 300°C, respectively. Asterisks show the site mean directions after 200 Oe AF demagnetization. Solid symbols are plotted on the lower hemisphere, open symbols on the upper hemisphere.

the magnetic directions of samples above the horizon of Z-12 are all normal in polarity. The sample Z-13 represents the uppermost horizon of reversed polarity, situated about 40 meter above the Biotite volcanic ash layer. Therefore the Brunhes/Matuyama boundary is temporarily assumed to exist in this horizon. This result of paleomagnetic dating of the Kisen River section keeps a good conformity with the result of fission track dating of the Biotite volcanic ash (0.70 m.y., Nishimura and Yokoyama, 1975). The sample Z-12 does not have the significant precision in the grouping of the magnetic directions both after the AF and thermal demagnetization. Intermediate states of remanent polarity are observed in the sample of Z-15 and Z-16, on which the AF and thermal demagnetization gave almost same directions. These three samples and another one, Z-14, which has the normal polarity between reversely magnetized samples, may be possibly representing the transitional feature of the paleomagnetic field. Then the Brunhes/Matuyama transition seems to be recorded within about 10 meter thick strata in the Kobiwako Group.

It should be noted, however, that these intermediate states of magnetic polarity could be partially caused by incomplete demagnetization of the secondary components of remanent magnetization. There is no experimental means, at present, to distinguish the paleomagnetic signals of original DRM from those of secondary chemical overprints. So the only method to confirm the validity of the present paleomagnetic results is reproduction of the data from the parallel sections with various lithology, sedimentary environment and sedimentation rate. Paleomagnetic survey of the other section in the vicinity of the Kisen River is expected to be made on the Brunhes/Matuyama boundary.

REFERENCES CITED

- Hayashida, A., T. Yokoyama, K. Takemura, T. Danhara and S. Sasajima (1976). *Paleolim. Lake Biwa Japanese Pleist.*, 4, 96.
- Ikebe, N. and T. Yokoyama (1976). *ibid.*, 4, 31.
- Kukula, G. and H. Nakagawa (1977). *Quaternary Res.*, 7, 283.
- Maenaka, K., T. Yokoyama and S. Ishida (1977). *ibid.*, 7, 341.
- Niitsuma, N. (1976). *J. Geol. Soc. Japan*, 82, 163.
- Nishimura, S. and S. Sasajima (1970). *Chikyu Kagaku (Earth Sci.)*, 24, 222
- Nishimura, S. and T. Yokoyama (1973). *Proc. Japan Acad.*, 49, 615.
- Nishimura, S. and T. Yokoyama (1975). *Paleolim. Lake Biwa Japanese Pleist.*, 3, 138.
- Ouliac, M. (1976). *Earth Planet. Sci. Lett.*, 29, 65.
- Roggenthen, W. M. and G. Napoleone (1977). *Geol. Soc. Amer. Bull.*, 88, 378.
- Watkins, N. D., D. R. Kester and J. P. Kennett (1974). *Earth Planet. Sci. Lett.*, 24, 113.
- Yokoyama, T. (1975). *Paleolim. Lake Biwa Japanese Pleist.*, 3, 114.

PALEOMAGNETISM AND K-Ar AGE OF THE VOLCANIC ROCKS FROM KURO-SHIMA ISLAND, KAGOSHIMA PREFECTURE

Masato JOSHIMA*, Ken SHIBATA*, Koji ONO and Osamu UJIKE**

*Geological Survey of Japan, Hisamoto 135, Takatsu-ku, Kawasaki-shi, 213

**Shikoku Branch Office, Geological Survey of Japan, Ban-cho 1-10-6, Takamatsu-shi, 760

Kuro-shima is an island located 50 km off the southernmost end of Kyushu and 30 km to the west of Satsuma-Io-jima of the Kikai Caldera which lies on the front of the West Japan Volcanic Belt (Fig. 1).

Kuro-shima is 5 x 4 km in the E-W and in the N-S directions. The highest point of the island, Yagura-dake, is 622 m above sea level and lies a little to the south of the center of the island. The island is a dissected stratovolcano of pyroxene andesite, the center of which approximately coincides with the highest point. Although most part of the flank of the volcano is cut by deep valleys, slopes to the north-northwest and to the west seem to preserve the original surface of lava flows, shown as stippled areas in Fig. 2, suggesting their young formation in the island (Ujike and Ono, 1977).

Paleomagnetism

As measurements of paleomagnetic direction, using a portable fluxgate magnetometer in the field, revealed that most rocks of the island were reversely magnetized except normally magnetized younger flows, oriented samples were collected for laboratory measurements.

Most samples were collected along the road encircling the volcano at its lower flank, with some others collected at the sea coast and near the summit (Fig. 2). Stratigraphic relations among them have not determined

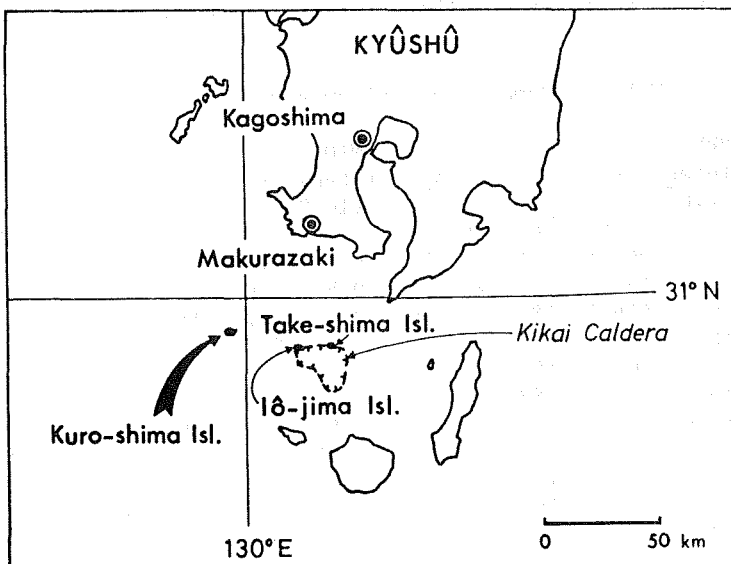


Fig. 1 Index map

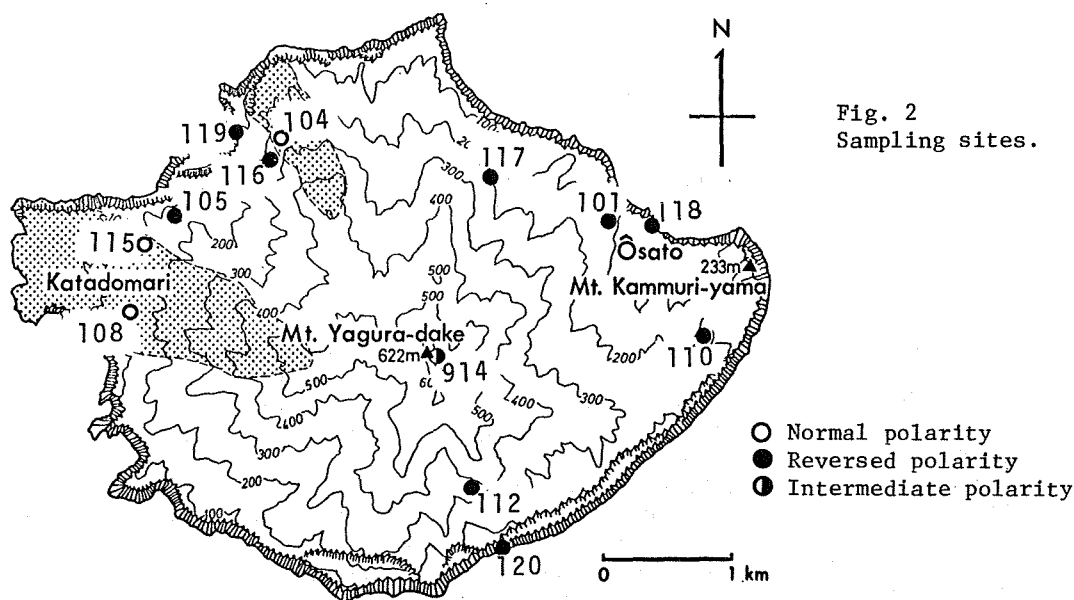


Fig. 2
Sampling sites.

except that KR120 at the south coast probably represents the lowermost horizon among those collected and that samples of three sites, KR104, KR108 and KR115, are from younger flows, as previously stated, than others.

35 specimens from 13 sites were drilled and cut in the laboratory from the oriented samples. Remanent magnetization, before and after the demagnetization in the alternating field of 100 oersted, were measured using a spinner magnetometer MD-1, made by PAR. Results are shown in Table 1.

As for the direction of NRM, specimens from 3, 7 and 3 sites of all 13 sites had normal, reversed and intermediate polarity respectively. Most specimens were magnetically stable and did not practically change their direction by the a.f. demagnetization but specimens of 2 sites of intermediate direction changed to reversed polarity resulting in 3, 9 and 1 of normal,

Table 1 Summary of paleomagnetic data

Sample N	NRM				RM100				Suscep- tibility (10^{-6})	
	Intensity (10^{-4})	D	I	α_{95}	Intensity (10^{-4})	D	I	α_{95}		
KR101	5	4.79 ±1.97	163	-6	38	3.96 ±0.81	177	-38	4	2613 ±113
KR104	3	14.8 ±0.15	-4	43	21	6.10 ±1.61	-4	36	13	1993 ± 93
KR105	5	10.1 ±3.1	177	-47	5	9.85 ±3.0	181	-50	4	980 ±126
KR110	5	29.5 ±16.7	188	-31	6	32.4 ±17.2	187	-37	4	755 ±295
KR115	3	16.9 ±1.0	-15	46	11	7.12 ±0.58	-12	34	13	2128 ±205
KR116	3	8.01 ±6.0	190	-25	15	9.23 ±4.9	190	-37	14	1306 ±237
KR117	3	10.1 ±4.2	83	-22	10	4.46 ±0.89	179	-52	31	2350 ±434
KR118	3	14.6 ±7.5	197	-32	16	13.8 ±6.7	193	-46	12	2025 ±424
KR108	1	11.6	8	53		3.97	-1	44		1919
KR112	1	5.99	149	-23		3.02	161	-26		2335
KR119	1	5.44	193	-35		4.55	185	-48		2300
KR120	1	40.0	158	-43		42.4	160	-49		1671
KR914	1	124.	-45	-28		14.2	-85	-44		1727
N group	7		-7	46	8		-7	36	6.5	
R group	27		171	-33	12.8		182	-43	4	

Intensity and susceptibility are in emu/cm^3 .

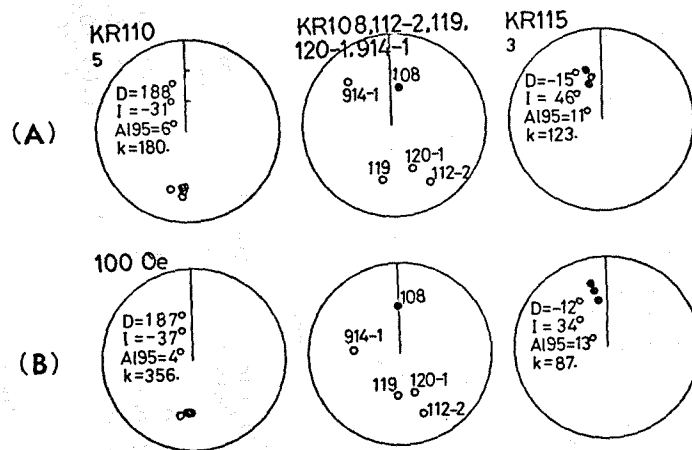
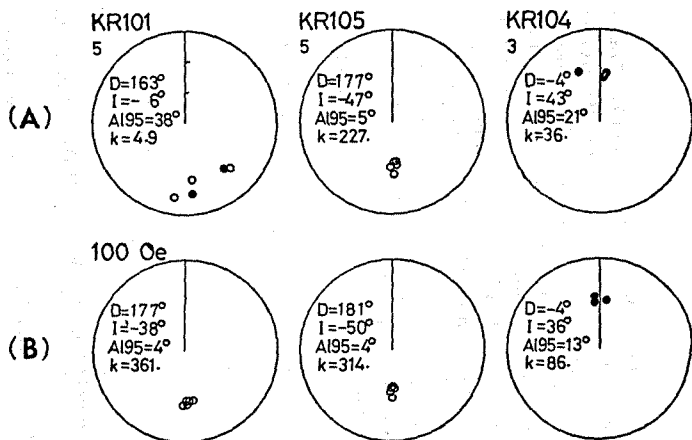


Fig. 3 (A) Directions of NRM. (B) After the a.f. demagnetization of 100 oersted.

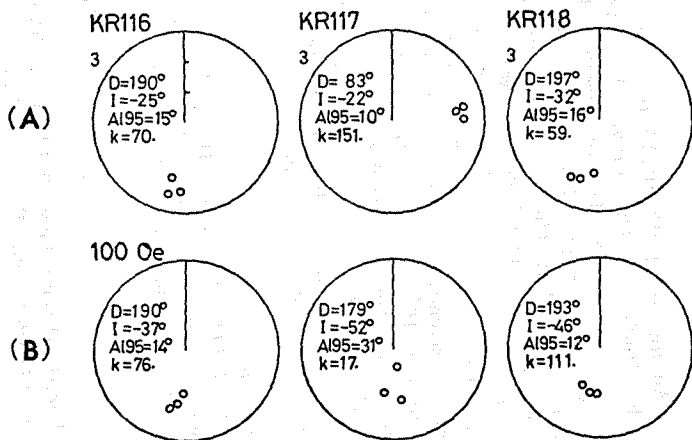


Fig. 4 Mean direction of remanent magnetization for groups of normal and reversed polarity. Circles : NRM, squares : after the a.f. demagnetization of 100 Oe. Open : upper direction. Closed : lower direction.

reversed and intermediate direction.

The intermediate direction, only one left, of the specimen 914-4, which was collected near the summit of the Yagura-dake, seems to be unreliable as it had extraordinary high intensity of NRM compared with other specimens from the island and was unstable in the a.f. demagnetization.

Directions of remanent magnetization of specimens taken from a site and, also, those of all specimens of normal and reversed, are reasonably well-concentrated after the a.f. demagnetization (Figs. 3, 4).

K-Ar age

One sample, KR112-1, was radiometrically dated by the K-Ar method. The sample, collected at the south flank of the volcano, is reversely magnetized and is probably of an intermediate horizon in the group of reversed polarity. The result of the measurements is shown in Table 2.

Table 2 Results of K-Ar age dating

Sample No.	Material	K ₂ O (%)	⁴⁰ Ar rad (10 ⁻⁶ mlSTP/g)	Atm ⁴⁰ Ar (%)	Age (m.y.)
KR112-1	Whole rock	1.33, 1.36	0.0439	91.8	1.01 ±0.17
			0.0456	95.8	1.05 ±0.35
			0.0444	76.9	1.03 ±0.10
					1.03 ±0.13

$$\lambda\beta = 4.962 \times 10^{-10}/y, \quad \lambda e = 0.581 \times 10^{-10}/y, \quad {}^{40}\text{K}/\text{K} = 0.01167 \text{ atom \%}$$

(Steiger and Jäger, 1977)

An age of 1.03 ±0.13 m.y. is correlated to a horizon a little lower than the beginning of the Jaramillo normal event, 0.97 m.y.*, in the Matuyama reversed epoch and is conformable to the reversed polarity of the sample.

Normally magnetized lavas are lying on the group of reversed rocks. Considering that the life of a usual stratocone of andesite is less than a few hundred thousand years, mostly less than one hundred thousand years, that the size of the Kuro-shima volcano is not large, and that the absence of a remarkable time gap in the sequence of lava flows especially at the base of normally magnetized flows, the probable time span of the Kuro-shima rocks is around 1×10^5 years or less. Then, the horizon of the overlying, normally magnetized flows is probably not in the Bruhnes normal epoch but in the Jaramillo normal event. Though we have only one radiometric age for rocks of Kuro-shima volcano, the whole range of rocks of the volcano is likely to span in age from somewhat older than 1.0 m.y. to around 0.9 m.y.

References

- Cox, A. (1969) Science, 163, 237.
Steiger, R. H. and Jäger, E. (1977) Earth Planet. Sci. Lett., 36, 359.
Ujike, O. and Ono, K. (1977) Bull. Volc. Soc. Jap., 22, 283.

(to be submitted to Bull. Volc. Soc. Jap.)

* Recalculated from 0.95 m.y. (Cox, 1969), according to decay constants of Steiger and Jäger (1977).

MAGNETOSTRATIGRAPHY OF THE PLIO-PLEISTOCENE AGÉ GROUP
IN THE NORTHERN PART OF MIE PREFECTURE, JAPAN

Keiji TAKEMURA and Masayuki TORII

Department of Geology and Mineralogy, Faculty of Science, Kyoto University,
Kitashirakawa, Sakyoku, Kyoto 606, Japan

Introduction

The Plio-Pleistocene sediments in Kinki and Tokai Districts are considered to be the most attractive deposits, because those sediments intercalate many tephra and yield many vertebrate and plant fossils. Throughout the Pliocene and Early Pleistocene, three sedimentary basins existed in the Second Setouchi Inland Sea (Ikebe, 1956). Sediments in those sedimentary basins are composed of clastic materials such as gravels, sands and muds with thin seams of lignite and volcanic ash layer. They are called the Osaka, Kobiwako and Tokai Groups from west to east.

Recently, by the help of the studies on fission track age (Nishimura and Sasajima, 1970; Nishimura and Yokoyama, 1973, 1974, 1975) and magnetostratigraphy (Ishida et al., 1969; Torii et al., 1974; Hayashida et al., 1976; Maenaka et al., 1977), precise stratigraphy and chronology of the Plio-Pleistocene in Kinki and Tokai Districts have been much advanced. In this manner, the informations from the Osaka and Kobiwako Groups have been accumulated and emended by such methods newly developed. Those from the Tokai Group, however, have been left behind. Especially, the Agé Group is the thickest and the most continuous sequence in the Tokai Group, but the informations from the sediments have been fragmental. In this paper, we will report natural remanent magnetization (NRM) of volcanic ash layers intercalated in the Agé Group in the northern part of Mie Prefecture.

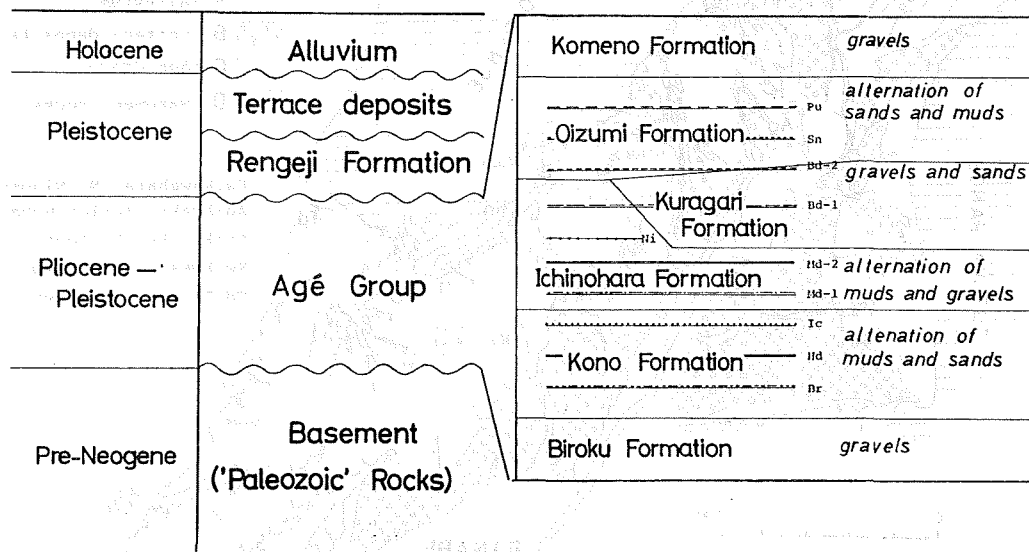


Fig.1 Stratigraphy of the Agé group in the northern part of Mie Prefecture

Geological outline of the Agé Group in the northern part of Mie Prefecture

The Agé Group in the northern part of Mie Prefecture (Inabe and Kuwana district) is developed in the foothills of the Suzuka and Yoro Mountains. It rests on the Paleozoic rocks with unconformity and is covered unconformably with Pleistocene Rengeji Formation and Terrace deposits. The Agé Group attains about 950m thick in the foothills of the Yoro Mountains, and about 800m in the foothills of the Suzuka Mountains. It is divided into six formations. They are the Biroku, Kono, Ichinohara, Kuragari, Oizumi and Komeno Formations in ascending order (Fig.1).

Volcanic ash layers, at least 25, are confirmed in those sediments and 12 of them are available as good marker beds. To those volcanic ash layers, the names of the Biroku (Br), Higashidani (Hd), Ichinohara (Ic), Minamidani-1 (Md-1), Minamidani-2 (Md-2), Ninose (Ni), Otsujishinden (Ot), Bando-1 (Bd-1), Bando-2 (Bd-2), Sonohara (Sn), Pumice (Pu) and Rokkoku (Rk) volcanic ash layer in ascending order (Takemura, 1978). 55 samples were collected from volcanic ash layers for NRM measurement along 7 routes.

Methods and Results

Fig.2 shows the sampling localities of the ash layers. Hand samples were collected carefully from a fine part of volcanic ash layer. Collected samples were divided into some specimens, which were mounted in cubic plastic capsules of 2cm in each side. The NRM's of specimen were

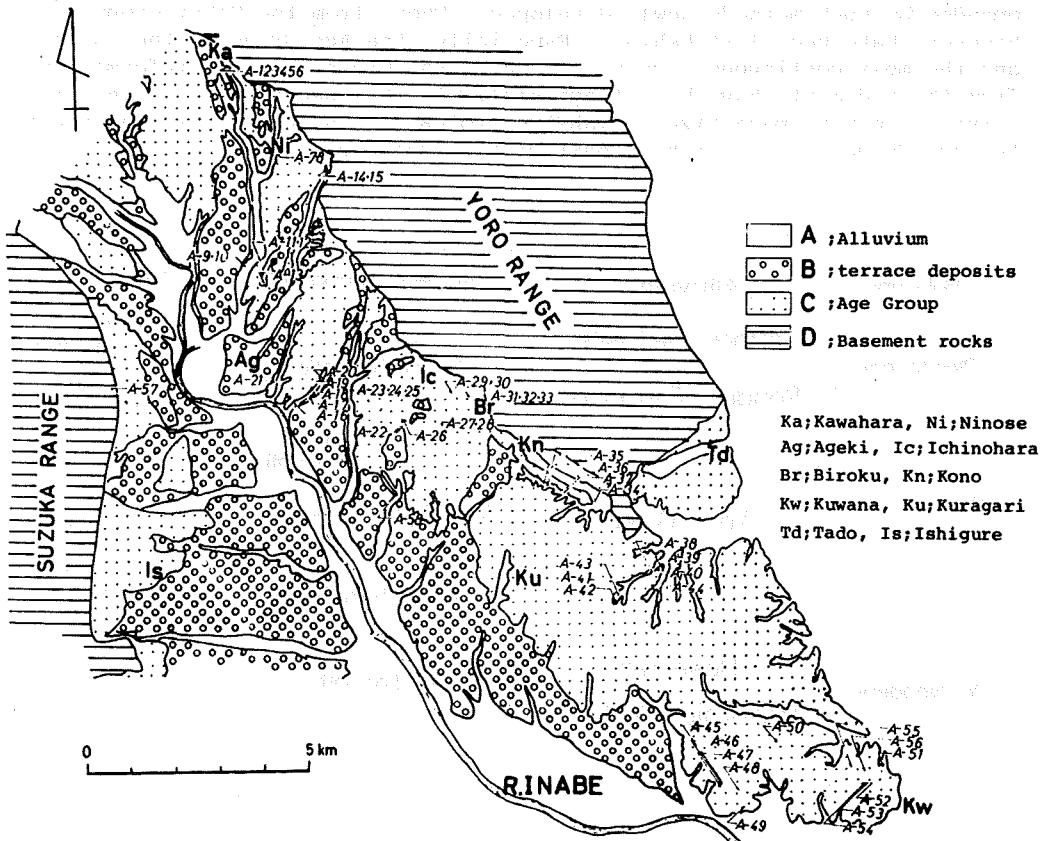


Fig.2 Map showing the sampling sites for NRM measurement

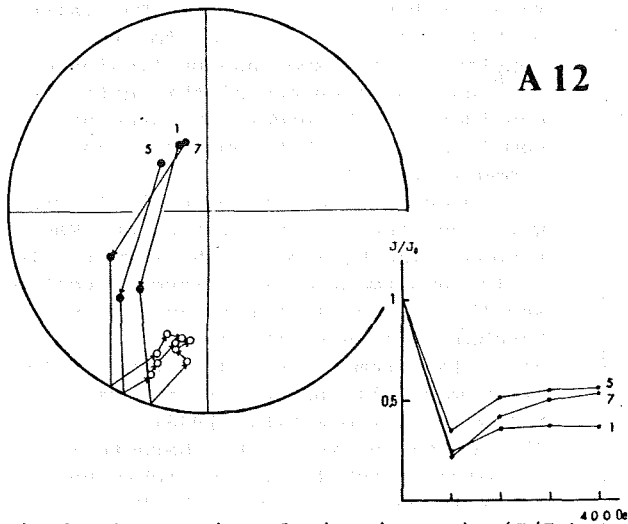


Fig.3 Changes in relative intensity (J/J_0) and direction with progressive alternating field demagnetization of the NRM of A-12 (Pumice volcanic ash layer)

below the Bd-2. The ash layers between Md-2 and Hd ash layer have normal polarity. On the other hand, those below Hd ash layer have reversed polarity.

measured with the Schonstedt spinner magnetometer (SSM-1A). Progressive alternating field demagnetization was carried out on three or five pilot specimens from each site, in steps in peak field value of 100, 200, 300 and 400 Oe. Most of the specimens show stable remanence except a few which have fairly low intensity of remanence. They are A-14, A-24, A-25, A-30 and A-50. Significant removal of normal secondary component is observed for Pumice and Ninose volcanic ash layer as shown in Fig.3.

These results are summarized in Table 1. From the result shown in Table 1 and Fig.1, it is evident that the ash layers above Md-2 have reversed polarity except for the unnamed ash layer just

Table 1 Results of NRM measurement

Sample No.	Locality No.	Locality	Volcanic ash layer	Magnetic polarity
A-9	YA 1358	Mukohira	unnamed	R
A-11	YA 1359	Mukohira	Pumice v.a.	R
A-12	YA 1359	Mukohira	Pumice v.a.	R
A-13	YA 63	Nishikaino	Pumice v.a.	R
A-1	YA 1412	Kawahara	unnamed	R
A-2	YA 1412	Kawahara	unnamed	R
A-5	YA 1412	Kawahara	Bando-1 v.a.	R
A-6	YA 1412	Kawahara	Bando-1 v.a.	R
A-7	YA 1357	Ninose	Ninose v.a.	R
A-8	YA 1357	Ninose	Ninose v.a.	R
A-14	YA 67	Koharaisshiki	Ichinohara v.a.	—
A-15	YA 67	Koharaisshiki	Ichinohara v.a.	N
A-21	YA 72	Nishikoyamadani	Rokkoku v.a.	R
A-16	YA 96	Higashikoyamadani	unnamed	R
A-17	YA 109	Higashikoyamadani	unnamed	R
A-18	YA 111	Higashikoyamadani	Pumice v.a.	R
A-19	YA 120	Higashikoyamadani	unnamed	R
A-20	YA 121	Higashikoyamadani	Bando-2 v.a.	R
A-22	YA 289	N.Bandoshinden	Bando-2 v.a.	R
A-25	YA 58	N.Bandoshinden	unnamed	—
A-24	YA 58	N.Bandoshinden	unnamed	—
A-23	YA 58	N.Bandoshinden	Bando-1 v.a.	R
A-26	YA 291	N.Bandoshinden	unnamed	R
A-27	YA 419	S.Ichinohara	Ninose v.a.	—
A-28	YA 419	S.Ichinohara	Ninose v.a.	R
A-29	YA 715	N.Ichinohara	Ichinohara v.a.	N
A-30	YA 715	N.Ichinohara	Ichinohara v.a.	—
A-31	YA 643	Biroku	Biroku v.a.	R
A-32	YA 643	Biroku	Biroku v.a.	R
A-33	YA 643	Biroku	Biroku v.a.	R
A-36	YA 846	Konominamidani	Minamidani-2 v.a.	N
A-35	YA 845	Konominamidani	Minamidani-1 v.a.	N
A-37	YA 811	Konominamidani	Ichinohara v.a.	N
A-34	YA 781	Kono	Biroku v.a.	R
A-44	YA 981	Chikarao	Pumice v.a.	R
A-39	YA 977	Chikarao	unnamed	R
A-40	YA 977	Chikarao	Bando-2 v.a.	R
A-42	YA 1026	Chikarao	Minamidani-1 v.a.	N
A-43	YA 1015	Chikarao	Minamidani-1 v.a.	N
A-41	YA 1025	Chikarao	Ichinohara v.a.	N
A-38	YA 979	Chikarao	Ichinohara v.a.	N
A-45	YA 1449	Nukata	unnamed	R
A-46	YA 1449	Nukata	unnamed	R
A-47	YA 1450	Nukata	unnamed	R
A-48	YA 1461	Nukata	Bando-2 v.a.	R
A-49	YA 1076	Nukata	unnamed	N
A-50	YA 1161	Okushinden	Bando-1 v.a.	—
A-51	YA 1133	Nishibessho	Pumice v.a.	R
A-52	YA 1422	Nishibessho	Bando-2 v.a.	R
A-53	YA 1422	Nishibessho	Bando-1 v.a.	R
A-54	YA 1422	Nishibessho	unnamed	R
A-56	YA 1404	Nishibessho	Minamidani-2 v.a.	N
A-55	YA 1137	Nishibessho	Higashidani v.a.	N
A-57	SA 91	River Tashida	Ichinohara v.a.	N

Discussion

Adding to the above-mentioned results of NRM measurements, the following data are available for magnetostratigraphy.

1). Fission track age of the Ichinohara volcanic ash layer at YA 888 in Kono is 3.0m.y. Fission track age of the Rokkoku volcanic ash layer at

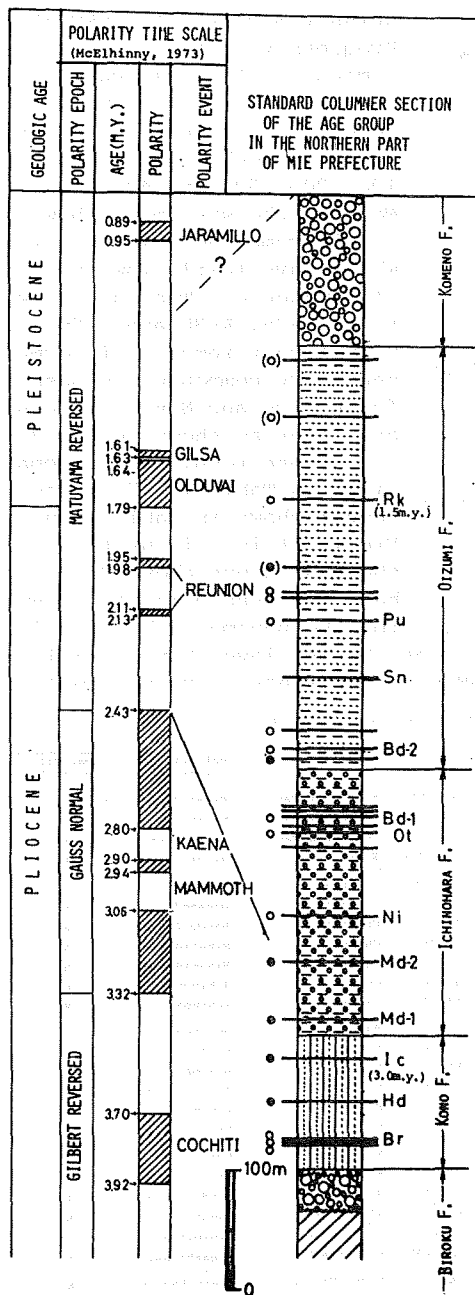


Fig.4 Magnetostratigraphy of the Agé Group in the northern part of Mie Prefecture (); Data by Maenaka et al. (1977)

○ ; reversed polarity
● ; normal polarity

*) Dr. Takuo Yokoyama; Doshisha University

YA 72 in Rokkoku is 1.5m.y. The value of $6.85 \times 10^{-7}/y^{-1}$ is used for the decay constant of the spontaneous fission of U^{238} and the accuracy of this data is considered to be under 20% concerning sample errors (T.Yokoyama, personal communication*).

2). Occurrences of *Stegodon akashiensis* were reported at Kaminoyamada and Kamikasada. The horizon of the former site is the uppermost of the Oizumi Formation, and that of the latter is just above the Sonohara volcanic ash layer.

3). Plant remains yielded from the Agé Group were all included in the range of *Metasequoia flora*(Miki, 1948).

4). On the basis of the characteristics of volcanic ash layer, the Ichinohara ash layer is correlated with the Masugi ash layer and the Pumice ash layer is correlated with the Mushono ash layer in the Kobiwako Group.

It can be considered that the Agé Group in the northern part of Mie Prefecture deposited in the age between the Gauss Normal Epoch and the early Matuyama Reversed Epoch(Fig.4).

References

- Hayashida,A., T.Yokoyama, K.Takemura, T.Danbara and S.Sasajima(1976) *Paleolim.Lake Biwa Japanese Pleist.*, 4, 96
- Ikebe,N.(1956) *Proc.8th Pacific Congr.*, 2, 446
- Ishida,S., K.Maenaka and T.Yokoyama(1969) *Jour.Geol.Soc.Japan*, 25, 183
- Maenaka,K., T.Yokoyama and S.Ishida(1977) *Quat.Res.(USA)*, 7, 341
- Miki,S.(1948) *Mineral.Geol.*, 9, 3
- Nishimura,S. and S.Sasajima(1970) *Chikyu Kagaku*, 24, 222
- _____ and T.Yokoyama(1973) *Proc.Japan Acad.*, 49, 615
- _____ and _____(1974) *Paleolim.Lake Biwa Japanese Pleist.*, 2, 38
- _____ and _____(1975) *ibid.*, 3, 138
- Takemura,K.(1978) *Master Thesis of Kyoto University*
- Torii,M., S.Yoshikawa and M.Itihara(1974) *Rockmagnetism and Paleogeophysics*, 2, 34

PALEOMAGNETIC RESULTS AND FISSION TRACK AGES OBTAINED FROM
THE WESTERN AND NORTHERN SULAWESI, EAST INDONESIA.

By

Sadao SASAJIMA*, Susumu NISHIMURA**, Kimio HIROOKA***,
Yoichiro OTOFUJI*, Theo Van LEEUWEN**** and Fred HEHUWAT*****

- * Dep. Geology and Mineralogy, Kyoto Univ., 606 Sakyo Kyoto, Japan
- ** Inst. Earth Science, Kyoto Univ., 606 Sakyo Kyoto, Japan
- *** Inst. Earth Science, Toyama Univ., 930 Gohoku, Toyama, Japan
- **** P. T. Rio Tinto Indonesia, Cilandak Commercial Estate Bld. 411,
Cilandak, Kebeyoran Timur, Jakarta, Indonesia
- ***** National Inst. Geology and Mining-LIPI, Jl. Cisitu No. 21, Bandung,
Indonesia

1. Introduction

Fairly large number of speculations about the tectonic history of Sulawesi have so far been reported in close association with whose complex feature of geology and geophysical characteristics. The most noticeable ones among them would be those by Katili (1975, 1978), Audley-Charles et al. (1972) and Audley-Charles (1974). They have mentioned in their publications that those ideas should be confirmed by the paleomagnetic method before establishment. On the other hand, based on the reconnaissance paleomagnetic survey in southwest and southeast Sulawesi, Haile (1978) substantiated quite separate paleogeographic positions of these two regions at the Early

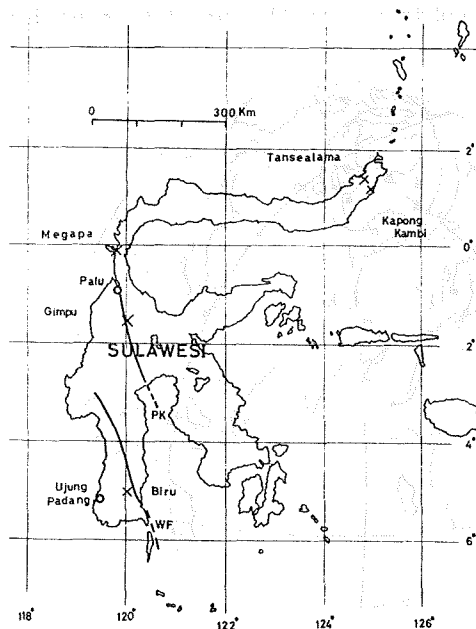


Fig 1. Location map showing the sampling sites.
x = the sampling sites.
PK: Palu-Koro fault. WF: Watampone fault.

Cretaceous period. One of our main purposes of studies is to choose the most plausible one from various hypotheses.

Reconnaissance paleomagnetic investigation combined with the fission track age dating in Sulawesi, Indonesia has been carried out. Most rock samples were collected from the Biru area (E120.2°, S5.0°), east of Ujung Padang (Makassar), Southwest Sulawesi, where the geological map (1/50,000 scale) was already completed by the P. T. Rio Tinto Bethlehem Indonesia. The other spot samplings were performed around Palu and the southern area of Menard. The sampling localities are shown in Fig. 1.

2. Geologic setting

Recently, geological map of the whole Sulawesi has been published by the geological survey of Indonesia (Sukanto, 1975). But detailed geologic map with a large scale is not well established, excepting a few area.

As shown in Fig. 1, the most prominent faults in Sulawesi, the Watampone fault and Palu-Koro strike-slip fault (Tjia and Zakaria, 1974), pass near our sampling areas, therefore, special cares were paid in collecting undisturbed rock-samples. In the Biru area there develop various kinds of Neogene volcanic complex overlaid with granodiorite and shallow neritic sedimentary formations with the age of the Eocene to the Late Cretaceous. The broad stratigraphic sequence along with the sampling sites in the Biru Area is schematically shown in Table 1. Samples for paleomagnetic study were taken from 18 sites in the Biru area and the other 5 sites in the northern regions.

3. Results

Several number of samples from acid igneous rocks and tuffs with different horizons were subjected to the age determination by use of the



Fig 2. Paleomagnetic Poles since the Late Cretaceous.

- K: the Late Cretaceous
- LM: the Paleocene to the Early Miocene
- R: the Middle Miocene to the Recent

Table 1. Fission-track age of Zircons

Sample	No. of grain	Spontaneous fission-track density (cm ⁻²)	Induced fission-track density (cm ⁻²)	Fission-track age (years)
Langi	1	7.47 x 10 ⁶ = ρ _s	5.15 x 10 ⁶ = ρ _i	62 x 10 ⁶ = T
Volcanics	2	6.61	4.35	65
	3	5.11	3.57	61
	4	6.12	4.08	64
	5	7.25	4.71	66
	6	5.67	4.05	60
				63 ± 2.2

Neutron dose = 0.70 x 10¹⁵ (cm⁻²) = Φ

ID 108	1	1.65 x 10 ⁶	4.25 x 10 ⁶	25
	2	1.08	3.86	18
	3	1.21	5.21	15
	4	1.11	3.56	20
	5	1.20	5.15	15
	6	1.50	5.07	19
				19 ± 3.4

Neutron dose = 1.05 x 10¹⁵ (cm⁻²).

Pammusurang Volcanic Complex	1	1.63 x 10 ⁶	3.88 x 10 ⁶	18
	2	1.43	5.10	12
	3	1.07	4.57	10
	4	1.10	3.92	12
	5	1.60	5.25	13
	6	2.20	5.89	16
	7	0.89	3.78	10
				13 ± 2.8

Neutron dose = 0.70 x 10¹⁵ (cm⁻²)

$$(T = 6.12 \times 10^{-8} \cdot \frac{\rho_s}{\rho_i} \cdot \Phi)$$

Table 2. Stratigraphic Sequence of Sampling Site in the Biru Area

Geological Age	Thickness (m)	Lithological Unit	Fission Track Age	Paleomagnetic Sampling Site*
Pliocene	350 +	Lemo Volcanics		ID 114, ID 115
		~~~~~		
Upper to Middle Miocene	250	Pammusurang Volcanic Complex	13 m.y. (ID 116)	ID 116, ID 117 ID 118
		~~~~~		
		Intrusion of Granodiorite and Quartzdiorite	19 m.y. (ID 108)	ID 101, ID 108 ID 109, ID 110
		~~~~~		
Mid. Miocene	200 +	Upper Tonassa Limestone		
		~~~~~		
Upp. Eocene	100-250	Lower Tonassa Limestone		ID 103
		~~~~~		
Paleocene	400 +	Langi Volcanics	63 m.y. (≈ID 105)	ID 102, ID 104 ID 105, ID 106 ID 107
		~~~~~		
		relation uncertain? (not exposed)		
Upp. Cretaceous	1000 +	Marada Sandstone		ID 111, ID 112 ID 113

* : Rock kind of the sample can be referred to Table 3.

≈ : Sample for fission track dating was taken from the intercalated tuff layer within Andesite lavas; its sampling site was near the paleomagnetic sampling site ID 105.

~~~~~ : unconformity

———— : conformity

fission track dating technique. A few samples which contained considerable euhedral zircon crystals with rich U-concentration has been determined their ages. Detailed description of the dating method can be referred to the previous paper by Nishimura (1973). The results so far obtained are listed in Table 1 and 2.

The remanent magnetizations of the specimen before and after stepwise a.f.-demagnetization treatments were measured by means of a spinner magnetometer (Schonstedt SSM-1A). After the remanent stability tests of the pilot specimens about a half of samples were discarded from further paleomagnetic research owing to their unreliable nature. The paleomagnetic properties and their relating data are summarized in Table 3. In the second column of this table, the star-marked samples are discarded in calculating the paleomagnetic poles.

#### 4. Discussion

From the Table 3 it appears that since the middle Miocene (13 m.y. BP.) to the Recent all the VGPs significantly group about the present north pole, suggesting that the paleomagnetic pole position is consistent with the north pole within the range of errors. Contrary to this, the VGPs for pre-Middle Miocene rocks show more or less scattered distribution. It may be very difficult to lead the reasonable unique explanation of the paleomagnetic feature based on these lesser grouping of VGPs. Needless to say, such a divergence of the VGPs cannot be reconciled merely with the polar wandering and the paleosecular variation for the period concerned. The fact might be explained by the occurrence of a revolutionally intense tectonic event which has resulted in a fairly large anticlockwise rotation ( $-45^\circ$ ) of the southwestern Sulawesi during the interval ranging 63 to 13 m.y., most probably 19-13 m.y. BP..

Another reason of the lesser grouping of the VGPs can be explained by the extensive block movements of which tilting corrections were not possible because of the igneous nature of the samples. A large number of faults parallel to the Palu-Koro fault and their conjugate minor faults which are existing in the Biru area should have caused extensive differential movements of the faulted blocks. If we assume that the scatter of VGPs is mostly resulted from the block movements and the paleosecular variation, we can almost regard the average VGPs as the representative of the paleomagnetic pole position during the period.

As shown in Fig. 2 the paleomagnetic pole for the period between the Paleocene and the Early Miocene epoch takes the position neighbouring to the Cretaceous paleomagnetic pole position for the Malaya Peninsula ( $E35^\circ$ ,  $N44^\circ$ ; McElhinny et al., 1974). In this instance, the VGPs of ID 104, 106 and 110 are disregarded in calculating the paleomagnetic pole as they are assumed to indicate the transitional poles during polarity reversal. Besides, it is interesting to refer Haile's (1978) recent report that the Cretaceous paleomagnetic poles for the Malaya Peninsula and West Kalimantan ( $E21^\circ$ ,  $N41^\circ$ ), and the Jurassic to Early Cretaceous paleomagnetic pole for the southwest arm of Sulawesi ( $E35^\circ$ ,  $N44^\circ$ ) show a good agreement in each other.

One of his important conclusions is that the three regions have formed part of the same plate which has rotated anticlockwise  $35^\circ$ - $50^\circ$  since the Cretaceous. However, he has failed paleomagnetically to make clear of the time of occurrence of the anticlockwise rotations. In the present study it is inferred that the S.W.-arm of Sulawesi could have been rotated during the time ranging 63 to 13 m.y., most probably in the period, 19-13 m.y. BP.

Very recently Katili (1978) has reported a sophisticated view of the tectonic evolution of Sulawesi since the Miocene, with an emphasis on the

Table 3. Summary of Paleomagnetic Data of Sulawesi

| Geological Age          | Site          | Rock Type     | N      | AC peak field | D         | I        | $\alpha_{95}$ | Long. ( V. G. P. ) | Lat. (N) |
|-------------------------|---------------|---------------|--------|---------------|-----------|----------|---------------|--------------------|----------|
| Recent                  | Tansealama    | Tuff          | 7      | 100           | -13.2     | 10.0     | 4.5           | 50.9E              | 76.3     |
| Pliocene                | Kampong Kombi | Ignimbrite    | 9      | 100           | -5.1      | 15.1     | 2.9           | 86.8E              | 81.8     |
|                         | ID 114        | Tuff          | 11     | 100           | 0.6       | -24.1    | 6.1           | 64.4E              | 82.4     |
| Miocene                 | Megapa        | Granite       | 9      | 200           | -6.4      | 11.1     | 17.2          | 72.1E              | 81.4     |
| Upper to Middle Miocene | ID 118*       | Basalt        | 13     | 200           | -43.6     | -26.4    | 7.6           | 15.0E              | 46.2     |
|                         | ID 116        | Ignimbrite    | 11     | 100           | -2.1      | -10.9    | 3.3           | 16.5E              | 87.8     |
|                         | mean          |               |        |               | -5.1      | -5.2     | 6.8           | 54.9E              | 84.4     |
| Lower Miocene           | ID 101        | Quartzdiorite | 9      | 200           | 127.3     | -32.8    | 3.4           | 55.2E              | 33.2     |
|                         | ID 108        | Granodiorite  | 9      | 200           | -21.9     | -13.3    | 6.4           | 24.4E              | 68.1     |
|                         | ID 109        | Granodiorite  | 9      | 300           | -67.3     | -6.7     | 12.2          | 28.5E              | 22.9     |
|                         | ID 110*       | Granodiorite  | 8      | 400           | -14.3     | 58.3     | 19.9          | 104.5E             | 44.1     |
| Paleocene               | ID 102        | Andesite      | 11     | 200           | 129.6     | -35.4    | 2.7           | 58.0E              | 34.7     |
|                         | ID 104*       | Andesite      | 6      | 200           | 116.7     | 67.1     | 7.7           | 21.9W              | 20.8     |
|                         | ID 105        | Andesite      | 11     | 200           | -53.9     | -20.7    | 3.8           | 20.4E              | 36.4     |
|                         | ID 106*       | Andesite      | 8      | 200           | -13.0     | 63.0     | 6.4           | 108.0E             | 39.2     |
|                         | ID 107        | Andesite      | 9      | 200           | -23.0     | -19.5    | 10.6          | 16.2E              | 66.7     |
|                         | mean          |               |        |               | -44.8     | 1.3      | 19.6          | 36.5E              | 44.8     |
| Upper Cretaceous        | Gimpu         | Sandstone     | 8      | 200           | 164.1     | 36.2     | 6.5           | 20.8W              | 65.6     |
|                         | ID 112        | Shale         | 10     | 300           | -26.1     | -36.2    | 7.8           | 1.1E               | 61.5     |
|                         | ID 113        | Sandstone     | 11     | 200           | -0.5      | -20.2    | 8.1           | 54.8W              | 84.6     |
|                         | mean          |               |        |               | -14.2     | -32.3    | 21.7          | 13.2W              | 71.3     |
| Location                |               |               |        |               |           |          |               |                    |          |
|                         | Tansealama    | 124°50'E      | 1°21'N |               | Gimpu     | 120°04'E | 1°42'S        |                    |          |
|                         | Kampong Kombi | 124°57'E      | 1°15'N |               | Biru (ID) | 120°10'E | 5°02'S        |                    |          |
|                         | Megapa        | 119°52'E      | 0°10'S |               |           |          |               |                    |          |

characteristics of the mobile zone tectonics. He has discussed the past and present geotectonic position of Sulawesi by elaborating on his previous idea of the westward thrust of Sulawesi to the direction of the Asian Continent (Katili, 1975).

In such circumstances, it is probable to consider that the proposed welding of both the western and eastern Sulawesi during the Pliocene epoch by Katili (1978) is modified in age as being 19-13 m.y. BP., the early to middle Miocene. Besides, the bending of the northern Sulawesi during the welding (Katili, 1978) was not evidenced by the present paleomagnetic studies.

It might be supposed with some reservation that the assumed anticlockwise rotation (about 45 degrees) of the S.W.-arm of Sulawesi during the period 19-13 m.y. BP. was caused by the anticlockwise rotation of New Guinea (Green and Pitt, 1967) and/or the northwestwards drift of New Guinea that was thought by Audley-Charles et al. (1972).

Our Cretaceous VGPs are too small in number to average out the paleosecular variation of the period, but when we assume the mean VGPs as the paleomagnetic pole, it is significantly apart from the Cretaceous three paleomagnetic poles mentioned above. We have no convincing explanation of the discrepancy. Discussion on the discrepancy of two Cretaceous paleomagnetic poles those by Haile (1978) and the present authors from the S.W.-arm of Sulawesi should be awaited further paleomagnetic investigations.

## 5. Conclusion

If we accept the tectonic evolution proposed by Katili it may be better to regard his welding time of the Pliocene as the early to middle Miocene epoch (19-13 m.y.). By this improvement the intense tectonic movement is much reasonably understood by the supposed anticlockwise rotation of New Guinea during the Miocene (Green and Pitt, 1967) and westward rapid movement of New Guinea (Audley-Charles et al, 1972).

Furthermore, our paleomagnetic result since the middle Miocene to the Recent cannot prove the bending of the northern part of the western Sulawesi during and subsequent to the welding of the eastern Sulawesi at the Pliocene epoch (Katili, 1978).

The Cretaceous paleomagnetic poles from the S.W.-arm of Sulawesi obtained by Haile (1978) and the present authors are not consistent, however, the hypothesis of the Gondwana origin of the western Sulawesi (Ridd, 1971; Audley-Charles et al., 1972) cannot be supported by all of them.

## References

- Audley-Charles, M. G., Carter, D. J. and Milsom, J. S. (1972) *Nature Phys. Sci.*, 239, 35-39.
- Audley-Charles, M. G., Carter D. J. and Milsom, J. S. (1974) *Geol. Soc. London Spec. Publ.* 4, 365-378.
- Green, R. and R. P. B. Pitt (1967) *J. Geomag. Geoelectr.* 19, 317-321.
- Haile, N. S. (1978) *Tectonophysics*, 46, 77-85.
- Haile, N. S., M. W. McElhinny and I. McDougall (1977) *Jour. Geol. Soc. Lond.* 133, 133-144.
- Katili, J. A. (1975) *Tectonophysics*, 26, 165-188.

- Katili, J. A. (1978) *Tectonophysics*, 45, 289-322.
- McElhinny, M.W., N.S. Haile and A.R. Crawford (1974) *Nature*, 252, 641-645.
- Nishimura, S. and T. Yokoyama (1973) *Proc. Jap. Acad.* 49, 615-618.
- Ridd, M.F. (1971) *Nature*, 234, 531-533.
- Sukanto, R. (1975) *Geologic map of Indonesia, sheet VIII: Ujung Padang, Scale 1:1,000,000. Geol. Surv. Indonesia.*
- Tjia, H. D. and T. Zakaria (1974) *Sains Malaysia*, 3, 65-86.

( to be submitted to *Tectonophysics*.)

AN EVIDENCE FOR THE OCCURRENCE OF ABOUT 80 M.Y. VOLCANIC  
ACTIVITY IN THE DECCAN TRAPS, INDIA

Ichiro KANEOKA

Geophysical Institute, University of Tokyo, Bynkyo-ku, Tokyo 113

The Deccan Traps, the largest lava plateau in the world with the volume of about  $(0.5 - 1) \times 10^6 \text{ km}^3$ , are mainly composed of tholeiitic basalts with minor amount of alkaline rocks (Kuno, 1969). From geochronological and paleomagnetic studies, they were estimated to have mainly erupted in relatively short period of several million years about 60 - 65 m.y. ago (Rama, 1968; Wellman and McElhinny, 1970; Kono et al., 1972; Kaneoka and Haramura, 1973). However, the investigated area are limited in these studies. Furthermore, their ages were determined by the K-Ar method whose results are affected by the condition of dated rocks and/or minerals as revealed for some Deccan samples (Kaneoka and Haramura, 1973). Deccan rocks are easily altered due to the climatic conditions, which apparently reduces the K-Ar age. Hence, there remains a possibility that an older volcanic activity of more than 65 m.y. occurred in the Deccan Traps. In this note,  $^{40}\text{Ar}$ - $^{39}\text{Ar}$  ages for two Deccan basalts in the western Ghat mountain are reported, which revealed the occurrence of about 80 m.y. volcanic activity in the Deccan Traps. The  $^{40}\text{Ar}$ - $^{39}\text{Ar}$  ages for the other regions were also determined and they generally show the ages of more than 60 m.y. Since the difference in the age from the same site is most typically seen for Igat Puri samples, they have been chosen to demonstrate the occurrence of an older volcanic activity than 65 m.y.

Fifteen successive lava flows with about 290 m thickness in total are exposed as a section between Kasara ( $19^\circ 40' \text{N}$ ,  $73^\circ 29' \text{E}$ ) and Igat Puri ( $19^\circ 42' \text{N}$ ,  $73^\circ 34' \text{E}$ ) about 105 km to the north east of Bombay. Samples were collected from this section by the Indo-Japanese scientific team as a joint program of Deccan basalt studies during the winter of 1972 and 1973. Among them, two samples were selected for  $^{40}\text{Ar}$ - $^{39}\text{Ar}$  dating from the uppermost and nearly the lowest lava flows to study the age difference between these lava flows.

The sample IG 15 is a tholeiitic olivine-augite basalt from the uppermost part of the successive lava flows, which is composed of olivine and augite phenocrysts with subophitic texture (Aramaki, personal communication, 1978). Olivine is partly altered. Groundmass is composed of clinopyroxene, plagioclase, some opaque minerals and partly altered mesostasis. The sample IG 02 was taken from the second flow from the bottom, which is also a tholeiitic olivine-augite basalt with similar mineralogical composition to IG 15.

These samples were dated by the  $^{40}\text{Ar}$ - $^{39}\text{Ar}$  method. Bern 4M (muscovite) was used as an age standard and the ages were calculated by using the newly recommended values for the decay of  $^{40}\text{K}$  (Steiger and Jäger, 1977).

The results are shown in Fig. 1a and b. As shown in Fig. 1a, all temperature fractions for the sample IG 15 lie well on the isochron with the age of 63.8 m.y. The intercept gives a

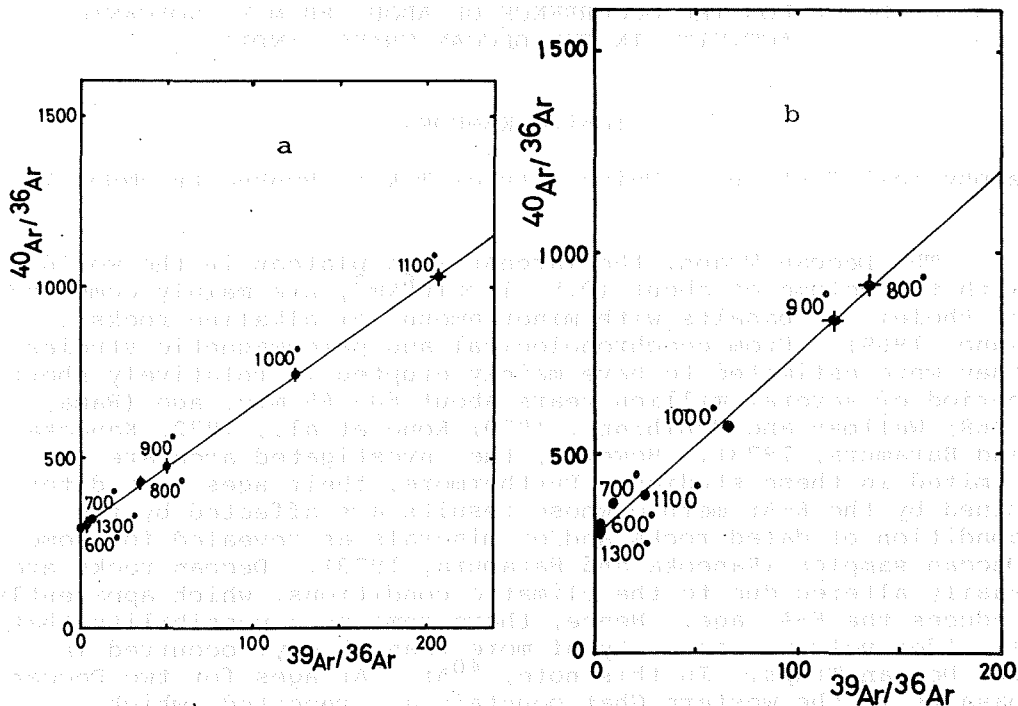


Fig. 1.  $^{40}\text{Ar}$ - $^{39}\text{Ar}$  isochron diagrams for olivine-augite basalts from Igat Puri in the Deccan Traps.

Samples were heated for one hour at each temperature which is indicated by figures at each plot. Horizontal and vertical bars at each plot indicate  $1\sigma$  (sigma) error range. Bern 4M muscovite (18.7 m.y.) was used as an age standard. All necessary corrections including those for interference products have been made.

(a) Sample IG 15; age:  $63.8 \pm 1.1$  m.y.; intercept:  $294.6 \pm 2.6$ ,

(b) Sample IG 02; age:  $83.6 \pm 4.2$  m.y.; intercept:  $258.3 \pm 19.3$ .

nearly atmospheric value for the  $^{40}\text{Ar}/^{36}\text{Ar}$  ratio. When the previously obtained K-Ar ages are recalculated by using the new decay constants for  $^{40}\text{K}$ , the apparent K-Ar ages increase by only about 0.3 m.y. for the age range of about 60 m.y. Hence, the age for the sample IG 15 is in very good accordance with the previously estimated ages for Deccan basalts.

On the other hand, the sample IG 02 shows an isochron which corresponds to the age of 83.6 m.y. for the  $800^\circ$  -  $1300^\circ\text{C}$  temperature fractions. The intercept for the  $^{40}\text{Ar}/^{36}\text{Ar}$  ratio seems to be a little lower than the atmospheric value, but cannot be discriminated from it due to its relatively large uncertainty. The  $700^\circ\text{C}$  fraction is apparently deviated to a little higher  $^{40}\text{Ar}/^{36}\text{Ar}$  ratio from the isochron, which may have been caused by loosely trapped radiogenic  $^{40}\text{Ar}$ . In spite of this, the total  $^{40}\text{Ar}$ - $^{39}\text{Ar}$  age for this sample shows a value of 83.9 m.y., which is essentially the same as that determined from the isochron. From the data array in Fig. 1b and the concordance between these ages, it is unlikely that this old age was caused due to the occurrence of excess  $^{40}\text{Ar}$  in this

sample.

These results suggest that there is a large age gap by about 20 m.y. between the lava flows for the samples IG 02 and IG 15. Although several gaps are observed geologically among the intermediate lava flows in this section (Aoki, personal communication, 1978), we cannot identify which boundary corresponds to the large age gap at present. Present results further give a clear evidence that an older volcanic activity of more than 65 m.y. occurred in the Deccan Traps, though it is not yet known to what extent it occurred. This fact may be an important key for clarifying the formation mechanism of the Deccan Traps. Even if the most lava flows might have extruded about 60 - 65 m.y. ago, the precursors had already extruded before that time at least by about 20 m.y. in the Deccan Traps.

Alkaline rocks from Girnar Hill and Pavagarh Hill seem to show almost the same or even a little older K-Ar ages than tholeiitic rocks from other localities (Kaneoka and Haramura, 1973). If we follow the hypothesis that alkaline rocks extrude after tholeiitic rocks during a series of magmatic differentiation, the above mentioned alkaline rocks may have belonged to the series of older volcanic activity than 65 m.y.

#### References

- Kaneoka, I. and H. Haramura (1973) *Earth Planet. Sci. Lett.*, 18, 229.  
Kono, M., H. Kinoshita and Y. Aoki (1972) *J. Geomag. Geoelectr.*, 24, 49.  
Kuno, H. (1969) *Amer. Geophys. Union, Geophys. Monogr.*, 13, 495.  
Rama, S.N.I. (1968) *22nd Int. Geol. Congr. 1964, New Delhi*, Pt. VII, 139.  
Steiger, R.H. and E. Jäger (1977) *Earth Planet. Sci. Lett.*, 36, 359.  
Wellman, P. and M.W. McElhinny (1970) *Nature*, 227, 595.

<sup>40</sup>Ar-<sup>39</sup>Ar AGES OF SOME YAMATO METEORITES FROM ANTARCTICA

Ichiro KANEOKA, Minoru OZIMA and Masahisa YANAGISAWA

Geophysical Institute, University of Tokyo, Bunkyo-ku, Tokyo 113

Yamato meteorites were firstly found in East Antarctica in 1969 by the Japanese Antarctic Research Expedition team (Yoshida et al., 1971). Since then, more than 1000 meteorites have been collected, among which all kinds of meteorites are included. In the present study, <sup>40</sup>Ar-<sup>39</sup>Ar ages of four Yamato meteorites are reported.

Investigated samples are : Yamato 74640 (H5-6), Yamato 74190 (L5-6), Yamato 74159 (Eucrite) and Yamato 74097 (Diogenite). USGS standard LP-6 (biotite) was used as the age monitor. Samples were heated for one hour at each temperature, ranging from 600°C to 1500°C. Ar extraction and measurement were made separately. For correcting interference Ar isotopes, following values were used by measuring neutron irradiated CaF<sub>2</sub> and K<sub>2</sub>SO<sub>4</sub>; (<sup>39</sup>Ar/<sup>37</sup>Ar)<sub>Ca</sub> = 7.0 x 10<sup>-4</sup>, (<sup>38</sup>Ar/<sup>37</sup>Ar)<sub>Ca</sub> = 3.9 x 10<sup>-3</sup>, (<sup>36</sup>Ar/<sup>37</sup>Ar)<sub>K</sub> = 5.5 x 10<sup>-4</sup>, (<sup>40</sup>Ar/<sup>39</sup>Ar)<sub>K</sub> = 7.0 x 10<sup>-2</sup>, (<sup>38</sup>Ar/<sup>39</sup>Ar)<sub>K</sub> = 6.7 x 10<sup>-2</sup>. After necessary corrections were made, <sup>40</sup>Ar/<sup>39</sup>Ar ages were calculated by using newly recommended decay constants for <sup>40</sup>K (Steiger and Jäger, 1977), which gives apparently younger ages by about 0.1 b.y. for the samples of about 4.5 b.y. compared to the older decay constants.

Fig. 1 shows the result for Yamato 74640. Although the lower temperature fractions show younger ages than the higher temperature ones, the apparent <sup>40</sup>Ar-<sup>39</sup>Ar ages increase to a plateau age of 4.41 ± 0.07 (1σ) b.y., which is represented by 1000° - 1350°C fractions, covering about 61% of the released <sup>39</sup>Ar. Although the 1500°C fraction apparently shows a higher

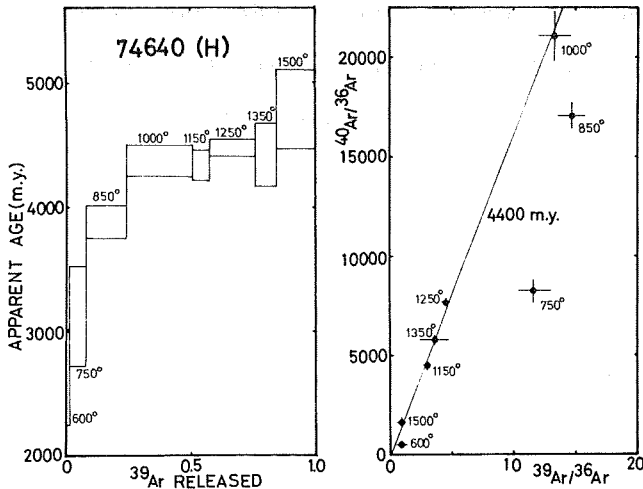


Fig. 1. <sup>40</sup>Ar-<sup>39</sup>Ar age diagram and <sup>40</sup>Ar/<sup>36</sup>Ar - <sup>39</sup>Ar/<sup>36</sup>Ar diagram for Yamato 74640 (H5-6). The uncertainties correspond to 1σ. The numbers in the figure indicate the degassing temperatures in Centigrade.

<sup>40</sup>Ar-<sup>39</sup>Ar age, we cannot give much weight on this value due to its large uncertainty. In the <sup>40</sup>Ar/<sup>36</sup>Ar - <sup>39</sup>Ar/<sup>36</sup>Ar diagram, the higher temperature fractions form a good isochron corresponding to 4.4 b.y., which goes through the zero point. Considering that the age of 4.4 b.y. corresponds to the age of 4.5 b.y. calculated by the old decay constants, we conjecture that the plateau age of 4.41 b.y. probably represents the time of formation for this sample. This value agrees well with those of other H-chondrites deter-

mined by  $^{40}\text{Ar}$ - $^{39}\text{Ar}$  method. For this sample, K-content is estimated to be  $800 \pm 150$  ppm by comparing the total  $^{39}\text{Ar}$  content with that of the standard sample (LP-6). Ca-content is also estimated to be  $1.0 \pm 0.2\%$  from the total  $^{37}\text{Ar}$  content.

On the other hand, Yamato 74190 shows completely different  $^{40}\text{Ar}$ - $^{39}\text{Ar}$  age pattern. In the  $600$ - $880^\circ\text{C}$  temperature fractions, about 46% of  $^{39}\text{Ar}$  released, where a lower plateau age of  $0.36 \pm 0.02$  b.y. is indicated. The apparent  $^{40}\text{Ar}$ - $^{39}\text{Ar}$  age increases gradually up to 1.3 b.y. in the highest temperature ( $1450^\circ\text{C}$ ) fraction. However, the  $920^\circ\text{C}$  and  $1050^\circ\text{C}$  fractions still show relatively young  $^{40}\text{Ar}$ - $^{39}\text{Ar}$  ages of 0.44 and 0.47 b.y. respectively. About 90% of  $^{39}\text{Ar}$  was released until  $1050^\circ\text{C}$  fraction. Such pattern is quite similar to those observed in many L-chondrites (Turner, 1969), which implies at least one major outgassing event for these L-chondrites about 0.3-0.5 b.y. ago. For present sample, the outgassing event may be suggested to be about 0.36 b.y. ago from the lower plateau age. Considering that such young event has not been observed for L-chondrites by other dating methods such as Pb-Pb and Rb-Sr methods, we conjecture that the outgassing event should have been short enough and the meteorites were never melted completely to keep solid elements in a closed system. Collision of L-chondrites is one of the most likely process for this event. K- and Ca-contents are estimated to be  $810 \pm 150$  ppm and  $0.69 \pm 0.14\%$ , respectively, for this sample from the total amounts of  $^{39}\text{Ar}$  and  $^{37}\text{Ar}$ .

Fig. 2 indicates the result for Yamato 74159, which shows a good plateau age of  $4.08 \pm 0.05$  b.y. for  $730^\circ\text{C}$ - $1250^\circ\text{C}$  fractions together with an isochron of the similar age. The higher temperature fractions ( $1350^\circ\text{C}$  and  $1500^\circ\text{C}$ ) indicate a higher  $^{40}\text{Ar}$ - $^{39}\text{Ar}$  age of about 4.4 b.y., though the uncertainty in these fractions is large (about 0.3 b.y.). The plateau age of about 4.1 b.y. is quite similar to that observed for Pasamonte (Podosek and Huneke, 1973). Furthermore, Takeda et al. (1978) reports that the Yamato 74159 is an eucritic polymitic breccia which has similar properties with Pasamonte with regards to the texture and pyroxene chemical trend.  $^{40}\text{Ar}$ - $^{39}\text{Ar}$  dating result is in accordance with this observation. Although the intermediate plateau  $^{40}\text{Ar}$ - $^{39}\text{Ar}$  age for Pasamonte agrees well with that of Yamato 74159, Pasamonte shows definitely older Sm-Nd and Pb-Pb ages of about 4.5 b.y. (Unruh et al., 1977). Hence, the age of about 4.1 b.y. probably represents the outgassing event on the achondrite parent body, such as the impact of meteoroids which did not disturb and Sm-Nd and Pb-Pb

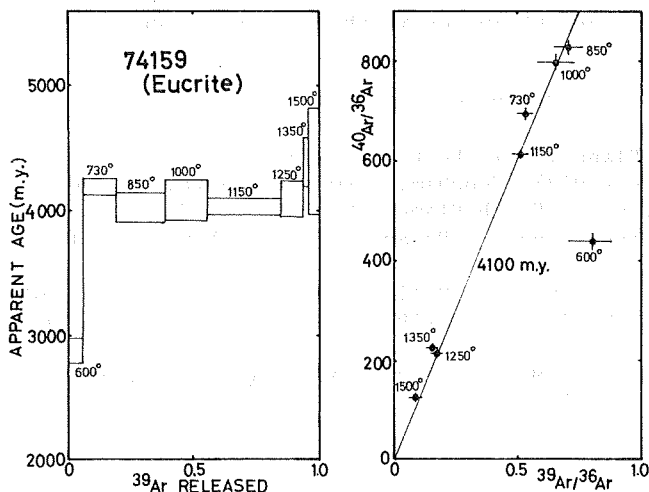


Fig. 2.  $^{40}\text{Ar}$ - $^{39}\text{Ar}$  age diagram and  $^{40}\text{Ar}/^{36}\text{Ar}$  -  $^{39}\text{Ar}/^{36}\text{Ar}$  diagram for Yamato 74159 (Eucrite).

systematics. K- and Ca-contents in this sample are estimated to be  $500 \pm 100$  ppm and  $6.7 \pm 1.3$  %, respectively, from the total amounts of  $^{39}\text{Ar}$  and  $^{37}\text{Ar}$ . These values agree reasonably well with those (K : 580 ppm; Ca : 6.78%) obtained by chemical analyses (Takeda et al., 1978), indicating the chemical characteristics of the basaltic chondrite.

Yamato 74097 shows an inverse staircase  $^{40}\text{Ar}$ - $^{39}\text{Ar}$  age pattern, ranging 1.1-1.3 b.y., whose ages are much younger than those of common achondrites and rather similar to that of Nakhilites (Podosek, 1973). Since the estimated K-content in this diogenite from the integrated  $^{39}\text{Ar}$  amount is less than 50 ppm, however, the calculated ages for this sample have larger uncertainties than the other meteorites. Ca-content is estimated to be  $0.51 \pm 0.10$  %.

Present results on  $^{40}\text{Ar}$ - $^{39}\text{Ar}$  ages are summarized in Table 1.

Table 1. Summary of  $^{40}\text{Ar}$ - $^{39}\text{Ar}$  ages of Yamato-74 meteorites

| Sample                      | Total | $^{40}\text{Ar}$ - $^{39}\text{Ar}$ age<br>minimum | (m.y.)*<br>maximum | Plateau             | Plateau range                                          |
|-----------------------------|-------|----------------------------------------------------|--------------------|---------------------|--------------------------------------------------------|
| Yamato-74640<br>(H5-6)      | 4317  | 2626<br>$\pm 383$                                  | 4790<br>$\pm 328$  | 4407<br>$\pm 71$    | 1000 - 1350°C<br>(61% of $^{39}\text{Ar}$<br>released) |
| Yamato-74190<br>(L6)        | 443.2 | 338.4<br>$\pm 35.5$                                | 1329<br>$\pm 103$  | 357.4<br>$\pm 32.4$ | 600 - 880°C<br>(46% of $^{39}\text{Ar}$<br>released)   |
| Yamato-74159<br>(Eucrite)   | 4043  | 2876<br>$\pm 98$                                   | 4398<br>$\pm 423$  | 4075<br>$\pm 49$    | 850 - 1250°C<br>(75% of $^{39}\text{Ar}$<br>released)  |
| Yamato-74097<br>(Diogenite) | 1190  | 1090<br>$\pm 87$                                   | $\sim 1270$        | 1100<br>$\pm 62$    | 1200 - 1500°C<br>(55% of $^{39}\text{Ar}$<br>released) |

\*  $^{40}\text{Ar}$ - $^{39}\text{Ar}$  age was calculated by using the following constants for  $^{40}\text{K}$ .  
 $\lambda_e = 0.581 \times 10^{-10} \text{yr}^{-1}$ ,  $\lambda_\beta = 4.962 \times 10^{-10} \text{yr}^{-1}$ ,  $^{40}\text{K}/\text{K} = 1.167 \times 10^{-4}$   
(Steiger and Jäger, 1977). Uncertainties in the ages represent  $1\sigma$ .

#### References

- Podosek, F.A. (1973) *Earth Planet. Sci. Lett.*, 19, 135.  
Podosek, F.A. and J.C. Huneke (1973) *Geochim. Cosmochim. Acta*, 37, 667.  
Steiger, R.H. and E. Jäger (1977) *Earth Planet. Sci. Lett.*, 36, 359.  
Takeda, H., M. Miyamoto, K. Yanai, and H. Haramura (1978) *Mem. Nat. Inst. Polar Res.*, 8, 170.  
Turner, G. (1969) *Meteorite Research*, P. Millman (ed.), Reidel Publ., 407.  
Unruh, D.M., N. Nakamura, and M. Tatsumoto (1977) *Earth Planet. Sci. Lett.*, 37, 1.  
Yoshida, M., H. Ando, K. Omoto, R. Naruse, and Y. Ageta (1971) *Antarct. Rec.*, 39, 62.

# PALEOINTENSITIES OF THE GEOMAGNETIC FIELD DETERMINED FROM RECENT FOUR LAVA FLOWS OF SAKURAJIMA VOLCANO

Hidefumi TANAKA

Department of Applied Physics, Tokyo Institute of Technology, Meguro-ku, Tokyo 152

## 1. Introduction

Sakurajima Volcano, located in Kagoshima Bay, southern Kyushu, Japan, has frequently erupted since the 8th century. The lava flows ejected from time to time provide an ideal material for an archeomagnetic study. However, only few paleomagnetic studies have been made of this volcano. Sasajima (1965) made a paleointensity study of the only one sample for each lava by applying the Thellier method. It is therefore worthwhile reexamining the paleointensities of the Sakurajima lavas using many more samples.

This paper aims at reporting the archeomagnetic results obtained by the Thellier method from the Bunmei (1471) and Anei (1779) lavas, and, at the same time, at checking the validity of the present method by comparing the intensities from the Taisho (1914) and Showa (1946) lavas to the actually-observed geomagnetic intensities.

It is believed that the Thellier method (Thellier and Thellier, 1959) is the most reliable method of measuring paleointensities because the linearity in the NRM-TRM diagram (Arai diagram; Nagata et al., 1963) provides, besides the paleointensity estimate, some evidence of the absence of undesirable effects such as changes in TRM characteristics during the heat treatment or superposition of secondary components. It is well known that magnetic properties of rocks often undergo changes during heat treatment in a laboratory (Kono and Tanaka, 1977; Kono, 1974; Coe and Grommé, 1973). In order to shorten the time required for heating and to minimize possible changes of magnetic properties of rock sample due to heat treatment, Kono (1974) proposed to perform the Thellier method by applying only one heating procedure. Although such a modified Thellier method works well in some cases, it is required to set rock samples with a high accuracy of orientation in contrast to the arbitrary sample orientation in the case of the ordinary double heating Thellier method.

The ordinary double-heating Thellier method is used in this study. A special furnace with a movable heater as shown in Fig. 1 is prepared for the present experiment in order to shorten the time needed for heating and cooling. Changes of magnetic properties of rock sample due to heat treatment can be made considerably smaller by such a quick experimental procedure. The ordinary Thellier method with double heatings can be performed within a very short time-range of one or two hours.

## 2. Magnetic Properties of Samples

Samples were collected from four lava flows, i.e. Bunmei (1471), Anei (1779), Taisho (1914), and Showa (1946) lavas of

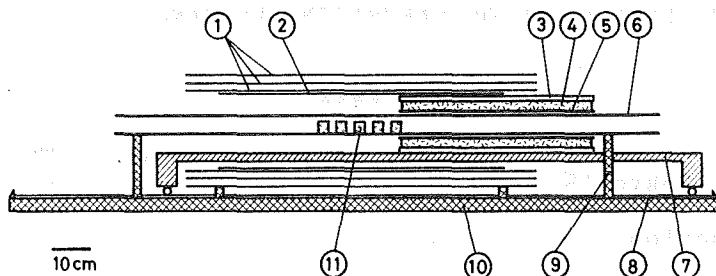


Fig.1. Vertical section of the furnace. 1: three-layer permalloy shield 2: solenoid coil 3: water jacket 4: asbestos 5: outer mullite tube with nichrom heater 6: inner mullite tube (fixed) 7: movable table supporting the water jacket 8: rail on which the table 7 moves 9: stand to hold the inner mullite tube 6 10: table supporting the device 11: sample. The movable heater system (3, 4, 5, and 7) can shorten the time needed for heating and cooling.

Sakurajima Volcano. The orientation was determined by means of a magnetic compass with a level with a possible error of 5 degrees or so. Three to five specimens from each lava flow were used in the paleointensity study, and the directions of natural remanent magnetization (NRM) of these samples are summarized in Table 1.

Changes with temperatures of saturation magnetization ( $J_s$ ) of samples were measured by a magnetic balance in a vacuum of  $10^{-5}$  Torr and a magnetic field of 5 KOe. Samples from the four lava flows contain two phases of ferromagnetic minerals with a high Curie temperature ( $T_c$ ) around 500 - 600 °C and a low  $T_c$  around 300 - 350 °C as listed in Table 1, and the  $J_s$ - $T$  curves are reversible. These facts indicate that titanomagnetite containing 35 - 40 percent ulvöspinel ( $Fe_2TiO_4$ ) is the main magnetic mineral, and that a part of the mineral changed into magnetite ( $Fe_3O_4$ ) through high temperature oxidation. The reversibility of  $J_s$ - $T$  curves indicates that these samples are suitable for paleointensity determination by the Thellier method.

### 3. Paleointensity Determination

Changes in the direction of the NRM component by the progressive heat treatment of the Thellier method are shown in Fig. 2, and the NRM-TRM diagram (Arai diagram) are shown in Fig. 3. The results of intensity determination are summarized in Table 2.

All the five specimens from Bunmei lava flow (1471) gave successful paleointensity values. Specimen SK 1-1-1 is characterized by a low blocking temperature. It appears that the experimental results are affected by unsuitable setting of heating temperatures to some extent, so that relatively short linear relation can be seen on the NRM-TRM diagram. But the estimated intensity of 0.581 Oe for this sample agrees with other values from the Bunmei lava within the error limit.

Table 1. NRM directions and magnetic properties of samples

| Unit           | Age  | Specimen | I    | D     | Jn                    | Low Tc | High Tc |
|----------------|------|----------|------|-------|-----------------------|--------|---------|
| Bunmei<br>lava | 1471 | SK 1-1-1 | 43.5 | 3.6   | $2.17 \times 10^{-3}$ |        |         |
|                |      | SK 1-2-1 | 38.1 | 7.4   | 2.82                  |        |         |
|                |      | SK 1-6-2 | 38.5 | 13.1  | 3.73                  |        |         |
|                |      | SK 1-8-2 | 38.5 | 22.4  | 3.06                  |        |         |
|                |      | SK 1-9-2 | 47.4 | 9.8   | 2.45                  | 319    | 563     |
| Anei<br>lava   | 1779 | SK 2-4-2 | 43.4 | 12.3  | 5.65                  | 303    | 492     |
|                |      | SK 2-8-2 | 37.8 | -2.0  | 4.87                  |        |         |
|                |      | SK 2-9-2 | 41.0 | 0.4   | 4.94                  |        |         |
| Taisho<br>lava | 1914 | SK 3-3-1 | 19.3 | 4.9   | 3.02                  |        |         |
|                |      | SK 3-4-1 | 11.3 | 7.4   | 3.22                  | 341    | 536     |
|                |      | SK 3-8-1 | 8.4  | -3.3  | 1.53                  |        |         |
| Showa<br>lava  | 1946 | SK 4-4-1 | 30.2 | -4.7  | 3.45                  |        |         |
|                |      | SK 4-5-2 | 43.9 | -5.6  | 3.37                  | 361    | 484     |
|                |      | SK 4-6-1 | 49.8 | -11.3 | 1.19                  |        |         |

I: Inclination ( $^{\circ}$ N) D: Declination ( $^{\circ}$ E) Jn: NRM intensity (emu/cc) Tc: Curie temperature ( $^{\circ}$ C)

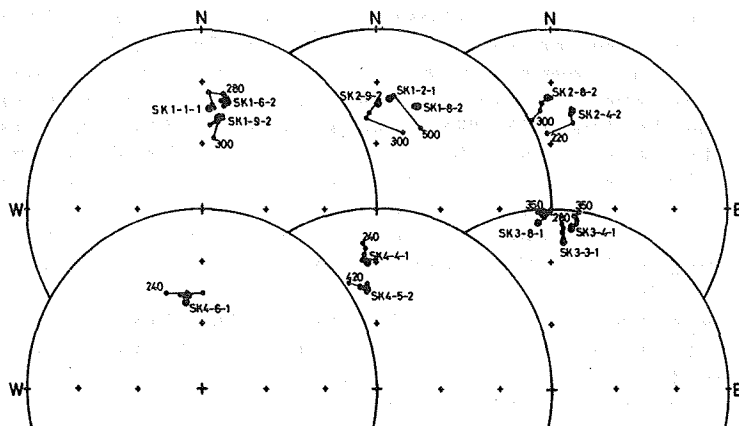


Fig. 2 Changes in the direction of NRM component by the progressive heat treatment of the Thellier method. Numerals indicate the temperature in degrees cintigrade at which deviations from the original NRM directions (indicated by larger circles) amounted to more than 10 degrees. NRM directions at temperatures higher than those are not shown in the figure. Solid and open circles indicate that NRM directions are downward and upward, respectively.

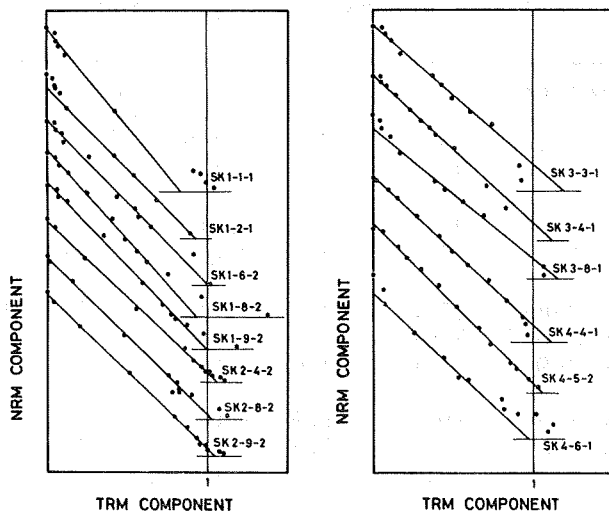


Fig. 3. The NRM-TRM diagram (Arai diagram) in the Thellier method. Intensities are normalized by those of the NRM of individual samples. The horizontal lines indicate the TRM axes for individual samples. Open symbols are the data excluded from the linear regression analyses due to some non-ideal behaviors.

Combining the result with those for other four specimens, the intensity is estimated as  $0.52 \pm 0.04$  Oe for 1471.

The blocking temperatures of three specimens from the Anei lava flow are low, and a small number of points fall on a straight line in the NRM-TRM diagram due to the unsuitable setting of temperatures. But the plots on the diagram fall on a straight line very nicely and the intensity values determined for the three specimens agree well with one another within the error limit. It seems likely, therefore, that these values are reliable. The mean intensity is obtained as  $0.46 \pm 0.01$  Oe for 1779.

Three specimens from the Taisho (1914) lava flow yield a mean intensity value of  $0.41 \pm 0.03$  Oe. Although the determined intensity values are a little smaller than the present geomagnetic intensity of 0.46 Oe, the Thellier method is successful with small experimental errors as shown in Fig. 3.

Three specimens from the Showa lava flow, which was ejected only 30 years ago, were studied. Specimen SK 4-5-2 gave an ideal NRM-TRM diagram although the change in the NRM direction in the course of progressive heating was not very small. Two other specimens also yielded reliable intensity estimates although some points deviate from a straight line at higher temperatures in the NRM-TRM diagram. The mean intensity as determined from the Showa lava,  $0.46 \pm 0.02$  Oe, agrees very well with the present-day geomagnetic intensity.

#### 4. Discussion

The intensity value determined for the Showa (1946) lava

Table 2. Paleointensity determination data

| Unit                     | Specimen | T <sub>1</sub><br>(°C) | T <sub>2</sub> | N  | -b                                     | s <sub>b</sub> | -r    | F<br>(Oe) |
|--------------------------|----------|------------------------|----------------|----|----------------------------------------|----------------|-------|-----------|
| Bunmei<br>lava<br>(1471) | SK 1-1-1 | 20                     | 200            | 6  | 1.187                                  | 0.071          | 0.993 | 0.582     |
|                          | SK 1-2-1 | 200                    | 500            | 5  | 0.990                                  | 0.011          | 1.000 | 0.485     |
|                          | SK 1-6-2 | 20                     | 600            | 11 | 0.998                                  | 0.023          | 0.998 | 0.489     |
|                          | SK 1-8-2 | 20                     | 350            | 9  | 1.089                                  | 0.024          | 0.998 | 0.533     |
|                          | SK 1-9-2 | 20                     | 260            | 7  | 1.029                                  | 0.033          | 0.998 | 0.504     |
|                          |          |                        |                |    | (F <sub>mean</sub> : 0.519 ± 0.040 Oe) |                |       |           |
| Anei<br>lava<br>(1779)   | SK 2-4-2 | 20                     | 220            | 6  | 0.934                                  | 0.019          | 0.999 | 0.458     |
|                          | SK 2-8-2 | 20                     | 260            | 7  | 0.962                                  | 0.017          | 0.999 | 0.471     |
|                          | SK 2-9-2 | 20                     | 260            | 7  | 0.931                                  | 0.009          | 1.000 | 0.456     |
|                          |          |                        |                |    | (F <sub>mean</sub> : 0.462 ± 0.008 Oe) |                |       |           |
| Taisho<br>lava<br>(1914) | SK 3-3-1 | 20                     | 420            | 10 | 0.844                                  | 0.026          | 0.996 | 0.413     |
|                          | SK 3-4-1 | 20                     | 420            | 9  | 0.897                                  | 0.020          | 0.998 | 0.440     |
|                          | SK 3-8-1 | 120                    | 490            | 8  | 0.792                                  | 0.027          | 0.997 | 0.388     |
|                          |          |                        |                |    | (F <sub>mean</sub> : 0.414 ± 0.026 Oe) |                |       |           |
| Showa<br>lava<br>(1946)  | SK 4-4-1 | 20                     | 420            | 11 | 0.903                                  | 0.010          | 0.999 | 0.443     |
|                          | SK 4-5-2 | 20                     | 530            | 13 | 0.977                                  | 0.013          | 0.999 | 0.478     |
|                          | SK 4-6-1 | 80                     | 240            | 5  | 0.909                                  | 0.045          | 0.996 | 0.445     |
|                          |          |                        |                |    | (F <sub>mean</sub> : 0.455 ± 0.020 Oe) |                |       |           |

T<sub>1</sub>, T<sub>2</sub> and N: temperature interval in which NRM-TRM relation is linear and the number of points in this interval b: slope of NRM-TRM linear regression line s<sub>b</sub>: standard error of the slope r: correlation coefficient F: paleointensity

(0.46 ± 0.02 Oe) agrees with the mean total force of 45,870 (1975) at Kanoya observatory about 20 km distant from Sakurajima Volcano. However, the value determined from the Taisho (1914) lava flow, i.e. 0.41 ± 0.03 Oe, is smaller than the present-day total intensity by about 10 percent. It is unlikely that the geomagnetic field on Sakurajima Volcano changed about 10 percent in a time span of 60 years, because the actually-observed total intensity in 1914 at magnetic observatories in Japan is almost the same as the present-day total force. It is surmised that this discrepancy is caused by magnetic anomaly predominating on the volcano. On Oshima Island about 100 km south of Tokyo, a total intensity value amounting to 0.51 ± 0.01 Oe, which is considerably larger than the actually-observed value, is obtained by means of the Thellier method (Kono, 1969). The magnetic field within a magnetized rock body is not equal to the external field H. The field becomes the vector sum of the external field and the demagnetizing field, namely H - NJ, where J is the remanent magnetization per unit volume and N is the demagnetizing factor (Coe, 1967; Stacey and Banerjee, 1974). When a specimen with a demagnetizing factor N<sub>0</sub> is used for the Thellier method, the slope of the straight line in a NRM-TRM diagram is equal to

$$\frac{H - NJ}{H_0 - N_0 J} \doteq \frac{H}{H_0} \left\{ 1 + J \left( \frac{N_0}{H_0} - \frac{N}{H} \right) \right\} \quad \text{---(1)}$$

where  $H_0$  is the magnetic field produced by the experimental device. Let us take an extreme case for which the rock body is assumed to be an infinitely extending layer with a uniform thickness and is magnetized perpendicular to its surface. The demagnetizing factor being  $\frac{1}{4}$ , the error involved in the estimate of the slope of a straight line in a NRM-TRM diagram is estimated as  $(8/3)\pi(J/H_0)$  from the equation (1) provided that the used specimen is a sphere, for which the demagnetizing factor amounts to  $(4/3)\pi$ , and that the magnetic field  $H$  is assumed to be equal to  $H_0$ . The error thus calculated amounts to 17 percent when  $J$  and  $H_0$  are assumed as 0.01 emu/cc and 0.5 Oe, respectively. In the case of the Taisho lava flow, the above estimate leads to a value amounting to 5.5 percent, and this error is believed to be close to its maximum. As the error thus estimated is not sufficiently large for the explanation of the estimated low value of the total intensity for 1914, the local magnetic anomaly prevailing around the lava flow may also be responsible for the estimated low value. It is very likely that the local magnetic anomaly is very large because of the strong magnetization of rock bodies around the sampling site. The fact that very low inclinations are observed for these specimens as shown in Table 1 and Fig. 2 seems to support the above supposition.

An intensity value,  $0.46 \pm 0.01$  Oe, which is almost the same as the present-day total intensity, is obtained for the 1779 lava. The paleointensity value obtained for the 1471 lava ( $0.52 \pm 0.04$  Oe) is larger than the present-day value by 13 percent. These values are somewhat smaller than those of Sasajima (1965) who reported total intensity values of 0.57 and 0.51 Oe for the Bunmei (1471) and Anei (1779) lavas, respectively. Sasajima measured only one specimen for each lava flow. The difference may represent the effect of the local magnetic anomaly and experimental errors.

The geomagnetic intensities thus determined from the Sakurajima lavas are compared with other data from Japan (Nagata et al., 1963; Sasajima, 1965; Kono, 1969) in Fig. 4. Although it is usual to convert the measured values to those at the equator for a worldwide comparison, no such procedure is made in the present case because the differences in the total intensity between the respective sites do not exceed 1,000  $\gamma$  at present according to the standard map of the total force in Japan. The new four data agree approximately with the secular trend of intensity changes. Although an intensity value by Nagata et al. (1963) estimated for 1070  $\pm$  70 deviates from the trend of other data, it can be concluded that the total intensity in Japan has been gradually decreasing since the 10th century when the total intensity was 1.5 times as large as the present-day value.

### Conclusion

Two recent lava flows, ejected in 1946 and 1914, and two historic (1779 and 1471) ones were used for geomagnetic paleointensity determination by making use of the Thellier method.

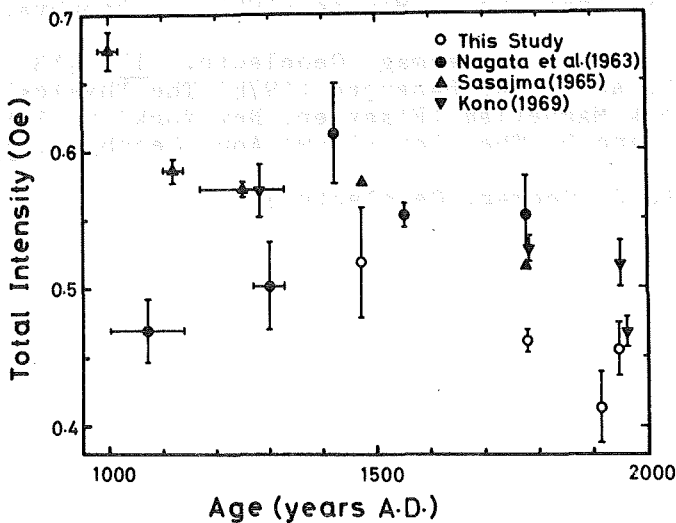


Fig. 4. Secular change of geomagnetic paleointensity in Japan for the last 10 centuries. Open circles indicate data determined in this study.

The former two lavas are useful for checking the validity of paleointensity determination by the Thellier method, which is slightly modified so as to make experimental time short, and the latter two lavas, for bringing out the secular variation of the total intensity on Sakurajima Volcano for the last five centuries.

The determined intensity for 1946 agrees well with the present-day value, while that for 1914 is smaller than the observed value by 10 percent. It can be said, however, that these results prove the correctness of paleointensity determination by the Thellier method because a difference of 10 percent or so can readily be explained by the local geomagnetic anomaly on a volcano. Possible errors in paleointensity experiments may also be about 10 percent at maximum.

The intensity value for 1471 is larger than the present-day value, by about 15 percent, but that for 1779 is almost the same as the present-day value. It is concluded that the total force tended to decrease at Sakurajima since the 15th century, and such a tendency agrees with the trend of the geomagnetic secular change over the last 10 centuries in Japan.

#### References

- Coe, R. S. (1967) *J. Geomag. Geoelectr.*, 19, 157.  
 Coe, R. S. and C. S. Grommé (1973) *J. Geomag. Geoelectr.*, 25, 415.  
 Kono, M. (1969) D. Sc. thesis (Univ. of Tokyo, Tokyo) p. 58.  
 Kono, M. (1974) *J. Geophys. Res.*, 79, 1135.  
 Kono, M. and H. Tanaka (1977) *Phys. Earth. Planet. Inter.*, 13, 276.

Nagata, T., Y. Arai and K. Momose (1963) J. Geophys. Res.,  
68, 5277.  
Sasajima, S. (1965) J. Geomag. Geoelectr., 17, 413.  
Stacey, F. D. and S. K. Banerjee (1974) The Physical Principles of Rock Magnetism (Elsevier, New York) p. 195.  
Thellier, E. and O. Thellier (1959) Ann. Geophys., 15, 285.  
(Submitted to J. Geomag. Geoelectr.)

# GEOMAGNETIC PALEOINTENSITIES DURING THE PAST 30,000 YEARS IN JAPAN

Hidefumi TANAKA

Department of Applied Physics, Tokyo Institute of Technology, Meguro-ku, Tokyo 152

Volcanic rocks of the past a few tens of thousand years are very suited to study the geomagnetic secular variation having time constant in the order of 1,000 years. Periodic variation with time of the averaged virtual dipole moment (VDM) was obtained for the past 8,500 years (Cox, 1968; Bucha, 1970), and it is important to investigate whether the VDM was also periodic in the time previous to 8,500 years. In Japan, many paleointensities for the past 10,000 years are obtained by the Thellier method (Nagata et al., 1963; Sasajima, 1965; Kono, 1969; Kitazawa, 1970; Kawai et al., 1975), but no data are reported for some time interval previous to 10,000 years B.P.. Recent progress in the tephrochronology and radiocarbon chronology is remarkable and some of lavas and pyroclastic flows in Japan for the past 30,000 years have well dated ages (Machida, 1976). These volcanic rocks are well suited for the investigation of the secular change of the geomagnetic paleointensity back to 30,000 years B.P.. In this report, six paleointensities are reported of the ages ranging from 3,000 to 30,000 years B.P..

Samples are collected from about 20 lava flows and pyroclastic flows in Japan as listed in Table 1. Most of pyroclastic flows have radiocarbon dated ages determined from the carbonated wood in the flows. The ages of most lava flows are precisely determined as the upper and lower layers have radiocarbon dated ages. The maximum temperatures of the pyroclastic flows at the time of formation are not known, but probably they are more than 300 - 400 °C.

Seven paleointensities are now obtained by the ordinary double heating Thellier method, and they are also contained in Table 1. The paleointensity experiments were applied to 32 specimens, and 19 of them gave reliable paleointensities. Samples from Hutago-yama lava have no orientation, but the obtained intensity values are reliable, because NRM's are stable and all the five specimens are agreed as to the intensity values. The paleointensity from Ito pyroclastic flow was determined using only two specimens sampled from one block of rock with no orientation, so it is necessary to reexamine the paleointensities using a few more specimens with orientations. The paleointensity experiment was successfully applied to Oosawa pyroclastic flow and concordant intensity values are obtained, but NRM directions of the specimens scatter much. This probably means that the temperature of the flow at the time of formation was not enough high and the NRM was not produced at that time. This explains the discrepancy of the two paleointensities obtained from the Oosawa pyroclastic flow (3,040 ± 50 years B.P.) and from the Oowakudani pyroclastic flow (2,900 ± 100 years B.P.). The latter gives an intensity value of  $0.60 \pm 0.08$  Oe agreeing with the worldwide secular trend of the paleointensity changes, while the former gives too

Table 1. Pyroclastic flows and lavas having radiocarbon dated ages in Japan (3,000 - 30,000 years B.P.)

| Flow unit         | Source  | Age (years B.P.)          | Paleointensity(Oe) |
|-------------------|---------|---------------------------|--------------------|
| Oowakudani p.f.   | Hakone  | 2,900 + 100               | 0.601±0.082        |
| Oosawa p.f.       | Fuji    | 3,040 ± 50                | 0.273±0.038        |
| Oohirayama p.f.   | Sambe   | 3,680 ± 90                |                    |
| Sanbe l.          | Sambe   | 4,480 > 3,680             |                    |
| Chojagahara p.f.  | Sambe   | older than Sambe l.       |                    |
| Shigaku p.f.      | Sambe   | 4,480 + 110               |                    |
| Hutago-yama l.    | Hakone  | 4,500 ± 500               | 0.451±0.028        |
| Ootagirigawa p.f. | Myoko   | 4,790 ± 100               |                    |
| Hunatsu l.        | Fuji    | younger than Saruhashi l. |                    |
| Saruhashi l.      | Fuji    | 8,530 + 170 >             | 0.453±0.032        |
| Akakura p.f.      | Myoko   | 8,640 ± 100               |                    |
| basalt            | Ooshima | 9,000 ± 500               |                    |
| Ukinuno p.f.      | Sambe   | 16,400 ± 400              |                    |
| Hikageyama l.     | Sambe   | older than Ukinuno p.f.   |                    |
| Kamiyama p.f.     | Hakone  | 19,640 + 550              | 0.383±0.019        |
| Ito p.f.          | Aira    | 22,000 ± 700              | 0.240              |
| Oota p.f.         | Sambe   | 25,600 ± 1,000            |                    |
| Kamiyama p.f.     | Hakone  | 28,200 ± 1,700            | 0.253±0.014        |

p.f.; pyroclastic flow l.; lava

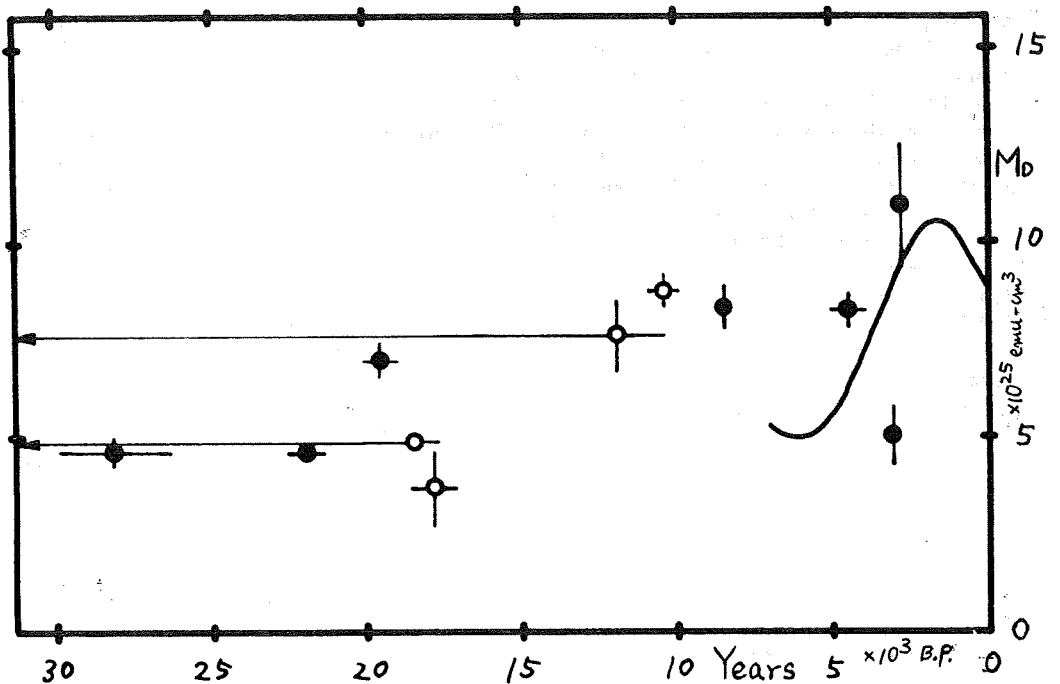


Fig. 1. Changes of the geomagnetic paleointensities for the past 30,000 years. Squares are data from this study. Open squares are data from Coe et al. (1978). Solid curve is the best fit sinusoid of Bucha (1970).

small value for 3,000 years B.P..

Six paleointensities except one from Oosawa pyroclastic flow were converted to the VDM's and are shown in Fig. 1 by squares with uncertainties. Open squares are paleointensity data reported by Coe et al. (1978) determined by dated lavas in Hawaii. As for the time later than 10,000 years B.P., the best fit sinusoid of Bucha (1970) is shown by solid curve. Two data from this study for the age of about 3,000 years B.P. and 4,500 years B.P. agrees with the trend of the sinusoid curve.

Further studies must be continued to deduce the secular change of the geomagnetic paleointensity back to 30,000 years B.P..

### References

- Bucha, V. (1970) Phil. Trans. Roy. Soc. Lond. A., 269, 47.  
Coe, R.S., S. Grommé and E.A. Mankinen (1978) J. Geophys. Res., 83, 1740.  
Cox, A. (1968) J. Geophys. Res., 73, 3247.  
Kawai, N., T. Nakajima, K. Tokieda and K. Hirooka (1975) Rock Mag. Paleogeophys., 3, 110.  
Kitazawa, K. (1970) J. Geophys. Res., 75, 7403.  
Kono, M. (1969) D. Sc. thesis (Univ. of Tokyo, Tokyo) p. 58.  
Machida, H. (1976) Geograph. Report. Tokyo Metropoli. Univ., 11, 109.  
Nagata, T., Y. Arai and K. Momose (1963) J. Geophys. Res., 68, 5277.  
Sasajima, S. (1965) J. Geomag. Geoelectr., 17, 413.

PALEOMAGNETISM AND PALEOINTENSITY STUDIES OF  
SCOTTISH DEVONIAN VOLCANIC ROCKS

Masaru Kono

Geophysical Institute, University of Tokyo, Bunkyo-ku, Tokyo 113.

1. Introduction

Devonian lavaflores of mainly andesitic rocks associated with the lower Old Red Sandstones are found near Perth, Scotland. Sallomy and Piper (1973) studied paleomagnetism of these rocks and concluded that the natural remanent magnetization (NRM) is stable to alternating field demagnetization and thermal demagnetization, and its direction well represents that of the ambient magnetic field in the Devonian. The flow mean directions of NRM in these lavas are widely scattered and do not show the usual bimodal distribution corresponding to normal (N) and reversed (R). In addition to N (NE and up) and R (SW and down) which represent the "normal" periods, Sallomy and Piper defined "transitional" polarity groups A (NE to E and down) and B (SE to S and up) and suggested that A and B (and some other "unclassified") groups represent times when the geomagnetic field was in transition, i.e., reversals or excursions. If their samples really represent the Devonian field well, such transitional periods seem to take much longer proportion of time (44 %) than they do in Tertiary (about 1-3 %). There is also some possibility that the lavas erupted in a relatively short interval when the field was actually undergoing reversals.

In the present paper, some additional flow units were sampled in the same area. They were demagnetized by AF method and some of the stable samples were further subjected to paleointensity determination by Thellier method. This study was carried out at University of Liverpool with assistance of John Piper, John Show and Rod Wilson.

Table 1. Scottish Devonian andesites: site, bedding and Curie temperatures.

| Site no. | Place           | Number of samples | Latitude (° ') | Longitude (° ') | Bedding angle |             | Curie temperature(s) (°C) |
|----------|-----------------|-------------------|----------------|-----------------|---------------|-------------|---------------------------|
|          |                 |                   |                |                 | Dip (°)       | Bearing (°) |                           |
| SC01     | Kilspindie      | 5                 | 56 25.2        | 356 44.4        | 12            | 315         | 585                       |
| SC02     | Black Bank      | 5                 | 56 26.2        | 356 43.7        | 15            | 315         | 580                       |
| SC03     | Black Bank      | 4                 | 56 26.2        | 356 43.7        | 15            | 315         | 578                       |
| SC04     | Ladywell        | 5                 | 56 26.2        | 356 43.0        | 15            | 315         | 570                       |
| SC05     | Craigneb        | 6                 | 56 26.3        | 356 41.9        | 21            | 315         | 560                       |
| SC06     | Dalreich Moor   | 6                 | 56 26.3        | 356 40.7        | 21            | 315         | 573                       |
| SC07     | Craigneb        | 6                 | 56 26.5        | 356 41.7        | 21            | 315         | 582                       |
| SC08     | Rait            | 5                 | 56 26.0        | 356 44.8        | 15            | 315         | 566, 685                  |
| SC09     | Woodwell        | 6                 | 56 26.3        | 356 46.2        | 11            | 315         | 538                       |
| SC10     | Kinnaird        | 6                 | 56 26.8        | 356 46.6        | 11            | 315         | 563, 679                  |
| SC11     | Collace Quarry  | 7                 | 56 28.2        | 356 43.1        | 21            | 305         | 557                       |
| SC12     | Ylack Hill      | 6                 | 56 28.3        | 356 44.7        | 21            | 305         | 569                       |
| SC13     | Abernyte        | 6                 | 56 28.2        | 356 47.9        | 11            | 295         | 551                       |
| SC14     | Northballo Hill | 6                 | 56 30.4        | 356 46.9        | 27            | 305         | 557                       |
| SC15     | Southballo      | 7                 | 56 30.0        | 356 47.5        | 21            | 315         | 535                       |

## 2. Paleomagnetism

Sampling localities and bedding angles are summarized in Table 1. Because of the folding of the Lower Old Red Sandstones of Strathmore region which took place in mid-Devonian times, the lavas dip gently towards northwest, but the rocks have never been affected by later thermal events (I. Patterson, private communication, 1976). One specimen from each sample was subjected to progressive AF demagnetization between 0 and 0.06 T (600 Oe). Flow units SC13 and SC15 showed erratic changes in directions of remanences, while the magnetization of SC01 was quite stable but the dispersion was very great. These flows were omitted from further considerations and the flow mean directions were determined from the remaining flows. The results are summarized in Table 2. The stability of NRM's in these flows is quite high and the median demagnetizing field (MDF) was greater than 0.04T except SC09 which has a mean MDF of 0.01T. As can be seen from the small confidence angles (Table 2), the reliability of these data is quite high. The mean directions of remanences can also be classified into N, R, as well as A and B, and the percentage of the "transitional" groups (A and B) is even higher (seven in a total of 12) than in the flow units of Sallomy and Piper (27 in a total of 61).

Table 2. Palaeomagnetic results.

| Site No. | AF  | N | I      | D     | R      | $\alpha_{95}$ | k    | Lat.   | Long. | Group |
|----------|-----|---|--------|-------|--------|---------------|------|--------|-------|-------|
| SC 02    | 400 | 5 | 14.3   | 54.9  | 4.8639 | 11.5          | 29.4 | 24.9   | 113.3 | A     |
| SC 03    | 500 | 3 | 14.0   | 45.8  | 2.9972 | 3.0           | 712  | 29.0   | 122.3 | A     |
| SC 04    | 500 | 4 | 13.6   | 86.7  | 3.9622 | 7.9           | 79.4 | 7.6    | 85.9  | A     |
| SC 05    | 600 | 6 | 10.2   | 68.8  | 5.9575 | 5.3           | 118  | 15.9   | 101.8 | A     |
| SC 06    | 600 | 6 | - 7.9  | 65.6  | 5.8575 | 9.6           | 35.4 | 9.8    | 109.5 | N     |
| SC 07    | 600 | 6 | 39.4   | 200.5 | 5.9500 | 5.7           | 100  | - 18.3 | 336.7 | R     |
| SC 08    | 600 | 5 | 42.7   | 84.7  | 4.9344 | 8.0           | 61.0 | 23.3   | 76.6  | A     |
| SC 09    | 200 | 6 | - 2.3  | 183.1 | 5.9918 | 2.3           | 611  | - 34.7 | 354.2 | B     |
| SC 10    | 600 | 6 | 43.0   | 93.4  | 5.9944 | 1.9           | 888  | 18.8   | 55.7  | A     |
| SC 11    | 600 | 5 | 56.8   | 176.8 | 4.9774 | 4.7           | 177  | 3.9    | 359.3 | R     |
| SC 12    | 200 | 6 | - 18.0 | 46.5  | 5.9807 | 3.5           | 260  | 14.0   | 129.2 | N     |
| SC 14    | 400 | 6 | - 43.0 | 52.7  | 5.9743 | 4.1           | 194  | - 2.8  | 130.7 | N     |

*Notes:*

AF, peak alternating field in 10<sup>-4</sup>T; N, number of samples; I, D, site mean inclination and declination after tilt correction; R, resultant length of N unit vectors;  $\alpha_{95}$ , k, semiaxis of the 95 per cent cone of confidence and precision parameter; Lat., Long., latitude and longitude of virtual geomagnetic pole; Group, polarity group defined by Sallomy & Piper (1973).

## 3. Paleointensity Experiments

Twenty-five specimens from 10 magnetically stable lava flows were used for paleointensity determination. Flow units SC02 and SC03 were excluded because large angular error was observed in AF demagnetization of the NRM's. The procedure used was the modified Thellier method proposed by Kono (1974) and employed by Kono and Ueno (1977). The specimens were heated and cooled in

air in a magnetic field of  $0.5 \times 10^{-4}$  T (0.5 Oe) at successively higher temperatures. Heating was carried out once to each temperature but, because the laboratory field direction was set perpendicular to the direction of the NRM component in the specimens, separation of remanence into NRM and TRM components was possible, with an assumption that the NRM direction is the same at every temperature step. Since this assumption was not strictly satisfied in some flow units, the "NRM" direction was defined as the direction of remanence after the NRM was demagnetized in a field-free space at 100°C.

Successful results are summarized in Table 3. The criteria of success was similar to those used by Kono (1974); more than six points in the linear interval and a correlation coefficient not less than 0.98. Fig. 1(a) shows the results of N and R polarity groups and Fig. 1(b) shows those of A and B groups. Results of the SC08 specimens (group A) are shown separately in Fig. 1(c). More than one estimates of paleointensity were determined for flow units SC04, 05, 06, 08, 09 and 12, where the internal consistency is reasonably good. A common feature among these results is that the NRM component (ordinate) does not decrease appreciably until 100 to 260°C while the TRM component (abscissa) increases steadily. This may indicate that the low blocking temperature component of NRM has been selectively demagnetized due to spontaneous decay or is masked by a viscous remanent magnetization (VRM) which is nearly antiparallel to the original remanence. Another notable fact is that above about 500°C the points deviate to the right from the linear lines indicated in the figures, or a larger TRM than expected is acquired. This is apparently due to some chemical changes taking place at higher temperatures, which is a very common feature of many paleointensity experiments using volcanic rocks (e.g., Kono, 1974; Kono and Ueno, 1977). However, in the present study these effects are not important and do not affect the validity of the experimental results; linear segments between 100-200°C and about 500°C define paleointensities with small ambiguity.

Table 3. Successful results of paleointensity experiments.

| Specimen  | $T_1$ | $T_2$ | N  | -b    | $S_b$ | -r    | F     |
|-----------|-------|-------|----|-------|-------|-------|-------|
| SC 0402-1 | 145   | 510   | 11 | 0.329 | 0.016 | 0.990 | 0.164 |
| SC 0403-2 | 145   | 480   | 11 | 0.334 | 0.020 | 0.983 | 0.167 |
| SC 0506-1 | 110   | 500   | 10 | 0.189 | 0.014 | 0.980 | 0.094 |
| SC 0507-1 | 110   | 500   | 9  | 0.142 | 0.006 | 0.994 | 0.071 |
| SC 0601-2 | 210   | 500   | 9  | 0.204 | 0.010 | 0.992 | 0.102 |
| SC 0604-2 | 425   | 570   | 5  | 0.142 | 0.008 | 0.995 | 0.071 |
| SC 0702-2 | 295   | 530   | 8  | 0.361 | 0.019 | 0.992 | 0.181 |
| SC 0802-1 | 20    | 500   | 11 | 0.189 | 0.009 | 0.990 | 0.095 |
| SC 0803-2 | 20    | 530   | 15 | 0.212 | 0.020 | 0.945 | 0.106 |
| SC 0804-1 | 20    | 570   | 13 | 0.142 | 0.008 | 0.981 | 0.071 |
| SC 0902-2 | 145   | 510   | 9  | 0.931 | 0.038 | 0.994 | 0.465 |
| SC 0903-2 | 145   | 510   | 12 | 0.702 | 0.032 | 0.990 | 0.351 |
| SC 1101-1 | 140   | 425   | 8  | 0.131 | 0.004 | 0.997 | 0.065 |
| SC 1201-1 | 260   | 490   | 7  | 0.272 | 0.017 | 0.990 | 0.136 |
| SC 1203-1 | 260   | 510   | 7  | 0.190 | 0.012 | 0.989 | 0.095 |
| SC 1206-2 | 145   | 435   | 9  | 0.191 | 0.011 | 0.989 | 0.096 |

Notes:

$T_1, T_2$ , temperature interval (°C) in which the NRM-TRM relation is linear; N, number of points in this interval; b, slope of the NRM-TRM linear regression line;  $S_b$ , standard error of the slope b; r, correlation coefficient of the regression line; F, paleointensity in  $10^{-4}$  tesla (Oe).

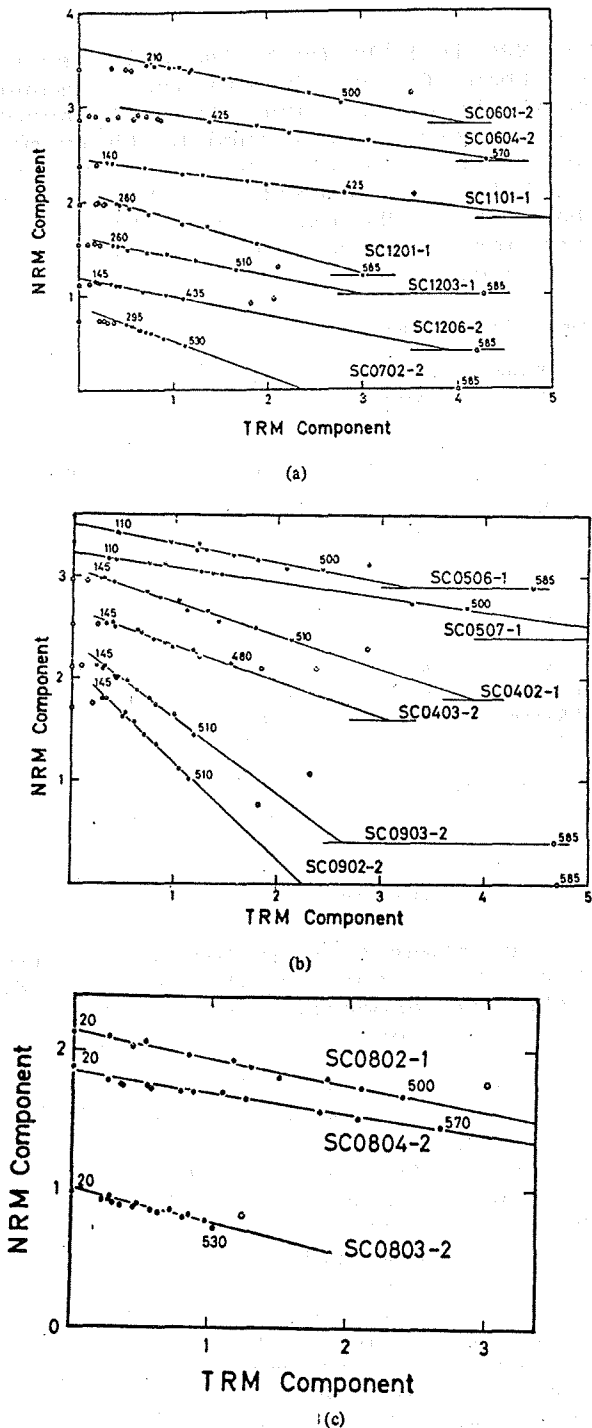


Figure Successful results of palaeointensity experiments shown in Arai diagrams (Nagata, Arai & Momose 1963). Diagrams for individual samples are 'stacked' by arbitrarily displacing them in the vertical direction. Horizontal bars indicate the abscissae for individual samples. Regression lines were determined from the solid circles in the temperature intervals ( $^{\circ}\text{C}$ ) indicated by the small numerals. Open circles are points excluded from the regression analysis because of the decay of NRM or the effect of VRM at low temperatures, or because of the changes in magnetic properties at high temperatures. (a) N and R polarity group samples. The scale is  $2 \times 10^{-4} \text{Am}^2/\text{kg}$  (emu/gr) for SC06 and SC07,  $2.5 \times 10^{-4} \text{Am}^2/\text{kg}$  for SC11 and  $1 \times 10^{-3} \text{Am}^2/\text{kg}$  for SC12. (b) A and B polarity group samples. The scale is  $1 \times 10^{-4} \text{Am}^2/\text{kg}$  for SC04,  $2 \times 10^{-4} \text{Am}^2/\text{kg}$  for SC05 and  $2.5 \times 10^{-3} \text{Am}^2/\text{kg}$  for SC09. (c) SC08 samples (polarity group A) which have NRM carried mostly by hematite. The scale is  $10^{-4} \text{Am}^2/\text{kg}$ . Note that the points are *not* displaced in this figure.

Most of the NRM in SC08 (and also SC10) seem to be carried by hematite. More than 70 % of the original remanence remains after demagnetization at the Curie temperature of magnetite. The existence of hematite is also ascertained by thermomagnetic analysis (Table 1) and by microscopic observation of polished sections, though the contribution of hematite to the total saturation moment is much less than 10%. The exceedingly high stability of the NRM to AF demagnetization of these samples is well understood in terms of hematite remanence.

Table 4. Summary of palaeointensity data.

| Flow unit               | Polarity group | Number of specimens successful/used | F, 10 <sup>-4</sup> T(Oe)* |             | Virtual dipole moment*<br>10 <sup>22</sup> Am <sup>2</sup> (10 <sup>23</sup> emu) |
|-------------------------|----------------|-------------------------------------|----------------------------|-------------|-----------------------------------------------------------------------------------|
|                         |                |                                     | Mean                       | Range       |                                                                                   |
| SC04                    | A              | 2/3                                 | 0.165                      | 0.164-0.167 | 4.2                                                                               |
| SC05                    | A              | 2/2                                 | 0.075                      | 0.071-0.094 | 1.9                                                                               |
| SC06                    | N              | 2/3                                 | 0.084                      | 0.071-0.102 | 2.2                                                                               |
| SC07                    | R              | 1/2                                 | 0.181                      | -           | 3.9                                                                               |
| SC08                    | A              | 3/3                                 | 0.084                      | 0.071-0.106 | 1.8                                                                               |
| SC09                    | B              | 2/2                                 | 0.397                      | 0.351-0.465 | 10.3                                                                              |
| SC10                    | A              | 0/3                                 | -                          | -           | -                                                                                 |
| SC11                    | R              | 1/2                                 | 0.065                      | -           | 1.2                                                                               |
| SC12                    | N              | 3/3                                 | 0.102                      | 0.095-0.136 | 2.5                                                                               |
| SC14                    | N              | 0/2                                 | -                          | -           | -                                                                                 |
| Mean of all the results |                | 8                                   | 0.144 ± 0.111              |             | 3.5 ± 2.9                                                                         |
| Mean of N and R groups  |                | 4                                   | 0.108 ± 0.051              |             | 2.4 ± 1.1                                                                         |
| Mean of A and B groups  |                | 4                                   | 0.180 ± 0.150              |             | 4.5 ± 4.0                                                                         |

\* Numbers after ± indicate standard deviations.

#### 4. Discussion and Conclusions

Results of paleointensity experiments are summarized in Table 4. In this table, the virtual dipole moment is defined as the moment of a hypothetical geocentric dipole which produce the magnetic field observed paleomagnetically at a point on the surface of the earth.

In all 16 paleointensity estimates corresponding to eight flow units were obtained. Flow mean was determined by averaging the individual results with weights of  $(1/s_p)^2$ . It may be concluded from Table 4 that the difference between the "normal" groups N and R and the "transitional" groups A and B is not significant statistically. At the start of the experiments, it was anticipated that A and B groups may show much smaller paleointensities compared to N and R groups. This supposition was based on the present-day knowledge of smaller field intensities at the times of magnetic reversals and on the conclusion of Sallomy and Piper (1973) that A and B groups may represent intermediate directions in transition periods. Although short periods of normal intensities may exist when virtual geomagnetic poles (VGPs) are near the equator (Dagley and Wilson, 1971; Shaw, 1975), transitional periods are characterized by the decline of intensity to 1/4 and 1/10 of the normal values (e.g., Dunn et al., 1971; Opdyke et al., 1973). That the paleointensities of A and B groups are not significantly different (and certainly not smaller than) those of N and R groups suggest that there is some error or at least inconsistency in our prejudices. Some of the possibilities are considered below.

- (1) Groups A and B may be spurious and do not correspond to real

transitional periods; the abnormal NRM directions are due to secondary components or caused by tectonic movements.

(2) The definition of polarity groups of Sallomy and Piper was in error. There is some ambiguity in the definition of "normal" field direction for Devonian times in the polar wander curve of the British Isles (Briden et al., 1973).

(3) A and B groups may really represent transitional periods but the characteristics of the geomagnetic field were much different in the lower Paleozoic. For instance, reversals may have taken much longer time and the intensity more or less stayed at the same level.

(4) A, B groups are much displaced from the mean of the N, R groups but actually the former are part of the latter. This implies that the secular variation was much larger in Scotland in Devonian than in recent or Tertiary times.

The possibilities (1) and (2) are very unlikely in the present case; there is no systematic difference other than NRM directions between these groups. If (3) is really correct, the division of field into "normal" and "transitional" types is not very helpful to the understanding of the nature of the geomagnetic field. In any case it is almost certain that we should expect characteristics of the geomagnetic field much different from the Tertiary regime.

We may make some speculations on the nature of the Devonian field; it may have been that the ratio of the multipole to dipole moments was much larger than those in Tertiary and recent times. If so, large secular variation is a direct consequence and we need not think A, B groups as "transitional". It may also explain the wide range of intensity fluctuations; the standard deviation is 84% of the mean compared to the values of 30-40% for various parts of Cenozoic (Kono, 1974). The difficulty in defining Devonian paleomagnetic poles may also be the result of this effect.

## References

- Briden, J.C., W.A. Morris and J.D.A. Piper (1973) *Geophys. J. Roy. Astron. Soc.* 34, 107.
- Dagley, P. and R.L. Wilson (1971) *Geophys. J. Roy. Astron. Soc.*
- Dunn, J.R., M. Fuller, H. Ito and V.A. Schmidt, *Science* 172, 840.
- Kono, M. (1974) *J. Geophys. Res.* 79, 1135.
- Kono, M. and N. Ueno (1977) *Phys. Earth Planet. Inter.* 13, 305.
- Nagata, T., Y. Arai and K. Momose (1963) *J. Geophys. Res.* 68, 5277.
- Opdyke, N.D., D.V. Kent and W. Lowrie (1973) *Earth Planet Sci. Lett.* 20, 315.
- Sallomy, J.T. and J.D.A. Piper (1973) *Geophys. J. Roy. Astron. Soc.* 34, 47.
- shaw, J. (1975) *Geophys. J. Roy. Astron. Soc.* 40, 345.
- (in press in *Geophys. J. Roy. Astron. Soc.* 56, 1978)

PALEOMAGNETIC STUDIES ON SUMATRA ISLAND: ON THE POSSIBILITY OF SUMATRA BEING PART OF GONDWANALAND.

By

Sadao SASAJIMA\*, Yoichiro OTOFUJI\*, Kimio HIROOKA\*\*,  
SUPARKA\*\*\*, SUWIJANTO\*\*\* and Fred HEHUWAT\*\*\*

- \* Dept. of Geology and Mineralogy, Kyoto University; 606 Sakyo, Kyoto, Japan
- \*\* Inst. of Earth Science, Toyama University; 930 Gofuku, Toyama, Japan
- \*\*\* National Institute of Geology and Mining-LIPE, Jl. Cisitu, Bandung, Indonesia

1. Introduction

Paleomagnetic investigation on Sumatra Island has been carried out 1976 as a part of the cooperation program between National Institute of Geology and Mining, Indonesia and Department of Geology and Mineralogy, Kyoto University, Japan.

Paleomagnetic samples which were taken from 53 sites amounting 570 in number, cover in their ages from the Permian to the Recent. The sampling route started from Medan, through around the Lake Toba, Sibolga, the Musala islet, Tonabatu, Hutanopan, Bukittinggi, Padang, Banko and ended at the southernmost Telukbetung. The sampling sites are shown in Fig. 1.

There have been so many arguments about the problem whether Sumatra region was a part of the Gondwanaland or the Laurasia. The main purpose of the paleomagnetic study on Sumatra is to find a clue to solve the problem.

2. Paleomagnetic results

Magnetic measurements before and after a.f.-demagnetization were performed by means of a Schonstedt SSM-1A spinner magnetometer. After the stability test of the remanences of pilot specimens, about one-half of samples were rejected for paleomagnetic use. Paleomagnetic properties of reliable rocks thus obtained after tilting corrections are listed in Table 1 together with computed virtual geomagnetic poles (VGP). As the radiometric ages are available only for a few rock samples, data in the table are arranged from the Permian to the Pleistocene in ascending order according

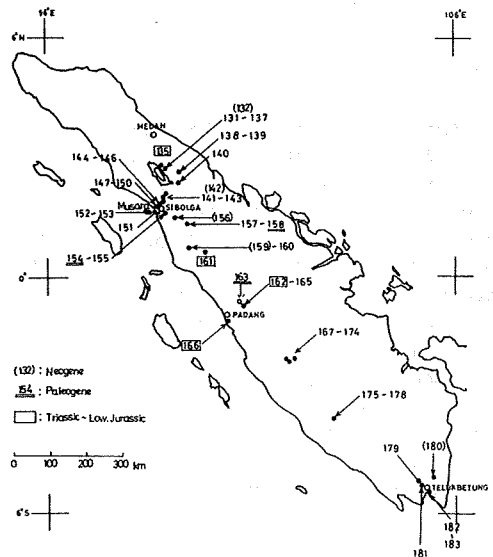


Fig. 1  
Sampling sites for paleomagnetic study.

Table 1. Summary of Paleomagnetic Data including Radiometric Ages of some Rocks

| Geological Age                | Site   | Rock type   | N  | AC peak field | D     | I     | $\alpha_{95}$ | Long. ( V. G. P. ) | Lat. (N) | Radiometric Age                                          |
|-------------------------------|--------|-------------|----|---------------|-------|-------|---------------|--------------------|----------|----------------------------------------------------------|
| Pleistocene                   | ID 138 | Ignimbrite  | 10 | 200           | 192.5 | 0.9   | 3.2           | 164.3W             | 77.4     | <sup>1)</sup> 1.2 m.y.                                   |
|                               | ID 158 | Tuff        | 10 | 100           | 0.6   | 7.5   | 3.4           | 114.1E             | 87.6     |                                                          |
|                               | ID 142 | Ignimbrite  | 11 | 100           | 12.7  | 15.2  | 4.5           | 164.1E             | 76.1     |                                                          |
| Plio-Pleistocene<br>Pliocene? | ID 156 | Dacite      | 7  | 200           | 11.3  | -8.2  | 3.3           | 145.1W             | 77.5     |                                                          |
|                               | ID 180 | Basalt      | 11 | 200           | 9.8   | -40.4 | 2.9           | 101.2E             | 69.6     |                                                          |
| Miocene                       | ID 132 | Diorite     | 8  | 200           | 6.3   | 16.1  | 7.3           | 147.1E             | 81.6     | <sup>2)</sup> 13.8 $\pm$ 3 m.y.<br><sup>3)</sup> 16 m.y. |
|                               | IDV 85 | Andesite    | 7  | 100           | 33.1  | 18.4  | 2.4           | 173.8E             | 55.8     |                                                          |
| Neogene                       | ID 176 | Shale       | 11 | 200           | 7.2   | -1.2  | 5.1           | 169.9E             | 82.2     |                                                          |
|                               | ID 177 | Shale       | 11 | 200           | -2.6  | -27.9 | 9.5           | 111.9W             | 76.4     |                                                          |
| Oligo-Miocene                 | ID 163 | Mudstone    | 9  | 100           | -13.3 | -15.6 | 7.2           | 18.3W              | 74.9     |                                                          |
| Eocene                        | ID 159 | Dacite      | 11 | 200           | -17.3 | -45.3 | 5.5           | 50.6W              | 57.8     | <sup>4)</sup> 47.7 m.y.                                  |
| Paleocene                     | ID 154 | Siltstone   | 9  | 100           | -6.1  | 35.7  | 7.8           | 81.0E              | 71.0     |                                                          |
| Paleogene                     | ID 166 | Black Shale | 10 | 200           | -2.6  | -41.9 | 9.6           | 73.7W              | 66.8     |                                                          |
|                               | mean   |             |    |               | 4.8   | -7.9  | 9.6           | 130.0E             | 83.8     |                                                          |
| Triassic                      | ID 133 | Black Shale | 7  | 100           | 5.0   | -34.3 | 19.1          | 93.7W              | 68.0     |                                                          |
|                               | ID 135 | Limestone   | 8  | 200           | 45.6  | 13.5  | 15.8          | 178.0W             | 44.4     |                                                          |
|                               | ID 161 | Limestone   | 7  | 300           | 199.9 | 28.0  | 11.7          | 130.9W             | 65.0     |                                                          |
| Up. Middle Triassic           | ID 162 | Limestone   | 14 | 300           | 241.3 | 31.2  | 8.2           | 151.0W             | 27.6     |                                                          |
|                               | mean   |             |    |               | 33.3  | -24.9 | 32.0          | 147.3W             | 54.6     |                                                          |
| Permian                       | ID 165 | Basalt      | 10 | 200           | -42.3 | -18.4 | 5.1           | 2.4W               | 47.0     | <sup>5)</sup> 248 $\pm$ 10 m.y.                          |

1) Nishimura et al. (1978) 2) Zen (1975) 3) Naeser (1975) 4) ORMDC (1971) 5) Shibata (1975)

to the geological determination. The most suitable alternating field values adopted for the cleaning of the secondary magnetization are listed in the fifth column of the table. It is worthy to note that about a half of Triassic paleomagnetic data comprises of the reversed polarity suggesting a very high reliability of the averaged paleomagnetic direction for the Triassic period. On the contrary, the remanent directions from Paleogene to the recent show considerable scattering around the present direction of the geomagnetic field for the sampling sites, which may be due partly to the secular variation and partly to the effects of presumable crustal movements after the emplacement of these igneous bodies; for most Tertiary igneous and pyroclastic rock samples tilting correction was not possible. The average Cenozoic remanent magnetization and related data are as follows;  $D_m=4.8^\circ$ ,  $I_m=-7.9^\circ$ , VGP:  $83.8^\circ\text{N}$  lat.,  $130.0^\circ\text{E}$  long.,  $\alpha_{95}=9.6^\circ$ ,  $k=19.6$ .

It would thus be reasonable to presume that the average paleomagnetic direction for all the Cenozoic data points to no considerable deviation from the axial dipole field direction. On the other hand, the pre-Cenozoic data in Table 1 show substantial changes in the paleomagnetic direction and VGP positions. If the VGP positions at Triassic period are different from the VGP's from other regions, we should expect that the Sumatra region experienced a land drift during the period between the Triassic and the early Tertiary. To evaluate such drift the average Triassic paleomagnetic pole for Sumatra is compared with, for example, that for the Russian Platform (McElhinny, 1973), which provides one of the best reference poles for Laurasian continent (Fig. 2).

### 3. Discussion

Since we are interested in the possible drift of Sumatra relative to the Laurasian Continent, we will first compare the Triassic VGPs from Sumatra and the Russian Platform, a representative stable block of the Laurasia. From the VGP for Sumatra ( $66.4^\circ\text{N}$ ,

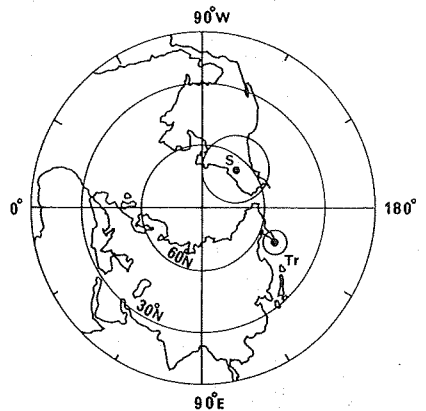


Fig. 2

Triassic paleomagnetic north pole for Sumatra in comparison with that for Russian Platform. S: Triassic VGP for Sumatra, Tr: VGP for Russian Platform.



Fig. 3

Possible paleo-latitudinal small circle on which Sumatra was situated in the Triassic Period as deduced from the VGP of Russian Platform.

137.9°W) and that for the Russian Platform (51°N, 154°E; McElhinny, 1973), we can depict the locus (paleolatitude small circle) on which Sumatra could have situated in the Triassic period (Fig. 3).

Alternatively if we use the VGP from the Western Europe (45°N, 143°E; McElhinny, 1973), we have, in a similar way, more southern paleo-latitude line on which Sumatra could have been situated in the Triassic. Needless to say that only from the paleomagnetic data we cannot determine uniquely the paleo-longitude of a concerned landmass. We need another constraint to fix the paleogeographic position of Sumatra. In this respect, we can favorably refer to the aspects of the ocean floor spreading in the East Indian Ocean which were described by sclater and Fisher (1974) and Johnson et al. (1976). Combining the supposed direction due to such ocean floor spreading against the Sumatra area with above-mentioned paleo-latitude for Sumatra, we can infer the possible paleogeographic position of Sumatra during the Triassic at 38°S, 100°E as shown in Fig. 3. In this inference we assume that the Sumatra landmass was dislocated to the present situation from the south latitudinal position by the ocean floor spreading mechanism.

Because of the insufficient knowledge in the present day paleomagnetism, we are unable to define a single universal magnetic pole for the Triassic period. Consequently it is much more safer to make a cross check to the above result referring to the Australian continent which was originally a part of the Gondwanaland. In Fig. 4 the Triassic paleomagnetic south pole for Sumatra is shown in comparison with that for Australia (47°S, 176°E; Embleton and Schmidt, 1977). It is clearly seen in the figure that VGP for Sumatra is situated far away from that for Australia. However, it is shown by computation that the two colatitudes of Sumatra for both VGPs are almost the same, and that the angle formed at central Sumatra (0° lat., 100°E long.) by the two paleomeridians through the two VGPs is 62.4°. It is implied that Triassic rocks located in both Sumatra and Australia might have been magnetized under the same dipole field represented by the Australian VGP. If it is the case the original position of Sumatra in the Triassic period relative to Australia might have been conserved through the breakup process of Australia from Antarctica. In this respect, it is of interest to mention Chamalaun's work (1977) that autochthonous Timor has been paleomagnetically evidenced to have formed a part of Australian continental block at least since the Upper Permian. Then, after the Triassic until the early Tertiary, Sumatra should have rotated clockwise by 62.4° presumably during the period of its breakup from Gondwanaland and/or during its northward drifting. This conclusion contradicts Ninkovich's speculation (1976) that in the late Cenozoic Sumatra rotated clockwise about 20 degrees and formed the present configuration.

By closing the spread ocean floor between Antarctica and Australia which is accompanied by Sumatra, we can draw Triassic paleogeographic

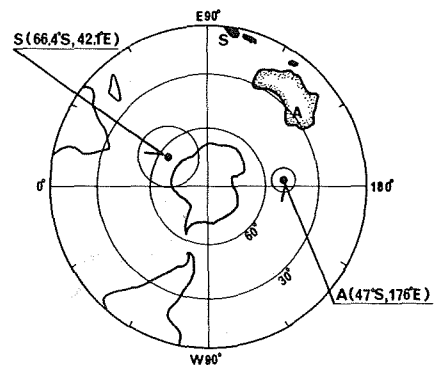


Fig. 4  
Triassic paleomagnetic south pole for Sumatra (S) in comparison with that for Australia (A).

position of Sumatra on the reconstruction map of Gondwanaland by Smith and Hallam (1970) (Fig. 5). It should be noted that such a paleomagnetic inference is supported by the ocean floor spreading pattern in the Wharton basin, East Indian Ocean (Sclater and Fisher, 1974).

The details of drifting processes of Sumatra are illustrated in Fig. 6 on the diagrams showing the history of the sea-floor spreading since the Late Cretaceous, which was originally drawn by Sclater and Fisher (1974). We can realize that the paleomagnetic reconstruction of Sumatra is quantitatively consistent with the history of the sea-floor spreading in the East Indian Ocean. As a result it is strongly suggested that the present position of Sumatra Island could have been almost established at the early Tertiary after drifting from the Gondwanaland. We have failed to find out any reliable Cretaceous paleomagnetic data even though more than 50 granitic rock-samples were collected. Therefore, the exact time of breakup of Sumatra from the Gondwanaland was not obtained.

#### 4. Conclusions

As a conclusive remark, it may safely be stated that at least during the Triassic period the Sumatra region belonged to the Gondwanaland, possibly a little north of the junction of the Indian and Australian Continents. Such a paleomagnetic conclusion has been substantiated by referring to not only the Triassic paleomagnetic pole for the Laurasian land, but also that for the Australian continent. Furthermore, it is noteworthy that such a paleomagnetic result is fully supported by recent findings of the ocean-floor spreading history in the East Indian Ocean.

The recent advocacy presented by Ridd (1971) that the Southeast Asia region had constituted a part of Gondwanaland, has been partially opposed by some paleomagnetic results from Malay Peninsula (McElhinny et al., 1974) and Kalimantan (Haile et al., 1977), but in the present result, it is strongly suggested that at least the Sumatra area was a part of the Gondwanaland during the Triassic period. Much more comprehensive work from many other branches of earth sciences will be required before the speculation is conclusively established.

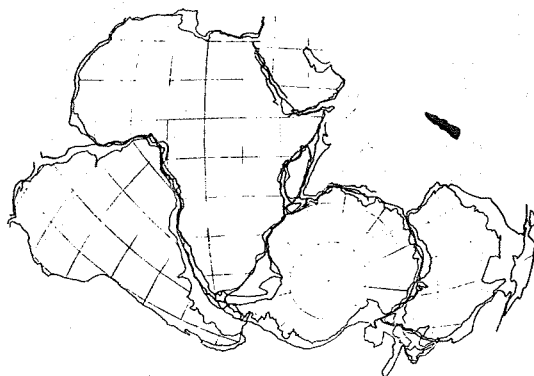


Fig. 5 Possible Triassic paleogeographic position of Sumatra drawn on the Gondwanaland reconstruction by Smith and Hallam (1970).

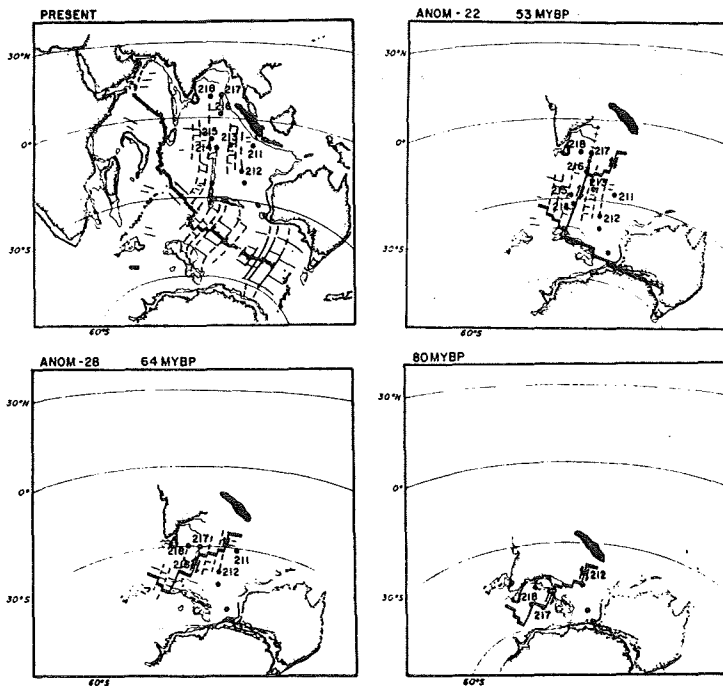


Fig. 6  
Northward drift of Sumatra being well matched with the history of sea-floor spreading of the Indian Ocean by Sclater and Fisher (1974).

#### References

- Chamalaun, F. H. (1977) *Earth Planet. Sci. Lett.*, 34, 107-112.
- Embleton, B. J. J. and P. W. Schmidt (1977) *Forth Int. Gondwana Sympo.*, abstract, Calcutta, India.
- Haile, N. S., M. W. McElhinny and I. McDougall (1977) *Jour. Geol. Soc. Lond.* 133, 133-144.
- Johnson, B. D., C. M. Powell and J. J. Veevers (1976) *Geol. Soc. Amer. Bull.*, 87, 1560-1566.
- McElhinny, M. W. (1973) Cambridge University Press., 206-212.
- McElhinny, M. W., N. S. Haile, and A. R. Crawford (1974) *Nature*, 252, 641-145.
- Ninkovich, D. (1976) *Earth Planet. Sci. Lett.*, 29, 269-275.

Ridd, M. F. (1971) *Nature*, 234, 531-533.

Sclater, J. G. and R. L. Fisher (1974) *Geol. Soc. Amer. Bull.*, 85, 685-702.

Smith, A. G. and A. Hallam (1970) *Nature*, 225, 139-144.

( to be submitted to *Nature* )

PALEOMAGNETISM OF THE OCEAN SEDIMENTS OF SHIKOKU BASIN  
AND DAITO AREA OBTAINED BY THE DEEP SEA DRILLING  
PROJECT, CRUISE LEG 58, BY GLOMAR CHALLENGER II

Hajimu KINOSHITA  
Department of Earth Sciences, Faculty of Science  
Chiba University, Yayoi-cho, Chiba

and

All scientists on board of the Glomar Challenger II, Leg 58

Paleomagnetic studies on the deep sea sediments, seamounts and the basaltic layers of the oceanic crust have extensively been carried out (refer to materials in group I). As to the northern part of the Pacific area there is a general trend that the oceanic plate has constantly been moving northward from Cretaceous through Pleistocene era. The same tendency has been found in the sediment cores recovered from the Atlantic Ocean basin as well (Sclater and Cox, 1970). The concept of the northerly drift of the Pacific Ocean crust for the last 100 to 150 Ma seems also to be confirmed by the sedimentological and the paleontological investigations

It is well known that the record of reversals of the (local) geomagnetic field can be found in the volcanic rocks as well as the depositional formations. Fine structures of reversing field have been studied by a large number of paleomagnetists (references, group II). As reviewed by Dagley (1974) recently a gross feature of the geomagnetic field assumes that the field intensity decreases far smaller and the semi-dipolar moment passes through the equator during the period of the field reversals. Here, the semi-dipole is stressed because most of the discussion on the orientation of the geomagnetic field around the reversing is based upon the dipole moment assumption though it is not evident yet if it is the case or not (Cox, 1964, group III). This type of study will certainly help us in an understanding of physical cause of the origin of the geomagnetic field.

In cores recovered by Deep Sea Drilling Project (DSDP) cruise, Leg 58, we have found an evidence of northerly movement of the northern tip of the Philippine plate which is coincidental with the finding of Louden (1977, group I). In a small valley of the Daito Ridge, a series of unbroken nannochalk cores was taken which enables us to analyze more than a couple of fine structures of the geomagnetic field reversals.

Looking at the facts that most of the earth's superficial materials (such as plates, continents, seamounts and so on) show a trace of northerly movement in a greater or lesser extent, the present authors are forced to account it for cosmological stimulations. The discussion which is based upon a oscillatory motion of the solar system within the Galaxy, is still crude and not conclusive yet, though.

Drilling sites 442 through 446 covered by Leg 58 cruise are shown in Fig.1. More detailed site and core descriptions will be found in the Initial Report of the DSDP Leg 58 cruise. Total number of about two thousands paleomagnetic minicores were cut out from sediment and hard rock cores, routinely every 1.5 meter of recovered cores.

Paleomagnetic measurements were made by well established techniques. Alternating field strength of 150 Oe (60 Hz) was selected for the demagnetization procedures and was fixed throughout the whole measurements. Results of measurements by a spinning magnetometer were calculated by an electronic computer. Only stable natural remanent magnetization (NRM) are picked up and analyzed statistically. Stability of NRM is checked as follows.

- 1 Koenigsberger's ratio  $Q_n$  exceeds 10.
- 2 Median destructive field is higher than 150 Oe.
- 3 Direction of NRM does not shift more than 10 degrees along a great circle when cleaned by AF 150 Oe.

Data on hard rock samples will be described in detail in the DSDP Initial Report, Leg 58, and therefore, will not be mentioned here.

Ages of recovered cores were determined by the paleontological investigation on nannofossils, radiolaria and foraminifera. Paleomagnetic data are divided by an appropriate geologic time scale and are analyzed statistically. Results

are plotted in Fig. 2. The paleolatitudes of the cores are estimated on an assumption that the geomagnetic dipole moment has been fixed parallel to the earth's rotational axis, thus oriented toward the geographic poles for the last 45 Ma.

Among cores from the Daito Ridge, Nos. 45, 46 and 47 nannochalk fossil cores are well consolidated and less broken. Relative change in declination and absolute values of inclination are easily measurable in detail. Paleomagnetic cores were cut out every 10 cm and whole cores cover just about 1 Ma (150 samples from a 15 meter interval). Results of measurements are shown in Fig. 3. Detailed core descriptions are presented in the Initial Report of the cruise.

From the absolute values of the NRM of

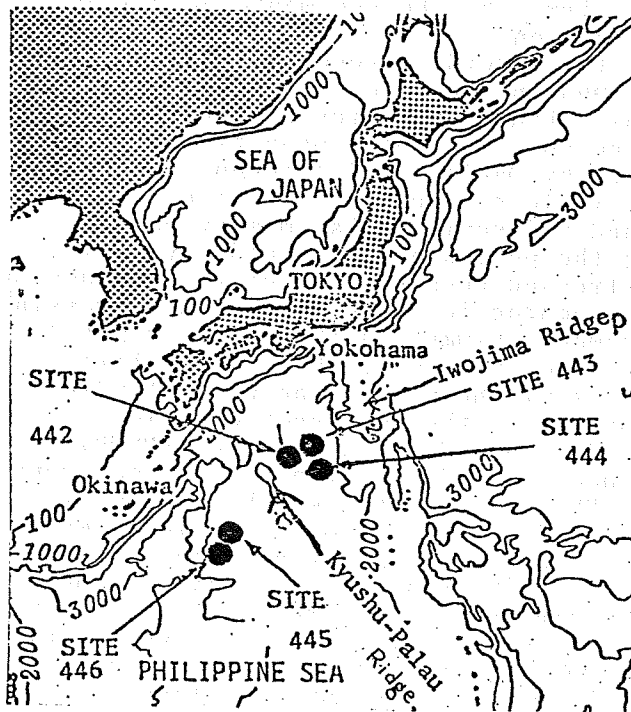


Fig. 1 Location of the drilling sites for DSDP, Leg 58.

sediments from the present area, it is concluded that the Daito Ridge located presently at the northern tip of the Philippine basin has been drifting northward for the last 45 Ma after it's formation.

Polarity changes observed in consolidated cores show a morphological similarity to those observed by other investigators. The geomagnetic field intensity decreased during the field reversals which was followed by a transfer of the semi-dipole axis toward the antipodal position and then the field intensity recovered to the normal value. It seems likely that the normal polarity was relatively more stable than the reversed one. Assumed a constant rate of sedimentation, the time constant of the field flip-flop seems to have been quite variable ranging from 1,000 to 30,000 years.

It is striking to learn that almost all the paleomagnetic data obtained so far show that the materials on the earth's surface are generally drifting northward for the last 100 -150 Ma.

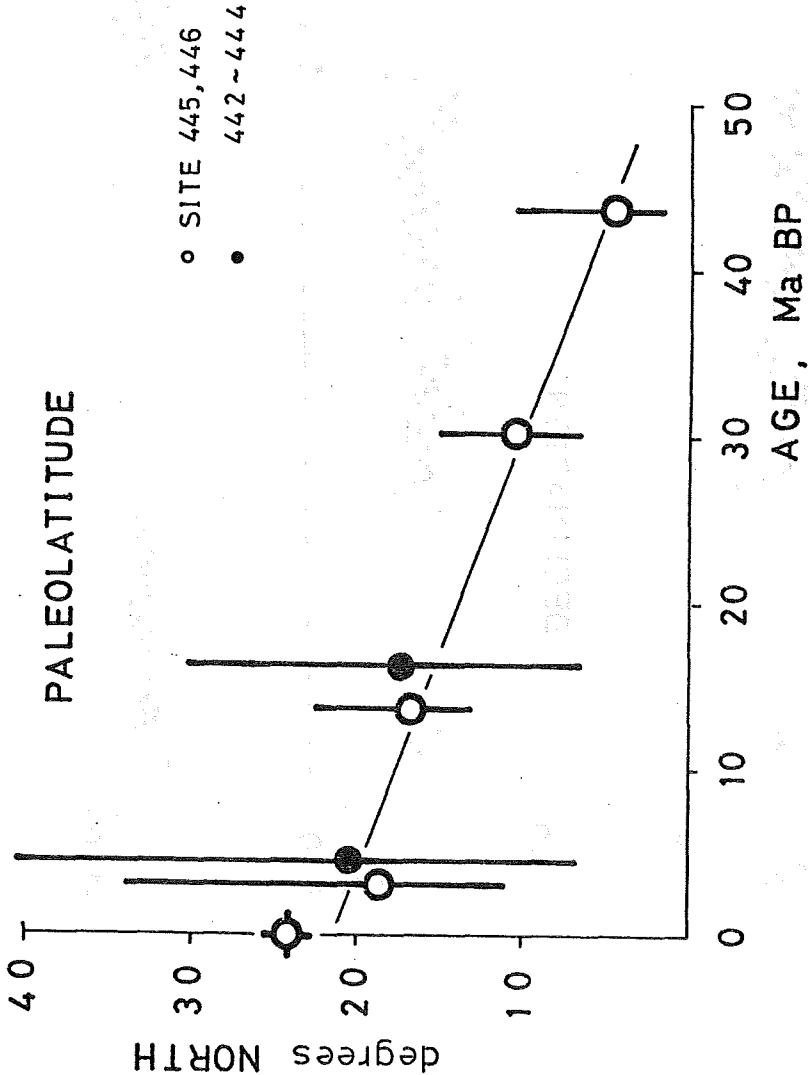


Fig. 2 Paleolatitude of the Daito Ridge and the Shikoku basin deduced from sediment magnetization paleomagnetically.

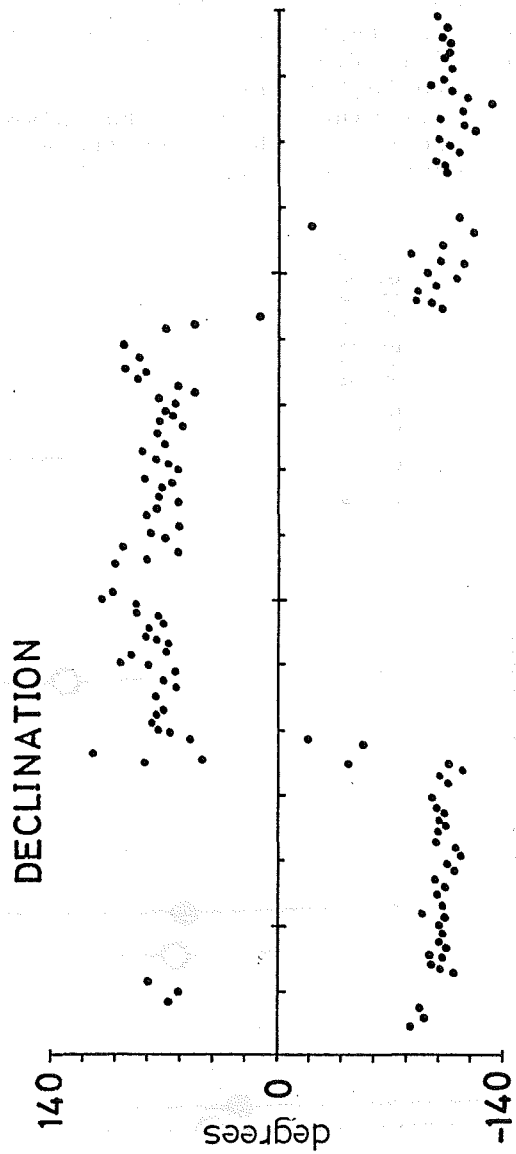
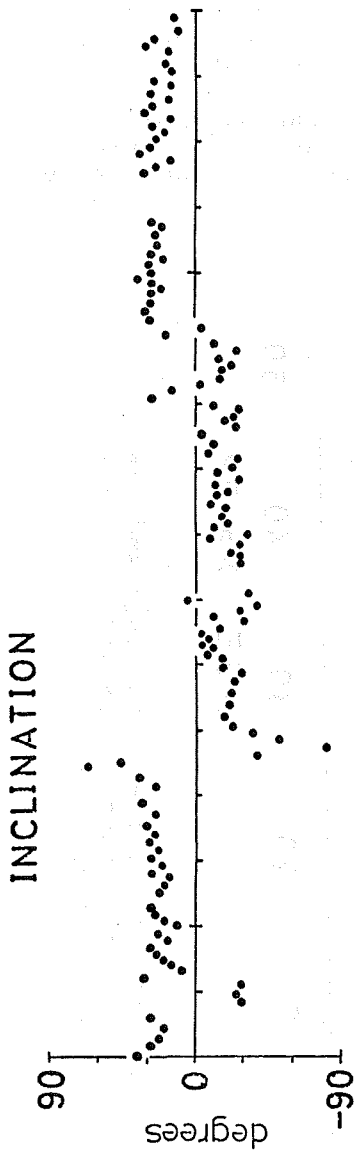


Fig. 3

Especially, the Pacific plate, the Philippine Sea plate, the Atlantic plate, the North American Continent, the Indian plate and also the Japanese Islands seem to have the common tendency. It is evident from the recent seismological data, that the Pacific plate is strongly pushed northward in general (Uyeda and Kanamori, 1978, group III). This fact can be explained as a result of a movement of the center of gravity of the earth with respect to time. This would possibly occur when the earth is floating in a general accelerating gravity field of the Galaxy in an oscillatory manner and the earth's interior is governed by a convective motion (of a fluid like material)

caused essentially by its own gravitational field. The model is something similar to a falling liquid droplet which has its own gravitational force (Chandrasekhar, 1961, group III) and a heat source or some driving force to cause convective motions. A slightly distorted pear shape of the earth may be accounted for by the present model. The Galaxy accelerating field seems to vary with time with the amplitude of  $4 \times 10^{-9}$  cm/sec<sup>2</sup> and the period of  $8 \times 10^7$  years. The time constant of this order is quite suggestive when we recall that the continental drift occurred in an episodic fashion with the order of 10 to 100 Ma.

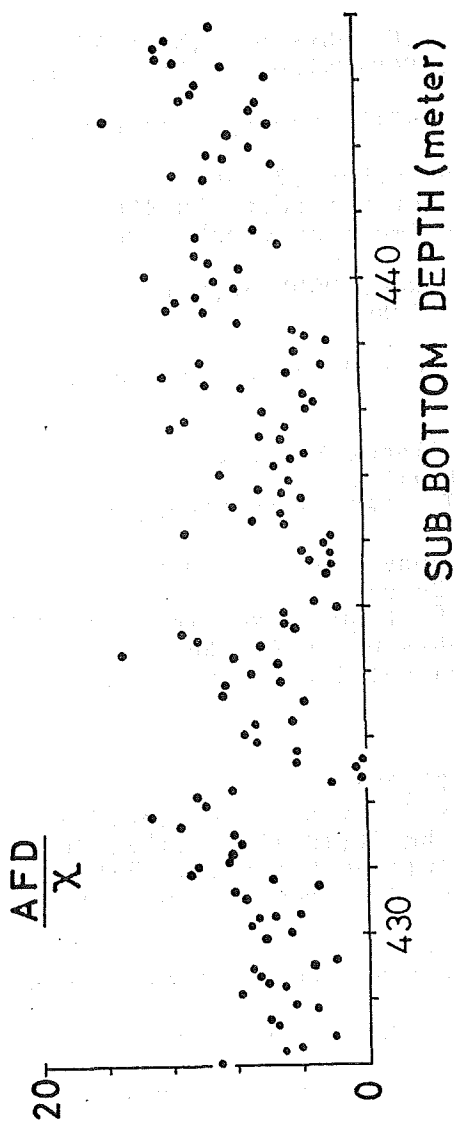


Fig. 3 (previous page)  
NRM orientation versus sub-bottom depth of consolidated nannochalk fossil cores taken at site 445, Daito Ridge.

(this page)  
Ratios of AFD'd NRM (in 150 Oe) to the initial susceptibility of the nannochalk cores.

Note; the sub-bottom depth are indicated on the foot of the last figure.

## REFERENCES

### (Group I)

- Clague D.A. and R.D.Jarrard(1973)Geol.Soc.America Bull.,84,1135.  
 Fitch T.J.(1972)J.Geophys.Res.,77,4432  
 Franchateau J.,C.G.A.Harrison,J.G.Sclater and L.M.Richards  
 (1970)J.Geophys.Res.,75,2035.  
 Gromme S. and F.J.Vine(1972)Earth Planet.Sci.Lett.,17,159.  
 Hammond S.R.,F.Theyer and G.H.Sutton(1974)Earth Planet.Sci.Lett.  
22,22.  
 Harrison C.G.A.,R.D.Jarrard,V.Vacquier and R.L.Larson(1975)  
 Geophys.J.Roy.astr.Soc.,42,859.  
 Heirtzler J.R.,G.O.Dickson,E.M.Herron,W.C.Pitman and X.LePichon  
 (1968)J.Geophys.Res,73,2119.  
 Jackson E.D.,E.A.Silver and G.B.Dalrymple(1972)Geol.Soc.America  
 Bull.,83,601.  
 Kalashnikov A.G.(1961)Izv.Akad.Nauk,Geophys.Ser.,No.9,1243.  
 Kawai N.,K.Hirooka and T.Nakajima(1969)Paleogeol.Paleoclim.  
 Paleoecol.,6,277.  
 Kawai N.,K.Nakajima and K.Hirooka(1971)J.Geomag.Geolectr.,  
23,267.  
 King R.F. and A.I.Rees(1966)J.Geophys.Res.,71,561.  
 Kodama K. and A.Cox(1978)Earth Planet.Sci.Lett.,38,436.  
 Lancelot Y. and J.Ewing(1973)Trans.American Geophys.Union,  
54,331.  
 Larson R.L. and W.Laurie(1975)Init.Rep.,DSDP,32,571.  
 Louden K.E.(1977)J.Geophys.Res.,82,2989.  
 McElhinny(1973)Nature,241,523.  
 Minster J.B.,T.H.Jordan,P.Molnar and E.Haines(1974)Geophys.  
 J.Roy.astr.Soc.,36,541  
 Morgan W.J.(1971)Nature,230,42.  
 Opdyke J.W. and A.Todd(1974)Earth Planet.Sci.Lett.,22,300.  
 Pierce J.W.(1976)J.Geophys.Res.,81,4173.  
 Sasajima S.,J.Nishida and M.Shimada(1968)Earth Planet.Sci.  
 Lett.,5,135.  
 Schouten H. and K.McCamy(1972)J.Geophys.Res.,77,7089.  
 Sclater J. and A.Cox(1970)Nature,226,934.  
 Vacquier V. and S.Uyeda(1967)Bull.Earthquake.Res.Inst.,45,815.  
 Vine F.J.(1968)Trans.American Geophys.Union,49,156.  
 Vine F.J. and H.H.Hess(1970)The Sea,vol.4,p-II,pp587-622.

### (Group II)

- Bucha V.(1970)J.Geomag.Geolectr.,22,253.  
 Dagley P. and E.Lawley(1974)Geophys.J.Roy.astr.Soc.,36,577.  
 Dunn J.R.,M.Fuller,H.Ito and V.A.Schmidt(1971)Sci.,172,840.  
 Harrison C.G.A. and B.L.K.Somayajulu(1966)Nature,212,1193.  
 Ito H.(1963)Ann.Progress Rep.Rockmag.Res.Group Japan,   ,87.  
 Ito H(1965)J.Geomag.Geolectr.,17,113.  
 Ito H.(1970)J.Geomag.Geolectr.,22,273.  
 Kawai N.,T.Nakajima,K.Hirooka and K.Kobayashi(1973)Proc.Japan  
 Acad.,49,820.  
 Kawai N.,Y.Otofuji and K.Kobayashi(1976)J.Geomag.Jeolectr.  
29,211.  
 Kawai N.,T.Sato,T.Sueishi and K.Kobayashi(1977)J.Geomag.  
 Geolectr.,28,395.  
 Larson E.E.,D.E.Watson and W.Jennings(1971)Earth Planet.Sci.  
 Lett.,11,391.  
 Momose K.,K.Kobayashi and T.Yamada(1959)Bull.Earthquake Res.

- Inst., 37, 433.
- Nomura S. (1967) J. Liberal Art Gumma Univ., 1, 11.
- Opdyke N.D., D.V. Kent and W. Lowrie (1973) Earth Planet. Sci. Lett. 20, 315.
- Petrova G.N., I.G. Kaporovich, Z.V. Makarova and R.S. Ruibak (1961) Geomag. Field in the Past and in the Present, pp220-227.
- Vlasov A.Y. and G.V. Kovalenko (1963) Izv. Akad. Nauk, Geophys. Ser., No. 4, 552.
- Watkins N.D. (1963) Nature, 197, 126.
- Wilson R.L., P. Dagley and A.G. McCormack (1972) Geophys. J. Roy. astr. Soc., 28, 213.
- Yaskawa K., T. Nakajima, N. Kawai, M. Torii, N. Natsubara and S. Horie (1973) J. Geomag. Geoelectr., 25, 447.
- Yukutake T. (1968) Phys. Earth Planet. Inter., 1, 93.
- van Zijl J.S.V., K.W.T. Graham and A.L. Hales (1962) Geophys. J. Roy. astr. Soc., 7, 23.
- van Zijl J.S.V., K.W.T. Graham and A.L. Hales (1962) Geophys. J. Roy. astr. Soc., 7, 169.

(Group III)

- Chandrasekhar S. (1961) Hydrodyn. Hydromag. Stability, pp220-271.
- Cox A. (1964) Geophys. J. Roy. astr. Soc., 8, 345.
- Uyeda S. and H. Kanamori (1978) Kagaku (Science), 48, 91.

## MAGNETIC ANOMALY LINEATIONS IN THE PHILIPPINE SEA

Hiroyuki MIKI , Nobuhiro ISEZAKI

Katsumi YASKAWA and Hiroo INOKUCHI

Department of Earth Sciences, Faculty of Science,  
Kobe University, Nada, Kobe 657, Japan

### 1. Introduction

The analysis of magnetic anomaly lineations in the Philippine Sea have been studied by Tomoda et al.(1975), Watts and Weissel (1975), Kobayashi and Isezaki (1976), Watts et al.(1977), Louden (1977), and so forth. As for the radiometric dating, Ozima et al.(1977) studied the rocks obtained by deep-sea drilling project (DSDP), Leg 31 (1971), and determined the age by the  $^{40}\text{Ar}$ - $^{39}\text{Ar}$  step-heating dating method (see Fig.1). We compiled magnetic data obtained during GDP period and got one of possible interpretations of lineations as shown in Fig.2 and Fig.6.

### 2. Magnetic Anomaly Lineations in the Shikoku Basin

We present the anomaly lineations in the Shikoku Basin in more detail than Tomoda et al.(1975) and Watts and Weissel (1975), and describe one of possible interpretations of lineations as shown in Fig.2 and Fig.3. The characteristic feature of this tentative lineations is that the lineations have no clear offset and appear to extend further south, at least to  $23^{\circ}\text{N}$  latitude, and is more similar to lineations of Watts and Weissel (1975) than those of Tomoda et al.(1975). However, it is possible that some fracture zones exist in the Shikoku Basin, because several magnetic anomaly lineations change the trend abruptly in the middle area of this basin. Then we have not attempted to map any fracture zone in this basin, as shown in Fig.2.

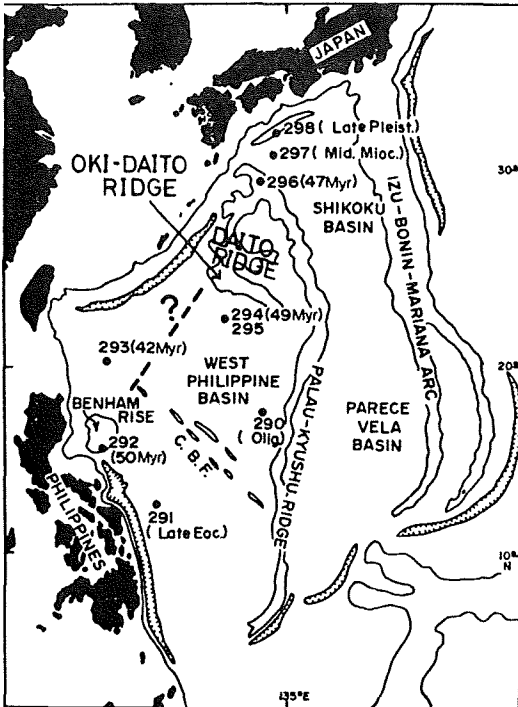


Fig.1 DSDP Leg 31 sampling sites :  $^{40}\text{Ar}$ - $^{39}\text{Ar}$  age (Myr) and minimum basement age estimated by microfossils are shown in a bracket (Ozima et al.(1977)).

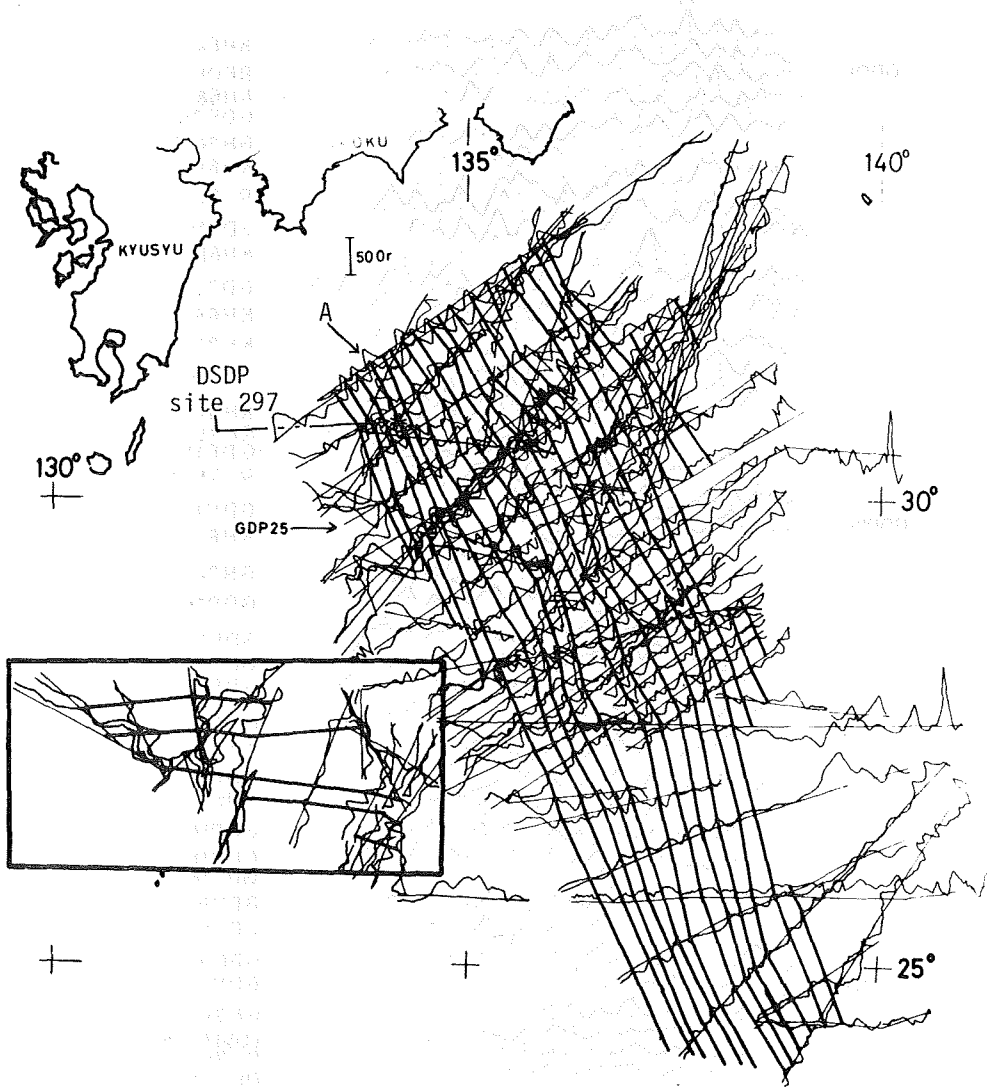


Fig.2 Geomagnetic total intensity anomaly lineations in the Shikoku Basin. The detail of the Amami Plateau and the Daito Ridge area, squared by the solid line, is shown in Fig.5. \* indicates the site 297 and Watts and Weissel (1975) identified that the magnetic lineation, which run on this site, as shown A in this Fig., is 6B. They estimated that the age of the crust at site 297 is about 24 m.y.B.P., and Tomoda et al.(1975) described that the age of this basement was approximately 20 m.y.B.P. (Isezaki and Miki (1978)).

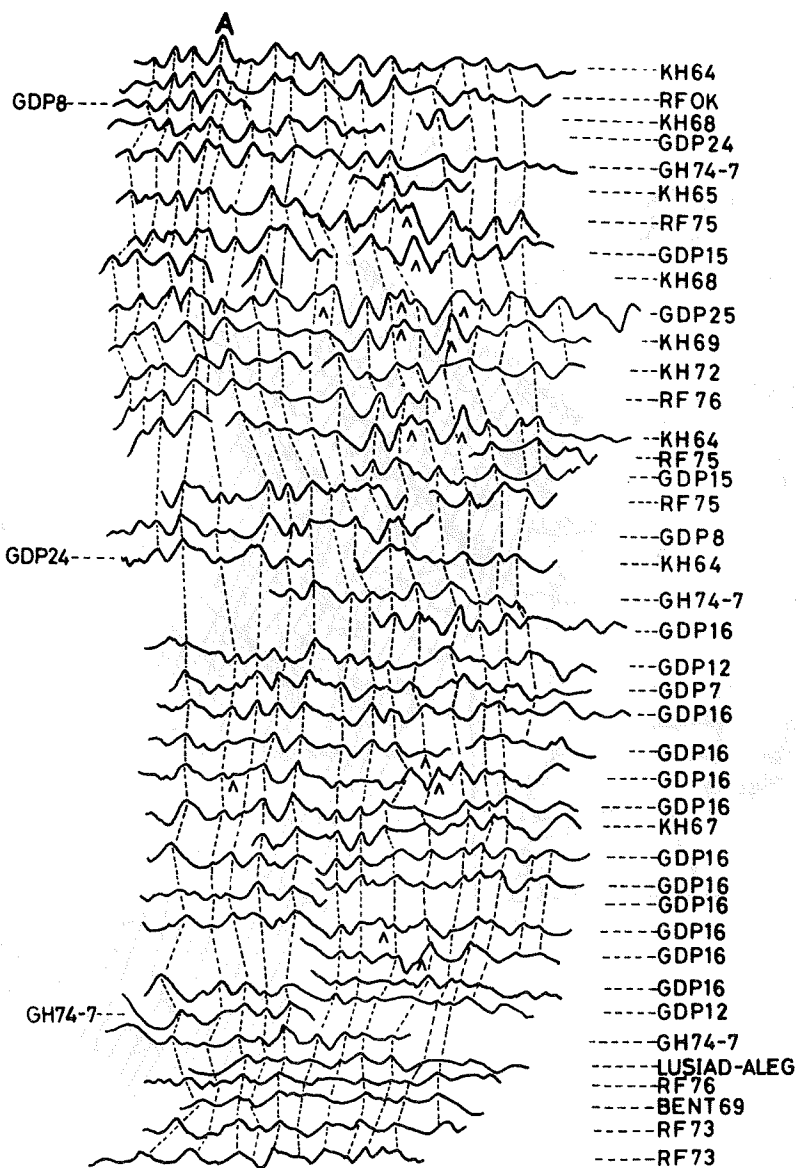


Fig.3 Anomaly profiles arranged from north to south to see the lineations in the Shikoku Basin. The lineation A is 6B which Watts and Weissel (1975) estimated.  $\Delta$  indicates a seamount (Isezaki and Miki (1978)).

Fig.4 shows the block model in the Shikoku Basin. The more exactly the calculated total and the absolute total intensity anomaly fit to observed  $t_0$  and  $t_a$ , the more confidently the block model becomes to be the truth (see Isezaki (1973)).

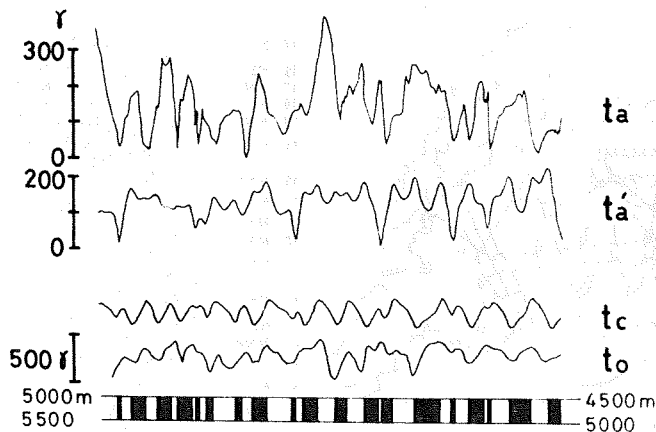


Fig. 4

The absolute total intensity anomaly  $t_a'$  calculated from the block model shown, and  $t_a$  calculated from the observed total intensity anomaly  $t_o$  of GDP 25 track (see Fig.2).

$t_a(x)$  is the absolute total intensity anomaly and defined by

$$t_a(x) = \sqrt{H(x)^2 + v(x)^2}$$

where  $H(x)$  : the horizontal intensity anomaly  
 $V(x)$  : the vertical intensity anomaly  
 $x$  : the positive direction is clockwise perpendicular to the strike of the lineation

$$t_c(x) = H(x) \cdot \cos I \cdot \sin(D-S) + V(x) \cdot \sin I$$

where  $t_c(x)$  : the total intensity anomaly  
 $I$  : inclination of the geomagnetic field  
 $D$  : declination of the geomagnetic field  
 $S$  : the strike of lineation measured clockwise from the geographical north

Adopted inclination and intensity of magnetization of block are  $45^\circ$  and  $7 \times 10^{-3} \text{emu/cc}$  respectively. Inclination and declination of the geomagnetic field at this place are  $45^\circ$  and  $-6^\circ$  respectively (Isezaki (1978)).

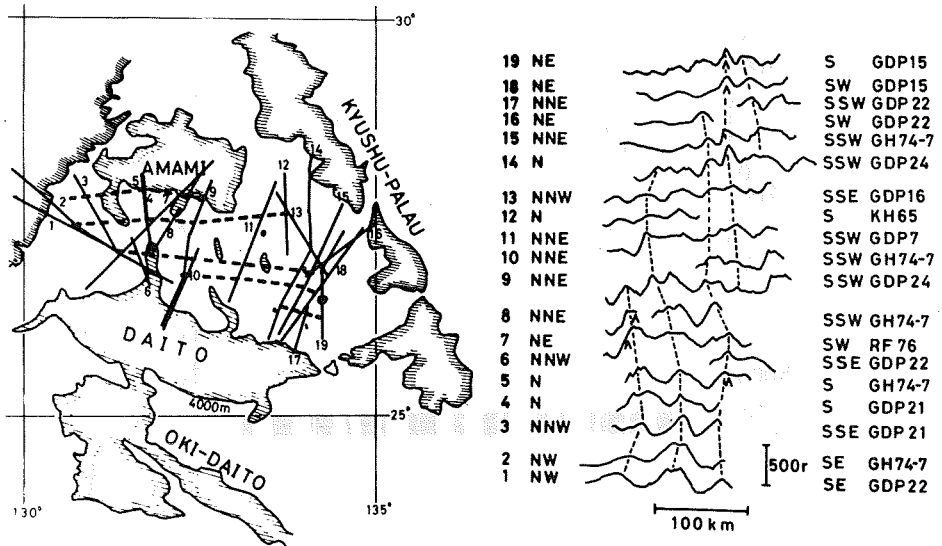


Fig.5 Geomagnetic total intensity anomaly lineations and profiles in the Amami Plateau and the Daito Ridge area. The solid lines are track lines and the broken lines represent lineations. A indicates a seamount (Isezaki and Miki (1978)).

### 3. Magnetic Anomaly Lineations in the Kita-Daito Basin

We call the small area "Kita-Daito Basin", between the Amami Plateau and the Daito Ridge. In this area, we found the magnetic lineations which run east-west (see Fig.5). Note that the peak-to-peak amplitudes of magnetic anomalies in the west of this area are appear to be smaller than one in the east. This phenomenon may relate to origin of the Kita-Daito Basin. These lineations will play a very important role in the problem of the origin of this area.

### 4. Magnetic Anomaly Lineations in the West Philippine Basin

We compiled the magnetic data, as shown in Fig.6. Ozima et al.(1977) described that the  $^{40}\text{Ar}$ - $^{39}\text{Ar}$  age is 49 Myr at site 294 and 42 Myr at site 293, and in the both of sites drill holes reached the basement (see Fig.1). These ages are different from the ages which were computed by the magnetic anomalies by Watts and Weissel (1975). There is no positive age evidence to suggest the spreading ocean ridge origin of the Central Basin Fault (CBF). The West Philippine Basin is significantly younger than the currently proposed magnetic anomaly lineations (Ozima et al.(1977)).

The U.S. Naval Oceanographic office shows the magnetic anomaly lineations in which area is squared by solid line in Fig.7. The strike of these lineations is NW-SE, and the strike of the eastern lineations is WNW-ESE, so we can not ignore the feature that the strike of lineations changes significantly. We think that a structural boundary may exist, as shown by

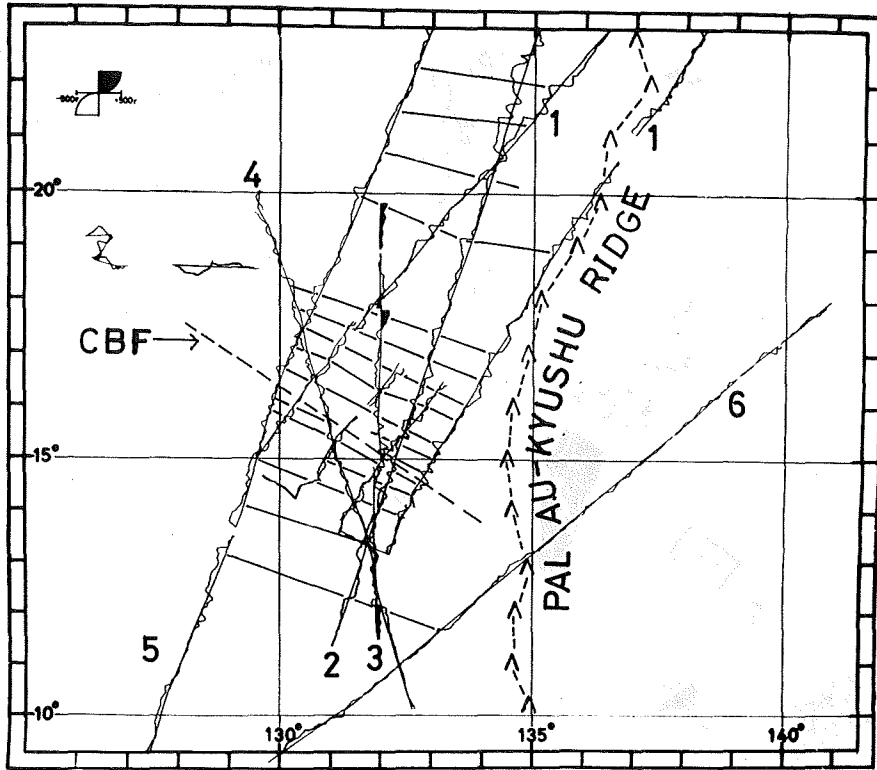


Fig.6 Geomagnetic total intensity anomaly lineations in the West Philippine Basin. The solid lines are lineations and the broken line represents the Central Basin Fault.  $\Delta$  ---  $\Delta$  line represents the Palau-Kyushu Ridge.

1. RF-73
2. UMI-63
3. KH72-1
4. RF-73-c
5. FUJI-67
6. SCAN-A Leg 4

the broken line in Fig.1 and Fig.7. Because the site 293 is the western area of this boundary and the age which estimated by the magnetic anomalies is the western area of this one, it is possible that the age in the site 293 may be different from the age in the eastern area.

And another possibility is that the CBF is not an old spreading center, because the strike of magnetic lineations is oblique to the trend of CBF, as shown in Fig.6.

The summarized magnetic lineations in the Philippine Sea are shown in Fig.7. We will try to determine the exact block model and to decide the age of magnetic lineations from the block model by the statistical method.

#### REFERENCE

1. S.Uyeda and Ben-Avraham (1972) Nature phys. Sci. 240 p.176
2. Ben-Avraham et al. (1972) Nature Vol.240 No.5382 p.453
3. Murauchi et al. (1974) Kaiyo-Kagaku (in Japanese) 6 p.56

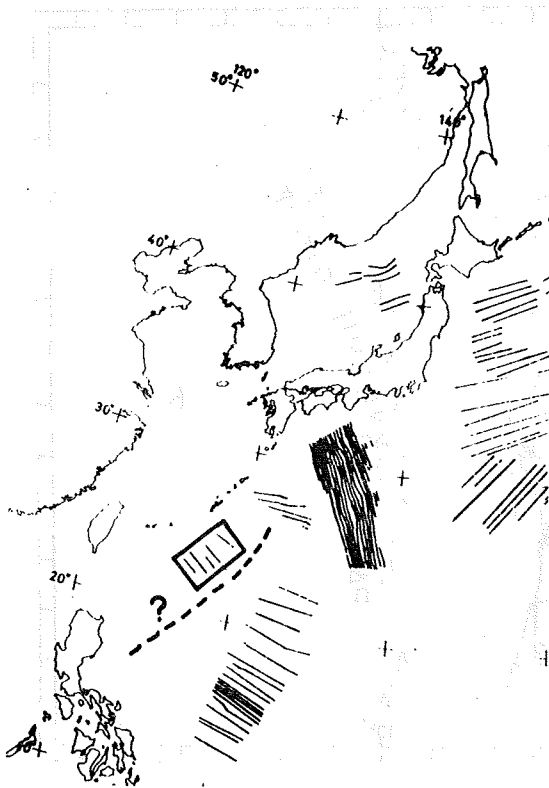


Fig.7  
 Geomagnetic total intensity anomaly lineations in the northwestern Pacific basin. Solid lines represent the lineated positive anomalies (Isezaki and Miki (1978)).

4. Y.Tomoda et al. (1975) J. Geomag. Geoelectr. 28 p.47
5. A.B.Watts and J.K.Weissel (1975) Earth planet. Sci. Lett 25 p.239
6. K.Kobayashi and N.Isezaki (1976) A.G.U. Monogr. 19 p.235
7. A.B.Watts et al. (1977) Tectonophysics 37 p.167
8. K.E.Louden (1977) J.G.R. Vol. 82 No.20 p.2989
9. M.Ozima et al. (1977) Nature Vol.267 No.5614 p.816
10. N.Isezaki (1978) (Submitted to J. Phys. Earth)
11. N.Isezaki and H.Miki (1978) (Submitted to J. Phys. Earth)
12. The U.S. Naval Oceanographic Office (1976) Map No.2405-2

AUTHOR INDEX

|                                                                                        |  |                   |     |
|----------------------------------------------------------------------------------------|--|-------------------|-----|
| All scientists on board of the Glomar Challenger II,<br>Leg 58                         |  | see KINOSHITA, H. |     |
| DOMEN, Haruo                                                                           |  |                   | 40  |
| DOMEN, Haruo                                                                           |  |                   | 47  |
| HAYASHIDA, Akira, S. SASAJIMA and T. YOKOYAMA                                          |  |                   | 55  |
| HEHUWAT, F                                                                             |  | see SASAJIMA, S.  |     |
| HEHUWAT, F                                                                             |  | see SASAJIMA, S.  |     |
| HIRAJIMA, Takao, Y. OTOFUJI and S. SASAJIMA                                            |  |                   | 27  |
| HIROOKA, Kimio                                                                         |  | see SASAJIMA, S.  |     |
| HIROOKA, Kimio                                                                         |  | see SASAJIMA, S.  |     |
| INOKUCHI, Hiroo                                                                        |  | see MIKI, H.      |     |
| INOUE, Yositungu                                                                       |  |                   | 5   |
| ISEZAKI, Nobuhiro                                                                      |  | see MIKI, H.      |     |
| JOSHIMA, Masato, K. SHIBATA, K. ONO and O. UJIKE                                       |  |                   | 65  |
| KANEOKA, Ichiro                                                                        |  |                   | 81  |
| KANEOKA, Ichiro, M. OZIMA and M. YANAGISAWA                                            |  |                   | 84  |
| KINOSHITA, Hajimu and All scientists on board of the<br>Glomar Challenger II, Leg 58   |  |                   | 111 |
| KONO, Masaru                                                                           |  |                   | 98  |
| LEEUWEN, T.V.                                                                          |  | see SASAJIMA, S.  |     |
| MAENAKA, Kazuaki                                                                       |  |                   | 49  |
| MIKI, Hiroyuki, N. ISEZAKI, K. YASKAWA and H. INOKUCHI                                 |  |                   | 118 |
| MOMOSE, Kan-ichi                                                                       |  |                   | 25  |
| MUROI, Isao                                                                            |  |                   | 34  |
| NISHIMURA, Susumu                                                                      |  | see SASAJIMA, S.  |     |
| ONO, Koji                                                                              |  | see JOSHIMA, M.   |     |
| OTOFUJI, Yo-ichiro                                                                     |  | see HIRAJIMA, T.  |     |
| OTOFUJI, Yo-ichiro                                                                     |  | see SASAJIMA, S.  |     |
| OTOFUJI, Yo-ichiro                                                                     |  | see SASAJIMA, S.  |     |
| OZIMA, Minoru                                                                          |  | see KANEOKA, I.   |     |
| SASAJIMA, Sadao                                                                        |  | see HIRAJIMA, T.  |     |
| SASAJIMA, Sadao                                                                        |  | see HAYASHIDA, A. |     |
| SASAJIMA, Sadao, S. NISHIMURA, K. HIROOKA, Y. OTOFUJI,<br>T.V. LEEUWEN, and F. HEHUWAT |  |                   | 73  |
| SASAJIMA, Sadao, Y. OTOFUJI, K. HIROOKA, SUPARKA,<br>SUWIJANTO and F. HEHUWAT          |  |                   | 104 |
| SHIBATA, Ken                                                                           |  | see JOSHIMA, M.   |     |
| SUEISHI, Tsutomu                                                                       |  |                   | 1   |
| SUPARKA                                                                                |  | see SASAJIMA, S.  |     |
| SUWIJANTO                                                                              |  | see SASAJIMA, S.  |     |
| TAKEMURA Keiji and M. TORII                                                            |  |                   | 69  |
| TANAKA, Hidefumi                                                                       |  |                   | 18  |
| TANAKA, Hidefumi                                                                       |  |                   | 87  |
| TANAKA, Hidefumi                                                                       |  |                   | 95  |
| TORII, Masayuki                                                                        |  |                   | 11  |
| TORII, Masayuki                                                                        |  | see TAKEMURA, K.  |     |
| UJIKE, Osamu                                                                           |  | see JOSHIMA, M.   |     |
| YANAGISAWA, Masahisa                                                                   |  | see KANEOKA, I.   |     |
| YASKAWA, Katsumi                                                                       |  | see MIKI, H.      |     |
| YOKOYAMA, Takuo                                                                        |  | see HAYASHIDA, A. |     |

